2013

Applications of Holographic Dualities

Dylan Judd Albrecht
College of William & Mary - Arts & Sciences

Applications of Holographic Dualities

Dylan Judd Albrecht

Williamsburg, Virginia

Master of Science, College of William and Mary, 2009
Bachelor of Science, University of Massachusetts Amherst, 2007

A Dissertation presented to the Graduate Faculty
of the College of William and Mary in Candidacy for the Degree of
Doctor of Philosophy

Department of Physics

The College of William and Mary
May 2013

UMI Number: 3578115

UMI

Dissertation Publishing

ProQuest®

APPROVAL PAGE

This Dissertation is submitted in partial fulfillment of
the requirements for the degree of

Doctor of Philosophy
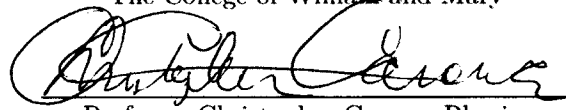
Dylan Judd Albrecht
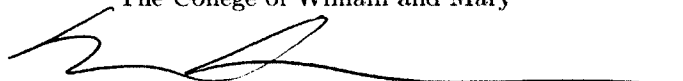
Approved by the Committee, May, 2013
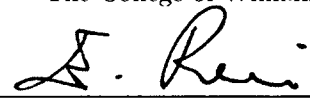
Committee Chair
Associate Professor Joshua Erlich, Physics
The College of William and Mary

Professor Christopher Carone, Physics
The College of William and Mary

Professor Marc Sher, Physics
The College of William and Mary

Assistant Professor Enrico Rossi, Physics
The College of William and Mary

Visiting Assistant Professor Daniel Vasiliu, Mathematics
The College of William and Mary

ABSTRACT

We introduce and review some of the building blocks to what is known as the AdS/CFT correspondence. We then present, using the framework of the correspondence, two applications: one to QCD (Chapters 2 and 3) and one to superconductivity (Chapter 4). The work presented in these chapters was carried out by the author and collaborators during the author's graduate studies.

TABLE OF CONTENTS

ACKNOWLEDGMENTS

For three pillars of support: Pam, Jeff, and Stephan.

LIST OF TABLES

LIST OF FIGURES

APPLICATIONS OF HOLOGRAPHIC DUALITIES

CHAPTER 1

Introduction

Properties of many physical systems can be studied using models where the interactions are governed by weak couplings. When couplings are small (weak) it is possible to solve the model perturbatively, order by order in the small coupling. However, there are many systems in nature where the coupling is not small, and the system is said to be strongly coupled. In this case, we lose the ability to do a perturbative expansion because higher order contributions are unsuppressed. For example, in Quantum Chromodynamics (QCD), the quantum field theory (QFT) of quarks and gluons, the coupling changes from weak coupling (at high energy) to strong coupling (at low energy). Within the confines of the defined quantum field theory (QCD), in order to make fundamental predictions at low energy, we must solve a strongly-coupled theory; that is, unless there is an alternative description, not necessarily a quantum field theoretical description, of the degrees of freedom which admits a weak-coupling expansion. If such an alternative (or dual) theory existed, one could perform a perturbative calculation and map the result back to, say, a matrix element of the strongly-coupled QFT. These two theories are said to be dual to one another and the mapping between the two is called a strong-weak duality.

In string theory, there are many dualities amongst the different types of string theories: some dualities (called T-duality) relate a compactification of a weakly-coupled string theory to another compactification of a (possibly the same) weakly-coupled string theory; other dualities are strong-weak dualities (called S-duality), which map a string theory at weak string coupling g_s to another (possibly the same) string theory at strong coupling $g'_s \sim 1/g_s$. It is important to note that many of these dualities are still conjectures. One of the most important dualities to come from string theory is called the AdS/CFT correspondence [1, 2, 3]. The correspondence relates a gravitational theory on $(d + 1)$-dimensional Anti-de Sitter (AdS) spacetime and d-dimensional conformal field theory (CFT), which lives on the boundary of that spacetime. It is a strong-weak duality, and because the CFT lives on the boundary of the dual theory it is called a holographic duality. Much of the original excitement concerning this duality was due to the fact that the boundary CFT (in the most precise form of the conjecture) is a four-dimensional, strongly-coupled SU(N) gauge theory on Minkowski spacetime, reminiscent of QCD. Since its inception, the AdS/CFT correspondence has spurred a plethora of models, some with applications to a variety of condensed matter systems. Even though many models don't necessarily adhere to the specifics of the strict form of the conjecture, the appeal of obtaining qualitative and possibly quantitative understanding of strongly-coupled physical systems is too great.

Modelling interesting physical systems using the framework of AdS/CFT has become an exciting and fast-growing area of research. In particular, AdS/CFT has provided motivation for extra-dimensional (holographic) models of QCD [4, 5, 6, 7, 8, 9, 10, 11, 12, 13]. Progress has been made in understanding properties of holographic models of superconductors and other condensed matter systems, including s, p, and d-wave superconductivity [14, 15, 16], the Nernst effect in the quantum critical regime [17], strange metallic behavior [18], enhancement of the superconducting gap compared to BCS theory [19], and Homes's empirical law for T_c as a function of low-temperature superfluid density and

normal-phase resistivity [20, 21]. In some models of holographic superconductors there is no hard zero-temperature gap [22]. AdS/CFT has been used to study finite temperature strongly-coupled plasmas (RHIC physics) [23], non-Fermi liquids [24], and the quantum Hall effect ([25], and references within). For some reviews on holographic models of condensed matter systems, see Refs. [19, 26, 27, 28, 29, 30, 31, 32, 33, 34].

The AdS/CFT correspondence represents a novel way to attempt to describe strongly-coupled systems at quantum criticality ([33], for an inspiring account). Finding correct qualitative features in a strongly-coupled system, where good theoretical techniques are in general lacking, is very encouraging. One notable success is the derivation of a holographic bound [35] on the ratio of shear viscosity (η) to entropy density (s), which appears to be saturated by the quark gluon plasma (see [36] for a recent status report). Furthermore, it is believed that strongly-coupled systems at quantum criticality relax back to equilibrium in the shortest possible time, governed by a specific form for the equilibrium time $\tau_{\mathrm{eq}}(T)$ [37]. As pointed out in Ref. [31], the AdS/CFT correspondence is the only known method in condensed matter physics that produces the correct form for $\tau_{\mathrm{eq}}(T)$ (see also [38]). Another (recent) interesting result is that holographic descriptions are the first to satisfy certain quantum critical conductivity sum rules [39]. The over-arching idea is that holographic methods involving quasinormal modes are more suited to strongly interacting quantum critical behavior than Boltzmann quasiparticle descriptions.

There are two major approaches to studying physical models using these holographic dualities: one is to study models derived from stable brane configurations in string theory, so-called topdown models, and the other is to study the correspondence involving (in general) a minimalistic set of fields not necessarily derivable from a string theory configuration, referred to as bottom-up models. In both cases, symmetries and quantum numbers are vital in constructing the model. The topics presented in this work focus on bottom-up, AdS/CFT models applied to study pions in QCD and simple s-wave holographic super-

conductors. First we will give some of the motivation for the AdS/CFT correspondence.

1.1 The Case for a Correspondence

There are a number of suggestive links between gauge theory and string theory, dating back to the early flux-tube description of QCD: the linear progression of meson masses (Regge behavior) and the confining potential, for example. The evidence becomes more concrete and precise when talking about four-dimensional SU(N), $\mathcal{N} = 4$ Supersymmetric Yang-Mills (SYM) at large N, as opposed to SU(3).[1] We will look at three basic ideas that give credence to AdS/CFT, which is the conjectured equivalence of the aforementioned SYM and a particular string theory. There are many excellent reviews [40, 41], and books [42, 43, 44, 45], which cover this topic. In the subsequent subsections we will follow, for the most part, the review by Aharony *et al.* Ref. [41]. First we will briefly review some general connections of large-N gauge theories and string theory, then we will move on to the identification of symmetries of the bulk and boundary AdS space, and touch on low-energy arguments leading to a specific conjecture.

1.1.1 Large-N Gauge Theory

As a concrete example, let's consider the gauge group of QCD, SU(3). The large-N version is simply the generalized gauge group SU(N). The impetus for working instead with SU(N) is we can calculate scattering amplitudes as an expansion in 1/N, taking N as large as we like. The hope is that results will resemble QCD, where N = 3 and the expansion in powers of 1/3 is some approximation to the large-N expansion [46]. Somewhat unexpectedly, the simplifications brought about by expanding in large N suggest

---

[1] Supersymmetry is a symmetry, in addition to the Poincaré symmetry group, which transforms bosons into fermions, and vice versa. The $\mathcal{N}$ generators (charges) of this transformation are fermionic operators, and they extend the operator algebra to a superalgebra containing the Poincaré group as a subgroup.

a connection to string theory [47], and features of large-N gauge theories provide evidence for gauge/string theory dualities in general. In QCD-like gauge theories, as $N \to \infty$, the glueball spectrum contains an infinite tower of narrow resonances [48, 46], in analogy to the spectrum of free string theory. Additionally, one of the most encouraging connections is that large-N gauge theory allows for a topological diagrammatic expansion (with $1/N$ acting as the coupling), which is the type of perturbative expansion present in string theory (with the string coupling g_s playing the role of $1/N$). This connection is based purely on large-N counting arguments, which we will now outline.

In large-N gauge theory the relevant diagrams in the perturbation series are planar diagrams (no lines crossing), as in the Fig. 1.1(a). Actually, the planar diagrams can be
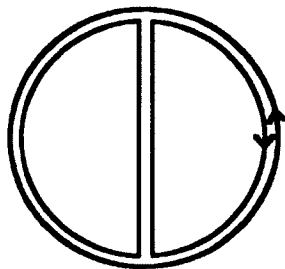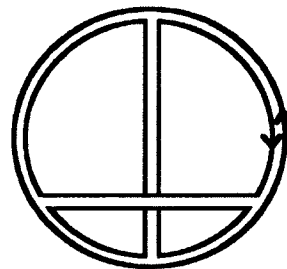
(a) Planar diagram.   (b) Nonplanar diagram.

FIG. 1.1: The planar diagram of (a) is $\mathcal{O}(N^2)$, with 2 vertices, 3 faces, and 3 propagators. The nonplanar diagram of (b) is $\mathcal{O}(1)$, with 4 vertices, 2 faces, and 6 propagators.

easily pasted onto a sphere, whereas nonplanar diagrams (with lines crossing) would be spheres but with handles at the line crossings. The weight of contributing diagrams can be ordered in terms of their topology – this is the advantage of expanding in terms of large N. The topological expansion mimics string perturbation theory, which involves sums over topologically distinct surfaces. In (closed) string perturbation theory, the diagrams are spheres, adding handles at higher order. A suggestive link between the two pictures goes

as follows. Imagine we have a gauge theory with Lagrangian, written schematically,

$$\mathcal{L} = \frac{1}{g_{\text{YM}}^2} \text{Tr} \left[d\Phi_I d\Phi_I + c^{IJK} \Phi_I \Phi_J \Phi_K + d^{IJKL} \Phi_I \Phi_J \Phi_K \Phi_L \right], \tag{1.1}$$

where $\Phi_I = \Phi_I^a T_{ij}^a = (\Phi_I)_j^i$, is a gauge field with the added index I, for generality. The gauge group generators, T_{ij}^a, are $N \times N$ matrices in the i, j indices. The final way of writing the gauge field, $(\Phi_I)_j^i$, is useful for organizing the large-N perturbative expansion. Each i, j index gets a line in the Feynman diagram, this is called double-line notation [47] and results in diagrams as in Fig. 1.1. We should note that we could consider diagrams with external lines — we would simply cut the outer loop and add a double line propagator – but this doesn't affect the counting. Additionally, the 't Hooft coupling defined as $\lambda = g_{\text{YM}}^2 N$, is to be held constant in the large-N limit.[2] The Lagrangian (1.1) implies each propagator (edge) contributes a factor of λ/N, each vertex contributes a factor of N/λ, and each loop (or face) contributes a factor of N, from summation over the fundamental representation indices. This means that each diagram is weighted by the following factor:

$$\left(\frac{\lambda}{N} \right)^E \left(\frac{N}{\lambda} \right)^V N^F = \lambda^{E-V} N^{V+F-E} = \lambda^{E-V} N^\chi \tag{1.2}$$

where $\chi = 2 - 2g$ and g is the number of handles. Diagrams with no handles (planar diagrams) dominate the perturbative expansion.

In closed string theory, diagrams for scattering closed strings can be deformed into genus-g Riemann surfaces [44]. Each loop (handle) of the diagram carries a factor of g_s^2, the string coupling constant, so the diagram is weighted by $g_s^{-\chi}$. We see that string theory and large-N gauge theory have similar topological perturbative expansions if we identify g_s with $1/N$.

---

[2]The reason to hold the combination $g_{\text{YM}}^2 N$ fixed is to maintain a scale: Λ_{QCD}.

1.1.2 Conformal Symmetry and AdS Isometries

Conformal symmetry in d-dimensions is defined by the set of transformations of the coordinates $(x \rightarrow x')$, the conformal transformations, that preserve the metric (g) up to a spacetime dependent scaling:

$$g'(x) = \Omega^2(x)g(x),$$ (1.3)

where $\Omega^2(x)$ is a real function. A "conformal metric" is defined only up to such a (conformal) rescaling – it is represented by an equivalence class.[3] The conformal transformations consists of, in addition to the Poincaré symmetry transformations, the scaling and special conformal transformations. The generators of the set of transformations are isomorphic to the $SO(2,d)$ group generators [49]. In order to define an action of the $SO(2,d)$ group on Minkowski space, we need to "add points at infinity," because the conformal transformations can map points to and from infinity (for a more detailed exposition see [2]). For example, in two-dimensional Euclidean space $\mathbf{R}^2$, we can project the plane onto the sphere and add a point at infinity to get the compact space $\mathbf{S}^2$, the two-sphere. One way to add these points at infinity for d-dimensional Minkowski space is to consider the space defined by the constraint

$$X_0^2 + X_1^2 - X_2^2 - \cdots - X_{d+1}^2 = 0,$$ (1.4)

in $(d+2)$-dimensional flat space with signature $(-,-,+,...,+)$; the ambient metric can be written as $ds^2 = -dX_0^2 - dX_1^2 + dX_2^2 + \cdots + dX_{d+1}^2$. If we consider the restriction $X_0^2 + X_1^2 = \sum_{i=2}^{d+1} X_i^2 = 1$, the ambient metric restricts to the product space $\mathbf{S}^1 \times \mathbf{S}^{d-1}$, with $\mathbf{S}^1$ representing the time component. This resulting space is a conformal compactification M_d of Minkowski space. To get a space with no closed time-like curves we can replace

---

[3]This is important because the boundary metric, extended from the bulk AdS metric, can only be defined up to conformal rescaling. When we study fields in AdS, changing the conformal factor results in identification of conformal scaling dimensions for boundary operators, consistent with a CFT interpretation.

the $\mathbf{S}^1$ factor by $\mathbf{R}^1$, arriving at the Einstein static universe with topology $\mathbf{R}^1 \times \mathbf{S}^{d-1}$. Another straightforward procedure for obtaining M_d is by performing a series of coordinate transformations on the standard Minkowski metric, and after identifying points on the conformal boundary (compactification) we then unwrap the closed time-like curve to obtain a conformal rescaling of the Einstein static universe metric, once again with topology $\mathbf{R}^1 \times \mathbf{S}^{d-1}$ [41]. We will see that M_d is the boundary of Anti-de Sitter space in $(d+1)$ dimensions.

Anti-de Sitter space in $(d+1)$ dimensions, AdS_{d+1}, can be defined as the hyperboloid in $(d+2)$-dimensional flat space [50]:

$$X_0^2 + X_1^2 - X_2^2 - \cdots - X_{d+1}^2 = R^2. \tag{1.5}$$

with a flat space metric with signature $(-,-,+,....,+)$. The parameter R is called the radius of AdS_{d+1}. This space has a manifest $\mathrm{SO}(2,d)$ isometry. If we send the coordinates to infinity while maintaining the hyperboloid relation, say αX_i goes to infinity by taking $\alpha \to \infty$, we can divide by α^2 to obtain Eq. (1.4), which amounts to setting $R = 0$ on the right-hand side of Eq. (1.5). This means that M_d is the boundary of AdS_{d+1}. Similarly to M_d in the previous paragraph, one can also perform coordinate transformations on AdS_{d+1}, followed by compactification, conformal rescaling and unwrapping of the closed time-like curve, to see that the boundary of AdS is a conformal rescaling of the Einstein static universe metric, with topology $\mathbf{R}^1 \times \mathbf{S}^{d-1}$, or M_d [41]. The key point is that the group of isometries of AdS space and the conformal symmetry group of the lower-dimensional boundary theory are the same group, $\mathrm{SO}(2,d)$.

One particularly convenient coordinatization of AdS space is given by Poincaré coordinates. One convenience is that in Poincaré coordinates the boundary of AdS space is a

conformal rescaling of the flat-space Minkowski metric:

$$ds^2 = \frac{R^2}{z^2} \left(dt^2 - d\vec{x}^2 - dz^2 \right), \quad 0 < z. \tag{1.6}$$

where $z \to 0$ is the boundary, $z \to \infty$ is the horizon, and here we have used the mostly-minus convention for the signature of the metric. It is clear that this metric preserves the isometries of Minkowski space. It also has a rescaling symmetry $(t, \vec{x}, z) \to (\alpha t, \alpha \vec{x}, \alpha z)$ for positive real α, which identifies the z-coordinate with (one over) the energy scale of the boundary theory. To see this we scale the z-coordinate of a localized object in the bulk to be closer to the boundary, i.e. $\alpha < 1$. As we can see from the metric (1.6), the scaling has the effect of scaling the boundary coordinates by $1/\alpha$, a large factor. This means that measuring distances in terms of the new coordinates $(\tilde{x}^\mu = \alpha x^\mu)$ the corresponding boundary object is in a much smaller region, or at higher energy. The resulting intuition is that $1/z \sim E$, where E is the energy scale of the boundary theory [51][4]. For this reason, the boundary is referred to as the UV-brane, whereas surfaces closer to the horizon are referred to as IR-branes. The form of the metric in Eq. (1.6) will be used throughout Chapters 2 and 3 with the following modification: we will terminate the geometry in the IR $(z \leq z_{\rm m})$ modelling confinement. In Chapter 4 we will study a black hole background asymptotic to the metric (1.6) in the UV.

We can add more symmetry (supersymmetry) to AdS. In this case we start matching and comparing aspects of the superconformal theory on the boundary and the supersymmetric gravitational theory in the bulk. The benefit of having so much symmetry is that aspects of the duality can be checked on both weak- and strong-coupling sides. In some cases, for example, correlators in the $\mathcal{N} = 4$ SYM match precisely with calculations in the

---

[4]In addition, this reference has a wonderful discussion of counting degrees of freedom in AdS space, which is important for a holographic interpretation.

dual string theory. We will not pursue a discussion of such matching here, and suggest following Refs. [40. 41]. However, we would like to note that there is ample supporting evidence for the correspondence with no known failures [44, 45]. Some have ventured to write the equation "AdS = CFT" ([52], for instance).

1.1.3 Low-Energy Descriptions of N D3-branes

Further motivation for the particular identification of type IIB string theory and $\mathcal{N} = 4$ SYM comes from considering two descriptions of a stack of N D3-branes. A D3-brane is a three (spatial) plus one (time) dimensional surface where open strings end. We can consider a number of such parallel surfaces where the endpoints of strings end on different surfaces, different D3-branes. As we take the position of these different branes to overlap, and yet still be distinguishable, the low-energy description contains four-dimensional (the four dimensions of the brane) massless vector particles transforming in the adjoint of the U(N) gauge group [44, 45]. The low-energy description of a stack of D3-branes is four-dimensional U(N) gauge theory. The U(1) factor of U(N) is related to the position of the collection of branes and is part of the low-energy degrees of freedom in which we are not particularly interested. As such, we are left with SU(N) gauge theory where upon including supersymmetry, we arrive at $\mathcal{N} = 4$, SU(N) gauge theory. Since closed strings are always present, and they happen to decouple from the branes in the low-energy limit [41], we have two decoupled sectors: the SU(N) gauge theory in four-dimensional Minkowski space and free closed string theory in 10-dimensional Minkowski space. The regime where the D-brane description is valid is $g_s N \ll 1$. Since the string coupling goes like the Yang-Mills coupling squared, this relation is equivalent to having small 't Hooft coupling, $\lambda \ll 1$ [44, 45].

Another description of the stack of branes is from the study of the resulting low-energy

effective type IIB supergravity. From the perspective of an observer far away from the branes, the low-energy fluctuations decouple into those far from the branes and those near the branes. Fluctuations far from the branes are described by free type IIB supergravity propagating in 10-dimensional Minkowski spacetime, whereas those close to the brane are described by type IIB supergravity in $AdS_5 \times S^5$. The claim is since these two ways of describing the low-energy physics of the same object both contain low-energy, free type IIB string theory in 10-dimensional Minkowski space, the other decoupled sectors should be equivalent. That is, more precisely, $\mathcal{N} = 4$ SYM is equivalent (dual) to IIB supergravity in $AdS_5 \times S^5$. The regime where the supergravity description is valid is $1 \ll g_sN$, or $1 \ll \lambda$.

Both of these descriptions are at fixed large-N, which means this is a strong-weak coupling duality. There is an important point here: these are two low-energy description which are valid in different regimes – large and small 't Hooft coupling. The idea is that the low-energy descriptions decouple for any g_sN, as we dial g_s from zero to strong coupling [45]. As such, the theories should really be equivalent.

1.2   The AdS/CFT Correspondence

The ideas of a duality were becoming clear, and in the late 90's there were a series of papers dedicated to making a concrete recipe for carrying out calculations [1, 2, 3, 53]. As we have seen, statement of the duality is one of a correspondence between a supergravity theory in $(d+1)$-dimensions and a conformal field theory in d-dimensions. The most well studied version is type IIB string theory on $AdS_5 \times S^5$ dual to large-N, SU(N), $\mathcal{N} = 4$ SYM in four dimensions. The gravitational theory is said to live in the bulk and the CFT on the boundary of the bulk spacetime. The dictionary defining the correspondence identifies to each higher-dimensional bulk field a lower-dimensional boundary source and operator.

Computationally the correspondence is written as

$$Z_{\text{CFT}}[\phi_0(x)] = e^{-S_{\text{SG}}[\phi_0]|_{\phi_{\text{cl}}}},$$ (1.7)

where on the left-hand side we have the generating functional for correlators of the operator $\mathcal{O}$, with source ϕ_0, and on the right we have the supergravity action S_{SG} evaluated on the classical solution to the $(d+1)$-dimensional equations of motion, ϕ_{cl}. We can rewrite the partition function as

$$Z_{\text{CFT}}[\phi_0(x)] = \langle e^{\int d^d x\, \phi_0 \mathcal{O}} \rangle_{\text{CFT}_d},$$ (1.8)

where, to emphasize this point, the source ϕ_0 and operator $\mathcal{O}$ arise from identification with the higher-dimensional field, and $\langle \cdots \rangle_{\text{CFT}_d}$ is the vacuum expectation value in the d-dimensional CFT. We can then calculate operator expectation values by taking functional derivatives with respect to the source.

To demonstrate concretely the recipe for performing holographic calculations, let us consider a scalar in AdS_{d+1}. We will follow Ref. [2], which appears to be the simplest and cleanest presentation of the type of calculations involved in the correspondence. We work in the Euclidean version of the correspondence where the AdS_{d+1} metric, written in Poincaré coordinates is

$$ds^2 = \frac{R^2}{z^2}(\eta_{\mu\nu} dx^\mu dx^\nu + dz^2).$$ (1.9)

where R is the curvature of AdS space and $\eta_{\mu\nu}$ is the flat Euclidean metric $(\delta_{\mu\nu})$. A salient point is we usually set a cutoff ϵ on the geometry, such that $z \geq \epsilon$, and assume to take the limit $\epsilon \to 0$ at the end of any calculation. We will be working in units of the AdS curvature and so we set $R = 1$. The action for a free complex scalar on AdS_{d+1} is

$$\mathcal{S} = \int d^d x\, dz\, \sqrt{g}\, \frac{1}{2}(|\partial_M \phi|^2 + m^2 |\phi|^2),$$ (1.10)

where the capital Latin indices range over all $(d+1)$ dimensions, whereas the lower-case Greek indices are reserved for the d-dimensional (boundary) coordinates. The equation of motion is

$$\frac{1}{\sqrt{g}}\partial_z\left(\sqrt{g}\,g^{zz}\partial_z\phi\right) + g^{\mu\nu}\partial_\mu\partial_\nu\phi - m^2\phi = 0. \tag{1.11}$$

Using the explicit form of the metric, the asymptotic solution for ϕ near $z = 0$ can be written:

$$\phi(x, z) \sim \phi_1(x)z^{\Delta_-} + \phi_2(x)z^{\Delta_+} + \cdots, \tag{1.12}$$

where $\Delta_\pm = d/2 \pm \sqrt{d^2/4 + m^2}$ and the dots represent higher powers in z. We will also define $\Delta \equiv \Delta_+$, to be used throughout, which implies $\Delta_- = d - \Delta$. So for instance, in five dimensions $(d = 4)$, if we choose $m^2 = -3$ we have $\phi(x, z) \sim \phi_1(x)z + \phi_2(x)z^3 + \cdots$, which is the particular case considered in Chapters 2 and 3. As we will see, this expansion in terms of $\phi_1(x)$ and $\phi_2(x)$ lends to the identification of ϕ_1 a source for the operator ϕ_2. We should note that upon integration by parts, the ϕ_1 term present in the $z = 0$ boundary term gives rise to an infinity. The ϕ_2 term, on the other hand, vanishes. For this reason, the ϕ_1 part of the asymptotic expansion is called the non-normalizable solution, while the ϕ_2 part is call the normalizable solution.

Before moving on to solving the equations of motion, we should discuss another important point. We chose a negative mass squared in the above example, but there is no stability problem as one would normally guess. Breitenlohner and Freedman [54] derived the following bound on the mass squared for a field in AdS$_{d+1}$: $m^2 \geq -d^2/4$. This means for the particular case considered in Chapters 2 and 3 with AdS$_5$, with a scalar of mass $m^2 = -3 > -4$, that there is no stability issue. We should also mention that there are subtleties for masses in the range $-d^2/4 < m^2 < -d^2/4 + 1$. It turns out, for masses in this range we can choose either the z^{Δ_+} or z^{Δ_-} part in the asymptotic expansion to be the operator and the remaining part the source [55]. Such a situation occurs for the model in

Chapter 4, with $d = 3$ and $m^2 = -2$, where we have $-9/4 < -2 < -9/4 + 1$. We will not pursue this discussion in detail further.

We will now go about solving the equation of motion Eq. (1.11). We will assume that the field $\phi(x, z)$ takes the value $\phi(x, \epsilon) \sim \epsilon^{\Delta^-} \phi_0(x)$. The idea is now to solve the for the Green's function $K_\Delta(x, x'; z)$, where $K_\Delta(x, x'; z)$ vanishes everywhere on the boundary except at one point[5], and satisfies

$$\phi(x, z) = \int d^d x' K_\Delta(x - x'; z) \phi_0(x').$$ (1.13)

This Green's function, called the bulk-to-boundary propagator, is proportional to the restriction of the bulk-to-bulk propagator $G_\Delta(x, z; x', z')$ to the boundary $z' \to 0$. The function G_Δ is a solution to the Laplace equation of motion with a delta function on the right-hand side. It turns out that the expression for the bulk-to-boundary propagator takes the form

$$K_\Delta(x - x'; z) = \pi^{-d/2} \frac{\Gamma(\Delta)}{\Gamma(\Delta - d/2)} \frac{z^\Delta}{(z^2 + |x - x'|^2)^\Delta}.$$ (1.14)

From this expression it is clear that

$$\phi_2(x) = \pi^{-d/2} \frac{\Gamma(\Delta)}{\Gamma(\Delta - d/2)} \int d^d x' \frac{\phi_0(x')}{|x - x'|^{2\Delta}}.$$ (1.15)

The strategy is to now evaluate the action on the equations of motion. In position space this is a bit tricky, though, due to divergences at small z, which don't appear when $m = 0$ [56]. One way of circumventing this issue is to define the field $\chi(x, z) = z^{-(d-\Delta)}\phi(x, z)$ [55]. The action written in terms of $\chi(x, z)$ no longer has a mass term. If we integrate the action by

---

[5]In other words, $\lim_{z \to 0} z^{\Delta - d} K_\Delta(x - x'; z) \to \delta^{(d)}(x - x')$.

parts and evaluate using the classical equation of motion we get

$$\mathcal{S}_{\mathrm{cl}} = \int d^d x \frac{1}{2} \left[\sqrt{g} \, g^{zz} z^{2(d-\Delta)} \chi(x, z) \partial_z \chi(x, z) \right] \Big|_{\epsilon}^{\infty} . \tag{1.16}$$

Assuming the fields vanish at infinity, we can focus on the ϵ boundary terms. The metric factors, combined with the additional z factor contribute $z^{d+1-2\Delta}$, and the χ term contributes terms that go like 1 and $z^{2\Delta-d}$, plus z^2 corrections, as can be seen from the asymptotic expansion. Looking at the various terms from using the expansion for χ, the non-divergent, nonvanishing contribution is from $\chi \rightarrow \phi_0(x)$ and $\partial_z \chi \rightarrow (2\Delta - d) z^{2\Delta - d - 1} \phi_2(x)$ [55]. Making this replacement, and using the explicit form for the function $\phi_2(x)$, we are left with

$$\mathcal{S}_{\mathrm{cl}} = -\int d^d x \int d^d x' (\Delta - d/2) \phi_0(x) \left[\pi^{-d/2} \frac{\Gamma(\Delta)}{\Gamma(\Delta - d/2)} \frac{\phi_0(x')}{|x - x'|^{2\Delta}} \right]. \tag{1.17}$$

We can identify the operator expectation value $\langle \mathcal{O}(x) \rangle_{\phi_0} = (2\Delta - d) \phi_2(x)$, which is be obtained from variation of the above action:

$$\langle \mathcal{O}(x) \rangle_{\phi_0} = (2\Delta - d) \phi_2(x) = \frac{\delta \mathcal{S}_{\mathrm{cl}}[\phi_0]}{\delta \phi_0(x)}. \tag{1.18}$$

Higher point functions are computed by taking more functional derivatives with respect to the source. We can determine, by inspection of Eq. (1.17), the expression of the two-point function and see that it has the correct form for an operator with conformal dimension Δ [49]. An n-point function has n fields connecting from the boundary to the bulk – "n operator insertions on the boundary".

So far we have only considered scalar fields propagating in AdS space, but this analysis can be carried out for other fields as well. A particularly important example for the remaining chapters is that of a gauge field A_M^a with gauge group G on AdS. Matching

symmetries, the group G should be a symmetry of the boundary theory as well. The AdS gauge field has a similar asymptotic expansion to the scalar field with zero mass: $A^a(x, z) \sim A_0^a(x) + J^a(x)z^d + \cdots$, where the '0' index of the source function $A_0^a(x)$ is not the Lorentz time component. Likewise, the ansatz for the generating functional is $\exp(\int_{M_d} J_\mu^a A^{a\mu})$. Carrying out a calculation similar to that for the scalar, the resulting two-point function has the form expected for a two-point function of conserved currents. The gauge field is dual to a conserved boundary current, J_μ^a, of a global symmetry group G [1, 2]. If we are interested in studying (holographically) a theory with a specific global symmetry we need the corresponding AdS gauge fields.

A natural way to attempt to extend the correspondence is to say that it is a correspondence between a bulk space $X \times W$ and a boundary space M, where X (a generalization of AdS_{d+1}) is a $(d+1)$-dimensional space with negative cosmological constant, and W (a generalization of the sphere in the product space) is a compact space. More precisely, a conformal compactification of X has the conformally compactified space M as its boundary, $\partial X = M$, in analogy to AdS_{d+1} and M_d. For example, we can try to find an X such that the boundary $\partial X = S^1 \times S^{d-1}$, where the first factor (periodic in time) indicates the theory is at finite temperature. There are two bulk solutions for X: one is an AdS-Schwarzschild black hole at high temperature, where the boundary theory is found to be in a deconfined phase, and the other AdS space at low temperature, where the boundary theory is in a confined phase [2, 57]. It is in this way that considering black hole geometries in the bulk is equivalent to turning on temperature in the boundary theory. The Hawking temperature of the black hole is identified with the temperature of the boundary theory. The physical intuition is that as the bulk horizon approaches the boundary, corresponding to a hotter black hole, the Hawking radiation is "heating up" the boundary.

1.2.1 Lorentz signature

There are significant differences when constructing the correspondence in AdS_5 with Lorentz signature. The main difference is that there are normalizable solutions to the wave equation, behaving as z^{Δ_+}, that must be taken into account [53]. This means the solution for $\phi(x, z)$ looks like

$$\phi(x, z) = \phi_{nn}(x, z) + \phi_n(x, z), \tag{1.19}$$

where ϕ_{nn} is the non-normalizable solution we discussed in the previous section, which asymptotes to z^{Δ_-} times the source function, and ϕ_n is a normalizable solution, which goes like z^{Δ_+} times a function of x near the boundary. We will look at the same scalar field but set $m = 0$, for simplicity, which gives $\Delta_- = 0$ and $\Delta_+ = d$, so we expect $\phi(x, 0) = \phi_0(x)$. This implies, choosing to switch to Fourier space, that

$$\phi(x, z) = \int \frac{d^d k}{(2\pi)^4} e^{ikx} f_\Delta(k, z) \phi_0(k), \tag{1.20}$$

where $f_\Delta(k, z)$ is the Fourier transform of the bulk-to-boundary propagator, satisfying $f_\Delta(k, 0) = 1$, and $\phi_0(k)$ is the Fourier transform of the boundary source function. The function $f_\Delta(k, z)$ satisfies the wave equation

$$\frac{1}{\sqrt{-g}} \partial_z \left[\sqrt{-g} \, g^{zz} \partial_z f_\Delta(k, z) \right] - g^{\mu\nu} k_\mu k_\nu f_\Delta(k, z) = 0. \tag{1.21}$$

Plugging in the explicit form for the metric this expression becomes

$$z^3 \partial_z \left[\frac{1}{z^3} \partial_z f_\Delta(k, z) \right] - k^2 f_\Delta(k, z) = 0. \tag{1.22}$$

The solution to this equation, imposing the $z = 0$ boundary condition, can be written as a linear combination of Hankel functions, of the first $(H_{d/2}^{(1)})$ and second $(H_{d/2}^{(2)})$ kind:

$$f_\Delta(k, z) = \epsilon^{\Delta-} \left(\frac{z}{\epsilon}\right)^{d/2} \cdot \frac{H_{d/2}^{(1)}(\sqrt{k^2}z) + C(k)H_{d/2}^{(2)}(\sqrt{k^2}z)}{H_{d/2}^{(1)}(\sqrt{k^2}\epsilon) + C(k)H_{d/2}^{(2)}(\sqrt{k^2}\epsilon)}. \tag{1.23}$$

where $C(k)$ is an arbitrary coefficient. This arbitrariness is another key distinction between the Lorentz and Euclidean correspondence, due to the presence of the normalizable solution. Written in terms of Hankel functions, the small z field asymptotics are not nicely separated, but for large z we find $H_{d/2}^{(1)} \sim e^{ikz}$ and $H_{d/2}^{(2)} \sim e^{-ikz}$. These asymptotic forms of the Hankel functions correspond to incoming-wave (e^{ikz}) and outgoing-wave (e^{-ikz}) contributions, at positive frequency. The terminology, incoming-wave and outgoing-wave, is with respect to an observer at infinity, or when we are dealing with a black hole geometry, with respect to the interior of the black hole. The choice of $z \to \infty$ boundary condition is thought to reflect the choice in type of Green's function: the physical intuition is that incoming-wave boundary conditions correspond to retarded Green's function, whereas outgoing-wave boundary conditions correspond to advanced Green's functions. In other words, for calculating retarded Green's functions nothing is propagating in from infinity (or coming out of the black hole).

Using the expression for the bulk-to-boundary propagator, we can add in the normalizable mode, represented by $\Phi(k)\phi_+(k, z)$:

$$\phi(k, z) = \Phi(k)\phi_+(k, z) + \phi_0(k)f_\Delta(k, z), \tag{1.24}$$

where $\phi_+(k, z)$ goes like $z^\Delta = z^d$ near the boundary. We can integrate the action by parts

and plug this solution into the remaining boundary terms:

$$
S_{cl} = -\frac{1}{2} \int d^d k z^{1-d} \left[\Phi(-k)\phi_+(k,z) + \phi_0(-k)f_\Delta(-k,z) \right]
$$
$$
\times \left. \partial_z \left[\Phi(k)\phi_+(k,z) + \phi_0(k)f_\Delta(k,z) \right] \right|_{z=\epsilon}^{z=\infty} .
$$

(1.25)

The surviving contributions are:

$$
S_{cl} = \int d^d k \left[\frac{d}{2}\Phi(-k)\phi_0(k) + \frac{1}{2}\phi_0(-k)\epsilon^\Delta \partial_z f_\Delta(k,z)\phi_0(k) \right]_{z=\epsilon}
$$
$$
- \int d^d k z^{1-d} \left[\frac{1}{2}\phi_0(-k)f_\Delta(-k,z)\partial_z f_\Delta(k,z)\phi_0(k) \right]_{z=\infty} .
$$

(1.26)

These terms require some discussion. The $z = \epsilon$ boundary term is meant to give the expectation value of a boundary operator when varied with respect to the source:

$$
\langle \mathcal{O} \rangle_{\phi_0} = \frac{d}{2}\Phi(-k) + \phi_0(-k)\epsilon^\Delta \partial_z f_\Delta(k,z)|_{z\to\epsilon}.
$$

(1.27)

The first term on the right-hand side is the contribution to the expectation value from the normalizable mode (in the absence of the source), whereas the second term is the familiar one we've already seen, the contribution to the expectation in the presence of the source – that is, "$(2\Delta - d)\phi_2(x)$".

The $z = \infty$ boundary term vanishes in the Euclidean case and for spacelike momenta. With Lorentz signature and timelike momenta, we can appeal to the solutions above. For large z the Hankel function have the asymptotic form:

$$
H^{(1),(2)}(kz) \sim (kz)^{-1/2}e^{\pm ikz}.
$$

(1.28)

Counting factors of z, and keeping track of factors of k from the normalization, the sur-

viving parts come from the derivative acting on the exponential giving

$$\int_{z=\infty} [\cdots] \propto \int_{z=\infty} d^d k \phi_0(-k)\phi_0(k) k^{2\Delta - d - 1}$$

$$\times \left(C^*(-k)e^{ikz} + e^{-ikz}\right) ik \left(e^{ikz} - C(k)e^{-ikz}\right).$$

(1.29)

So there is an oscillatory piece at infinity (see also [53, 58]), which if the ingoing- or outgoing-wave conditions are maintained, yields a purely imaginary, nonvanishing contribution to the action $\sim ik^{2\Delta - d}\mathrm{sgn}(\omega)$.

At this point it makes sense to define the "flux function" [3]:

$$\mathcal{F}(k, z) = f_\Delta(-k, z)\partial_z f_\Delta(k, z).$$

(1.30)

The Green's function calculated from the $\mathcal{S}_{\mathrm{cl}}$ is

$$G(k) = \frac{\delta^2 \mathcal{S}_{\mathrm{cl}}}{\delta\phi_0(-k)\delta\phi_0(k)} = -\mathcal{F}(k, z)\Big|_{z=\epsilon}^{z=\infty} - \mathcal{F}(-k, z)\Big|_{z=\epsilon}^{z=\infty}.$$

(1.31)

It turns out that the Green's function calculated from the action is real [58]; that is, there is no imaginary part. A retarded Green's function, though, is in general complex. Even if we only keep the $z = \epsilon$ boundary terms, the Green's function is still real. In fact, using $\mathcal{F}^*(k, z) = \mathcal{F}(-k, z)$, we would have $G(k) = -2\mathrm{Re}[\mathcal{F}(k, \epsilon)]$. The conjecture for computing retarded (advanced) Green's functions is to assign ingoing-wave (outgoing-wave) boundary conditions to the bulk-to-boundary propagator and calculate the Green's function as [58]:

$$G(k) = -2\mathcal{F}(k, \epsilon),$$

(1.32)

essentially claiming that $\mathcal{F}(k, \epsilon)$ is the object that we're interested in, even though procedurally we would be instructed to calculate only the real part.

A convenient way to discuss these Green's functions is in terms of a ratio of the coefficients in $\mathcal{F}(k, \epsilon)$. We have the near boundary, small z, behavior of the bulk-to-boundary propagator:

$$f_\Delta(k, z) \sim \frac{A(k)z^{d-\Delta} + \cdots + B(k)z^\Delta + \cdots}{A(k)\epsilon^{d-\Delta} + \cdots + B(k)\epsilon^\Delta + \cdots}. \tag{1.33}$$

When calculating the Green's function we have the leading, non-analytic (in k) behavior:

$$G(k) \sim \partial_z f_\Delta(k, z)|_\epsilon \sim \epsilon^{2\Delta - d - 1} \frac{B(k)}{A(k)} + \cdots . \tag{1.34}$$

Schematically, this comes from the crossterms of the numerator and denominator. The punchline is that black hole quasinormal modes satisfy ingoing-wave boundary conditions near the horizon, and $A(k) = 0$ near the boundary. So the black hole quasinormal modes correspond precisely to the poles of the Green's function [58].

As discussed before, we can turn on temperature by considering a black hole geometry. For a concrete example we take a metric of the following form:

$$ds^2 = \frac{1}{z^2} \left(-f(z)dt^2 + \eta_{\mu\nu}dx^\mu dx^\nu + \frac{1}{f(z)}dz^2 \right), \tag{1.35}$$

where $f(z)$, not to be confused with the bulk-to-boundary propagator, has a first order zero at a special location $z = z_{\rm H}$, defining the horizon. Later we will take the function $f(z) = 1 - (z^3/z_{\rm H}^3)$; that is, the background solution for an AdS_4-Schwarzschild black hole. The near-horizon field asymptotics can be described as ingoing- or outgoing-waves (like the zero temperature case) in terms of the horizon function:

$$f_\Delta(k, z) \sim f(z)^{\pm i\omega F(z_{\rm H})}, \tag{1.36}$$

where $F(z_{\rm H})$ is some function. We now have the ingredients to calculate real-time correlation functions at finite temperature in a strongly-coupled field theory.

In order to add superconductivity, we would need to identify an order parameter for a phase transition corresponding to the breaking of a U(1) symmetry. This additional parameter would violate what are known as black hole "no-hair" theorems (or more appropriately, conjectures). These "no-hair" theorems are a general set of arguments stating that stable black hole solutions are only described by a select set of quantum numbers (position, angular momentum, charge, and mass) with no other free parameters ([59], for a review). The models of Refs. [60, 14] circumvent the black hole "no-hair" theorems. In these models, for cold enough black holes, scalar fields condense near the black hole horizon and the new free parameter is the order parameter of the phase transition. In Ref. [14], the theory is a four-dimensional Abelian Higgs model coupled to gravity with a negative cosmological constant. The scalar condensation spontaneously breaks the gauge invariance, suggestive of superconductivity. Since the spacetime is asymptotically AdS_4, this result has a direct holographic interpretation in terms of AdS/CFT: the condensed scalar is dual to a nonzero scalar operator expectation value. The Lagrangian of Ref. [14] is

$$16\pi G_{\rm N}\mathcal{L} = R - \frac{6}{L^2} - \frac{1}{4}F_{\mu\nu}^2 - |\partial_\mu\psi - iqA_\mu\psi|^2 - m^2|\psi|^2, \qquad (1.37)$$

where the first two terms on the right-hand side are the gravity Lagrangian, and the last terms are the matter Lagrangian. It was found that for a large enough charge q and a cold enough black hole, there is an instability to scalar hair condensation. The argument goes as follows (see Ref. [14] for the subtleties involved). If we consider the static part of the Lagrangian with only A_0 and ψ nonzero, the scalar field has an effective mass (assuming

for the moment that we can use the metric (1.35) and scale out the charge):

$$m_{\text{eff.}}^2 = m^2 - \frac{z^2}{f(z)}(A_0)^2.$$ (1.38)

If the last term in the expression for m_{eff}^2 becomes big enough, which will occur near the horizon for nonzero A_0, then the indication is that the scalar field ψ condenses. If we rescale the fields by q and take the limit $q \to \infty$ (the "probe limit"), then the gravitational part of the action decouples from the matter action. This allows us to study the matter Lagrangian in the background (1.35), and justifies our assumptions leading to m_{eff}^2. The above model in the probe limit, and its dimensional deconstruction, will be the topic of Chapter 4.

We are now in a position to study the application of the AdS/CFT dictionary to a variety of physical models. In Chapter 2, we study a model with a minimal set of fields on a slice of AdS_5 space. The model will have an $SU(2)_L \times SU(2)_R$ gauge invariance with a field transforming as a bifundamental, corresponding to the operator $q_L \bar{q}_R$. This is a minimal holographic model of two-flavor QCD with the pattern of chiral symmetry breaking built in, yet we will discover some behavior inconsistent with well known models (Effective Field Theory, Lattice QCD, etc.), leading to an improved holographic calculation discussed in the sequel. In Chapter 3, we will continue studying the model from Chapter 2, and will find that nonlinear boundary conditions on the fields are required to maintain the pattern of chiral symmetry breaking beyond quadratic order in the field fluctuations -- this is important when considering phase transitions, for instance. In Chapter 4, we move on to possible condensed matter applications of AdS/CFT, where we review a holographic s-wave superconductor. The theory has a charged $U(1)$ scalar field in a four-dimensional AdS-Schwarzschild background spacetime; the boundary theory then has spacetime dimension three. As already discussed, this type of black hole background has an instability

to the development of scalar hair, at low enough temperature, signalling a possible superconducting phase transition. We will see how the application of an idea referred to as "deconstruction of extra dimensions" gives us a three-dimensional field theory which mimics, with the addition of a somewhat *ad hoc* boundary contribution, the physics of the holographic theory.

CHAPTER 2

Holographic Pions

In this chapter, we will study a holographic model of hadrons with a chemical potential turned on for isospin, μ_I. Our focus will be to look at the pion condensation phase transition (at zero temperature) that results, as a function of μ_I. Following the natural development of the model, we will discover that the transition from the hadronic phase to the pion condensate phase is first order except in a certain limit of model parameters. This analysis suggests that immediately across the phase boundary the condensate acts as a stiff medium approaching the Zel'dovich limit of equal energy density and pressure. Interestingly these results, which should follow almost entirely from symmetry considerations, disagree with results from other models, suggesting possible improvements to the holographic model. Such improvements will be considered in Chapter 3.

2.1 Holography and Isospin Chemical Potential

Dense nuclear matter generically carries net isospin and consequently has a nonvanishing isospin chemical potential, μ_I. The Relativistic Heavy Ion Collider (RHIC) and the Large Hadron Collider (LHC) are presently the premier laboratories capable of studying

the quark-gluon plasma phase of nuclear matter. The heavy nuclei in these experiments carry isospin, so the finite temperature system after collision has a nonvanishing isospin chemical potential. Neutron stars have still larger chemical potential, and the behavior of such objects depends on the phase structure of QCD in cold, dense environments [61, 62, 63, 64]. At large chemical potential it is expected that mesons condense, beginning with the pions at $\mu_I \sim m_\pi$ [65, 66, 67]. The phase diagram of QCD at high density has been explored via the chiral Lagrangian [68, 69], the Nambu-Jona-Lasinio model [70, 71, 72], and lattice QCD [73, 74, 75, 76]. The general consensus is that at low temperatures and vanishing baryon chemical potential there is a second order transition from the hadronic phase to a pion condensate phase at a critical isospin chemical potential μ_I around the pion mass $m_\pi \approx 140$ MeV, or larger at finite temperature.

We will study the behavior of matter with isospin chemical potential in a holographic model of hadrons [11, 12]. Related analyses in other holographic systems appear elsewhere (e.g. Refs. [79, 80, 81, 82]). Both explicit and spontaneous chiral symmetry breaking may be built into this extra-dimensional models, resulting in an effective description similar to extended hidden-local-symmetry models [77, 78]. The AdS/CFT correspondence maps sources and expectation values of field theory operators to backgrounds of extra-dimensional fields with corresponding quantum numbers. By studying fluctuations about a prescribed background, the model makes predictions for field theory observables. Motivation to study the hard-wall model of Refs. [11, 12] comes in light of recent suggestions that the pion condensate phase is absent in that model [83]. In contrast, we will discover the pion condensate phase and study its properties.

The hard-wall models [5, 6, 7, 11, 12] are the simplest holographic models which capture certain features of QCD. The hard-wall geometry is a region of 4+1 dimensional[1]

---

[1]The +1 in the spacetime dimensionality, when written explicitly as 4+1 as opposed to 5, always refers to time, not the extra spatial dimension of the holographic model.

(5D) Anti-de Sitter space preserving the isometries of 3+1 dimensional (4D) Minkowski space. The main motivation for this choice of spacetime is its simplicity, although arguments have been made to support the choice of Anti-de Sitter space in light of asymptotic freedom at high energies and evidence for an approximate conformal invariance in QCD at lower energies [84, 85]. The presence of a wall, which terminates the spacetime at what is referred to as the IR boundary, leads to a discrete spectrum of Kaluza-Klein modes identified via their quantum numbers with towers of hadronic resonances.

As discussed in the Introduction, global symmetries are lifted to gauge invariances in the holographic description. In order to include the approximate chiral symmetry of the up and down quarks, $SU(2)_L \times SU(2)_R$ gauge fields are included in the 5D model. To mimic the pattern of chiral symmetry breaking, a set of scalar fields transforming in the bifundamental representation of the chiral symmetry group is introduced. The quantum numbers of the scalar fields are those of the scalar quark bilinear $q_L^i \bar{q}_R^j$, where i and j are flavor indices which are now gauge indices. When we write the operator product $q\bar{q}$ we are implicitly tracing over the Lorentz structure. The scalar fields have a background profile which preserves the 4D Lorentz invariance of the spacetime but breaks the chiral symmetry to the diagonal isospin subgroup. If the non-normalizable mode of the scalar is turned on, then the theory is modified so as to explicitly break the chiral symmetry, as if by a quark mass; if the normalizable mode has a nonvanishing background then there is a spontaneous breaking of the chiral symmetry, as if by a contribution to the chiral condensate $\langle q_L^i \bar{q}_R^j \rangle$.

Next we would like to turn on a chemical potential for $SU(2)_V$, which is the vector subgroup of the chiral symmetry group $SU(2)_L \times SU(2)_R$. The chemical potential for the third component of isospin is a source for the isospin number density

$$N_3 = q_L^{\dagger i} \, T_{ij}^3 \, q_L^j + q_R^{\dagger i} \, T_{ij}^3 \, q_R^j, \tag{2.1}$$

which is the time component of the isospin current

$$J_V^{a,\nu} = \bar{q}^i \gamma^\nu T_{ij}^a q^j.$$ (2.2)

where $T^a = \sigma^a/2$ are the generators of the isospin SU(2). A source (say $v_0 = \mu_1$) for the isospin number density, written explicitly as $\mathcal{L} \supset \mu_1 N_3 = v_0 J^0$, couples to the current like the time component of a background gauge field: schematically, $\mathcal{L} \supset v_\mu J^\mu$. However, we would like to turn on a chemical potential in the boundary theory from the perspective of the bulk 5D model. Recall that the non-normalizable mode of the 5D gauge field acts as a source for the boundary current, represented by the normalizable mode. Hence, a non-normalizable background for the time component of the vector combination of 5D gauge fields should mimic an isospin chemical potential in the 4D effective theory.

In general, as the magnitude of the isospin chemical potential is increased above the pion mass, it becomes energetically favorable for a pion condensate to form. We will find that the phase transition is first order in the hard-wall model unless the 5D gauge coupling vanishes. The speed of sound c_s at high temperatures was conjectured to satisfy a "sound bound" $c_s^2 < 1/3$ [86, 87], where $c_s^2 = 1/3$ is the conformal limit. We will see that fluctuations in the condensate at zero temperature violate the "sound bound," except near the phase boundary and then only if the 5D gauge coupling is small enough. Violation of the sound bound at low temperature is not unusual [87] and has also been observed in certain D-brane systems [82] and in a holographic model describing matter at a Lifshitz point [88].

We will focus on the zero-temperature phase of isospin matter, which corresponds to the original hard-wall background without a black-hole horizon. For simplicity we will not include chemical potentials except for isospin, so the analysis presented here provides only a narrow cross section of the phase structure of the model. Extensions of these results to

nonvanishing temperature and baryon chemical potential, and to include strange quarks and Kaon condensation [89], may shed light on the phases of matter in neutron stars and other extreme environments.

2.2 Holographic Pion Condensation

We begin by defining the 5D theory, where we include a very minimal set of fields and interactions: the bifundamental X dual to $q_L \bar{q}_R$, and the $SU(2)_L \times SU(2)_R$ gauge fields. We will then turn on isospin chemical potential and solve for the linearized bulk pion equations of motion to find the instability to pion condensation. The instability occurs exactly when the pions are expected to condense, when $\mu_I = m_\pi$. Expanding the Lagrangian to quartic order in the pion fluctuations will then allow us to determine the order of the pion condensation phase transition, and calculate the number density and speed of sound.

The action for the 5D hard-wall model with chiral symmetry is given by [11, 12],

$$
\mathcal{S} = \int d^4x \, dz \, \sqrt{g} \, \mathrm{Tr} \left\{ |D_M X|^2 - M_X^2 \, |X|^2 - \frac{1}{4g_5^2} \left(F_L^2 + F_R^2 \right) \right\}, \tag{2.3}
$$

where $D_M X = \partial_M X - i L_M X + i X R_M$, $L_M = L_M^a T^a$ and $F_{MN}^L = \partial_M L_N - \partial_M L_N - i \left[L_M, L_N \right]$ (similarly for R), and we normalize the gauge kinetic term as in [11]. The mass for the field X is set to $M_X^2 = -3$, which is appropriate for the mass dimension of the operator $q_L \bar{q}_R$. As explained in the Introduction, the mass dimension for the operator dual to X is $\Delta_+ = \frac{4}{2} + \sqrt{4 + M_X^2} = 3$, which is consistent with $[q_L \bar{q}_R] = \frac{3}{2} + \frac{3}{2} = 3$, for fermions in four dimensions. The scalar fields X transform in the bifundamental representation of the $SU(2)_L \times SU(2)_R$ gauge invariance; that is, $X(x, z) \rightarrow U_L(x, z) X(x, z) U_R^\dagger(x, z)$, where $U_{L,R}(x, z)$ is an element of the $SU(2)_{L,R}$ gauge group. The spacetime in the hard-wall

model is a slice of AdS_5:

$$ds^2 = a(z)^2 \left(\eta_{\mu\nu} dx^\mu dx^\nu - dz^2 \right), \qquad \epsilon \leq z \leq z_m,$$

where $a(z) = 1/z$ in units of the AdS curvature scale, and $\eta_{\mu\nu}$ is the 4D Minkowski metric with mostly negative signature. Greek indices range from 0 to 3, and capital Latin indices from 0 to 4, with x^4 also denoted by z. This metric is the Poincaré patch Eq. (1.6) with an IR cutoff ($z = z_m$) to model confinement.

Chiral symmetry breaking is provided by the background solution, uniform in x^μ, to the X field equation of motion,

$$X_0(z) = \frac{1}{2} \left(m_q z + \sigma z^3 \right) \equiv \frac{1}{2} v,$$ (2.4)

where m_q is the quark mass matrix responsible for sourcing $\sigma = \langle \bar{q}q \rangle$, the chiral condensate. The bulk vector gauge field $V_M^a(x,z) = \frac{1}{2}[L_M^a(x,z) + R_M^a(x,z)]$ is dual to the boundary isospin vector current operator $J_V^{a\mu}(x)$. Working in the gauge $L_z^a = R_z^a = 0$, the linearized equations of motion for the transverse part of V_μ^a are

$$\partial_z \left(\frac{1}{z} \partial_z V_\mu^a \right) - \frac{1}{z} \partial_\alpha \partial^\alpha V_\mu^a = 0.$$ (2.5)

The background solutions, uniform in x^μ, for V_0^3 are of the form

$$V_0^3(z) = c_1 + \frac{c_2}{2} z^2.$$ (2.6)

where the coefficient of the non-normalizable mode, c_1, is identified with the chemical potential for the third component of isospin μ_I; and c_2 is proportional to the spontaneously generated background isospin number density, which we assume to vanish. Hence, the

background gauge field is constant,

$$V_0^{3} = \mu_{\mathrm{I}}. \tag{2.7}$$

In order to more easily identify the instability to pion condensation we will focus only on the pion fluctuations coupled to the background gauge field (2.7). This means we will be ignoring the vector gauge field fluctuations and the transverse axial gauge field fluctuations. The pions are identified with solutions to the linearized coupled equations of motion for the Goldstone modes in the scalar fields X, which mix with the longitudinal part of the axial vector field $A_\mu^a = (L_\mu^a - R_\mu^a)/2 \equiv \partial_\mu \phi^a$. We parametrize the Goldstone modes by fields π^a such that,

$$\begin{aligned} X &= X_0 \exp\left[i2\pi^a T^a\right] \\ &= X_0 \left(\cos b + i\,(n^a \sigma^a) \sin b\right), \end{aligned} \tag{2.8}$$

where $b = \sqrt{\pi^c \pi^c}$ and $n^c = b^{-1}\pi^c$. Plugging this parametrization into the action (2.3), we have the pion part of the action:

$$\begin{aligned} \mathcal{S}_\pi = \int d^4x\,dz\,\sqrt{-g} \Bigg\{ & 2X_0^2 \bigg(\partial_M(\cos b)\,\partial^M(\cos b) + \partial_M(n^a \sin b)\,\partial^M(n^a \sin b) \\ & - \frac{2\mu_{\mathrm{I}}}{a^2} \partial_0(n^c \sin b)\epsilon^{a3c} n^a \sin b - \frac{2}{a^2}\partial_\mu(n^a \sin b)\cos b\,\partial^\mu \phi^a \\ & + \frac{2}{a^2}\partial_\mu(\cos b)\,n^a \sin b\,\partial^\mu \phi^a + \frac{2\mu_{\mathrm{I}}}{a^2}\cos b\,\epsilon^{a3c} n^a \sin b\,\partial_0\phi^c \\ & + \frac{\mu_{\mathrm{I}}^2}{a^2}\sin^2 b\,n^c n^d \epsilon^{c3c}\epsilon^{d3c} + \frac{1}{a^2}\cos^2 b\,\partial_\mu\phi^a \partial^\mu\phi^a + \frac{1}{a^2}\sin^2 b\,n^a \partial_\mu\phi^a n^c \partial^\mu \phi^c \bigg) \\ & - \frac{1}{2a^4 g_5^2}\left(\mu_{\mathrm{I}}^2\left(\partial_i\phi^1 \partial^i\phi^1 + \partial_i\phi^2 \partial^i\phi^2\right) - \partial_z\partial_\mu\phi^a \partial_z\partial^\mu\phi^a + \mathcal{O}\left[(A_\mu^a)^4\right] \right) \Bigg\}, \end{aligned} \tag{2.9}$$

where contractions of Greek indices are done with $\eta_{\mu\nu}$ and those of capital Latin indices are done using the full metric g_{MN}.

The indication for an instability to condensation occurs when a mass term turns negative. To see this, we need only look at the behavior of the pion masses in the four-dimensional effective Lagrangian. To quadratic order in π^a and ϕ^a, the 5D action for the pion sector, written $\mathcal{S}_\pi \approx \mathcal{S}_\pi^{(2)}$, is

$$
\mathcal{S}_\pi^{(2)} = \int d^4x\, dz\, \Bigg\{ v^2 a^3 \left[\frac{1}{2}\partial_\mu \pi^a \partial^\mu \pi^a - \frac{1}{2}\partial_z \pi^a \partial_z \pi^a + \mu_\mathrm{I} \left(\partial_0 \pi^2 \pi^1 - \partial_0 \pi^1 \pi^2 \right) \right.
$$
$$
\left. + \frac{\mu_\mathrm{I}^2}{2}\left(\pi^1 \pi^1 + \pi^2 \pi^2 \right) - \partial_\mu \pi^a \partial^\mu \phi^a + \frac{1}{2}\partial_\mu \phi^a \partial^\mu \phi^a + \mu_\mathrm{I} \left(\pi^2 \partial_0 \phi^1 - \pi^1 \partial_0 \phi^2 \right) \right]
$$
$$
\left. - \frac{a}{2g_5^2}\left[\mu_\mathrm{I}^2 \left(\partial_i \phi^1 \partial^i \phi^1 + \partial_i \phi^2 \partial^i \phi^2 \right) - \partial_z \partial_\mu \phi^a \partial_z \partial^\mu \phi^a \right] \right\} . \quad (2.10)
$$

The linearized equations of motion for π^a and ϕ^a are:

$$
\phi^0 - \pi^0 = \frac{1}{v^2 a^3 g_5^2}\partial_z(a \partial_z \phi^0) \, ,
$$
$$
m_0^2 \phi^0 - m_0^2 \pi^0 = \frac{1}{v^2 a^3}\partial_z(v^2 a^3 \partial_z \pi^0) \, ,
$$

$$(2.11)$$

$$
m_\pm \phi^\pm - (m_\pm \mp \mu_\mathrm{I}) \pi^\pm = \frac{m_\pm}{v^2 a^3 g_5^2}\partial_z(a \partial_z \phi^\pm) \, ,
$$
$$
\left(m_\pm^2 \mp \mu_\mathrm{I} m_\pm \right) \phi^\pm - \left(m_\pm^2 \mp 2\mu_\mathrm{I} \frac{m_\pm}{v^2 a^3 g_5^2} \mu_\mathrm{I}^2 \right) \pi^\pm = \frac{1}{v^2 a^3}\partial_z(v^2 a^3 \partial_z \pi^\pm) \, ,
$$

where $\pi^1 = \frac{1}{\sqrt{2}}(\pi^+ + \pi^-)$, $\pi^2 = \frac{-i}{\sqrt{2}}(\pi^+ - \pi^-)$, and $\pi^3 = \pi^0$ (similarly for ϕ^a). These equations are evaluated in the pion rest frame ($\vec{q} = 0$), where we identify the pion frequency with the four-dimensional effective pion mass in the isospin background: $i\partial_t \pi^\pm(x) \to m_\pm \pi^\pm(x)$, assuming a plane-wave solution for $\pi^\pm(x)$. Working in the gauge $A^a_{Lz} = A^a_{Rz} = 0$, the fields satisfy the boundary conditions $\partial_z \phi^{\pm,0}(z_\mathrm{m}) = \phi^{\pm,0}(\epsilon) = \pi^{\pm,0}(\epsilon) = 0$. The boundary condition at z_m corresponds to the gauge-invariant condition $F^L_{z\mu}(z_\mathrm{m}) = F^R_{z\mu}(z_\mathrm{m}) = 0$, but this choice is not unique and is made for simplicity.

By eliminating $\phi^{\pm,0}$ we can obtain equations of motion for $\pi^{\pm,0}$ alone:

$$\partial_z \left[\tfrac{1}{v^2 a^3} \partial_z \left(v^2 a^3 \partial_z \pi^0 \right) \right] + m_0^2 \partial_z \pi^0 - g_5^2 v^2 a^2 \partial_z \pi^0 = 0,$$

$$\partial_z \left[\tfrac{1}{v^2 a^3} \partial_z \left(v^2 a^3 \partial_z \pi^\pm \right) \right] + \left(m_\pm^2 \mp 2\mu_I m_\pm + \mu_I^2 \right) \partial_z \pi^\pm \qquad (2.12)$$

$$-g_5^2 v^2 a^2 \partial_z \pi^\pm = 0.$$

Except for the replacement of the eigenvalue m_0^2 with $\left(m_\pm^2 \mp 2\mu_I m_\pm + \mu_I^2 \right)$, the fields $\pi^\pm$ and π^0 are solutions to the same differential equation with the same boundary conditions, with identical eigenvalues

$$m_0^2 = \left(m_\pm^2 \mp 2\mu_I m_\pm + \mu_I^2 \right). \qquad (2.13)$$

The neutral pion is unaffected by the chemical potential, so m_0 is identified with the pion mass in vacuum, m_π. In subsequent sections we will derive the 4D effective Lagrangian for the pion modes by integrating the action over the extra dimension. However, we can already argue for the quadratic part of the effective Lagrangian, which is enough to demonstrate the instability to pion condensation. The linearized equations of motion which follow from the effective Lagrangian should be consistent with the determination of $m_\pm$ in (2.13). Replacing $m_\pm$ with the operator $i\partial_0$ acting on the rest-frame plane wave solutions to the equations of motion, we have the rest-frame equation of motion

$$\left(-\partial_0^2 \mp 2i\mu_I \partial_0 + \mu_I^2 - m_\pi^2 \right) \pi^\pm(x) = 0. \qquad (2.14)$$

These linearized equations of motion follow from the 4D Lagrangian,

$$\mathcal{L}_\pm = \partial_\mu \pi^+ \partial^\mu \pi^- - (m_\pi^2 - \mu_I^2)\pi^+ \pi^- - i\mu_I(\pi^- \partial_0 \pi^+ - \pi^+ \partial_0 \pi^-). \qquad (2.15)$$

which we will derive more systematically later. From the sign of the pion mass term we

see that when $\mu_I > m_\pi$ there is an instability to condensation of the charged pions. The properties of the condensate phase depend on the pion interactions, which we address next.

2.3 Properties of the Pion Condensate Phase

Since the pattern of chiral symmetry breaking is built into our holographic model, we expect to reproduce predictions of the chiral Lagrangian, at least qualitatively. We will first carry out our analysis in the simpler situation where we take $g_5 \to 0$, in order to decouple the gauge fields, and then move on to the case of nonzero g_5. In both cases, the pion effective theory is determined by the action evaluated on the solution for the pion mode discussed in the previous section, integrated over the extra dimension. Expanding the 4D effective potential, $V_{\text{eff}}[\pi^\pm(x); \mu_I]$, to quartic order in the pion fluctuations and finding the minimum allows us to determine the nature of the pion condensation phase transition as a function of μ_I. We then derive expressions for the number density and speed of sound.

2.3.1 Decoupling the 5D Gauge Fields

The limit $g_5 \to 0$ provides the most direct comparison to previous results. In that limit the fluctuations of the 5D gauge fields decouple from the pion physics. The corresponding 4D effective theory is similar to the chiral Lagrangian with isospin chemical potential included as a background for a 4D isospin gauge field, as in Ref. [68]. In terms of the unitary fields

$$\Sigma = \exp\left[\frac{i\pi^a \sigma^a}{f_\pi}\right],$$

(2.16)

the leading order chiral Lagrangian is

$$\mathcal{L}_{4\mathrm{D}} = \frac{f_\pi^2}{4}\mathrm{Tr}\left(\nabla_\nu\Sigma\,\nabla^\nu\Sigma^\dagger\right) + \frac{m_\pi^2 f_\pi^2}{4}\mathrm{Tr}\left(\Sigma + \Sigma^\dagger\right). \tag{2.17}$$

where $\nabla_0\Sigma = \partial_0\Sigma - i\frac{\mu_{\mathrm{I}}}{2}\left[\sigma_3, \Sigma\right]$ and $\nabla_i = \partial_i$. Expanding to second order in the pion fields, the Lagrangian takes the form,

$$\begin{aligned}
\mathcal{L}_{4\mathrm{D}} &= \frac{1}{2}\partial_\mu\pi^a\partial^\mu\pi^a - \frac{1}{2}\left(m_\pi^2 - \mu_{\mathrm{I}}^2\right)\left(\pi^1\pi^1 + \pi^2\pi^2\right) \\
&\quad - \frac{1}{2}m_\pi^2\pi^3\pi^3 + \mu_{\mathrm{I}}\left(\partial_0\pi^2\pi^1 - \partial_0\pi^1\pi^2\right).
\end{aligned} \tag{2.18}$$

The instability when $|\mu_{\mathrm{I}}| > m_\pi$ signals the phase transition to a pion condensate phase. Estimation of the value of the condensate and related observables requires an extension of the analysis to higher order in the pion fields, which we perform in the holographic description.

By design, the analysis of the 5D model is similar to the chiral Lagrangian analysis above. In the limit $g_5 \to 0$, we neglect couplings to the longitudinal gauge field $\partial_\mu\phi^a$. The action (2.9) takes the form

$$\begin{aligned}
\mathcal{S}_{g_5=0} &= \int d^5x\sqrt{-g}\Big\{2X_0^2\left[\partial_M(\cos b)\,\partial^M(\cos b) + \partial_M(n^a\sin b)\,\partial^M(n^a\sin b)\right] \\
&\quad - 2\frac{\mu_{\mathrm{I}}}{a^2}\,\partial_0\left(n^c\sin b\right)\epsilon^{a3c}n^a\sin b + \frac{\mu_{\mathrm{I}}^2}{a^2}\,\sin^2 b\;n^c n^d\epsilon^{c3c}\epsilon^{d3c}\Big\}, \tag{2.19}
\end{aligned}$$

where $b = \sqrt{\pi^c\pi^c}$ and $n^c = b^{-1}\pi^c$ as before. The linearized equations of motion for the pion fields are now,

$$-m_\pi^2\pi^{0,\pm} = \frac{1}{v^2 a^3}\partial_z\left(v^2 a^3\partial_z\pi^{0,\pm}\right). \tag{2.20}$$

The condensate is a static configuration rotationally invariant in x^1, x^2, x^3. The action on

such configurations gives the condensate effective potential,

$$V_{\text{eff.},g_5=0} = \int dz\, v(z)^2 a(z)^3 \left\{ \frac{1}{2}\left(\frac{db}{dz}\right)^2 + \frac{1}{2}\sin^2 b \left(\frac{dn^c}{dz}\right)^2 \right.$$

$$\left. - \frac{\mu_I^2}{2}\sin^2 b\, n^c n^d \left(\delta^{cd} - \delta^{c3}\delta^{d3}\right) \right\}. \quad (2.21)$$

The effective potential increases with $|dn^c/dz|$, so $dn^c/dz = 0$ in the ground state. The profile of $b(z)$ is determined from the solution to the equations of motion for the pion Kaluza-Klein mode. Expanding to fourth order in the pion fields,

$$V_{\text{eff.},g_5=0} = \int_\epsilon^{z_m} dz\, v^2/z^3\, \frac{1}{2}\left\{ \left(\frac{d\pi}{dz}\right)^2 - \mu_I^2\left(\pi(z)^2 - \frac{\pi(z)^4}{3} + \cdots\right) \right.$$

$$\left. \times n^c n^d \left(\delta^{cd} - \delta^{c3}\delta^{d3}\right) \right\}$$

$$= \int_\epsilon^{z_m} dz\, v^2/z^3\, \frac{1}{2}\left\{ m_\pi^2 \pi(z)^2 - \mu_I^2\left(\pi(z)^2 - \frac{\pi(z)^4}{3} + \cdots\right) \right.$$

$$\left. \times n^c n^d \left(\delta^{cd} - \delta^{c3}\delta^{d3}\right) \right\}, \quad (2.22)$$

where we used the linearized equation of motion (2.20) in the last line.

For $|\mu_I| > m_\pi$ it is energetically favorable to turn on the charged pions. The pion field is normalized by its kinetic term in the effective 4D theory, so we define $\pi^a(z) = \tilde{\pi}(z)\,\pi^a$ such that

$$\int_\epsilon^{z_m} dz\, v^2 a^3\, \tilde{\pi}(z)^2 = 1, \quad (2.23)$$

and π^a is the pion condensate $\langle \pi^a \rangle$.

Minimizing $V_{\text{eff.},g_5=0}$ expanded to $\mathcal{O}\left[(\pi^a)^4\right]$, written $V^{(4)}_{\text{eff.},g_5=0}$, we find that the transi-

tion is smooth (second order), and for $\mu \gtrsim m_\pi$ we obtain,

$$\pi^+\pi^- = \frac{3}{4\tilde{\eta}}\left(1 - \frac{m_\pi^2}{\mu^2}\right),$$

(2.24)

where $\tilde{\eta} = \int_\epsilon^{z^m} dz\, v^2 a^3 \tilde{\pi}(z)^4$. We then find,

$$V_{\text{eff.},g_5=0}^{(4)}(\pi^\pm) = -\frac{3}{8\tilde{\eta}}\mu_I^2\left(1 - \frac{m_\pi^2}{\mu_I^2}\right)^2,$$

(2.25)

and the isospin number density is

$$n_I = -\frac{\partial V_{\text{eff.}}}{\partial \mu_I} = \frac{3\mu_I}{4\tilde{\eta}}\left(1 - \frac{m_\pi^4}{\mu_I^4}\right).$$

(2.26)

We can express $\tilde{\eta}$ in terms of f_π^2 in this model by the AdS/CFT determination of f_π. The correlator of a product of axial currents has a pion pole at zero momentum transfer in the chiral limit, with residue equal to f_π^2. The AdS/CFT correspondence determines the correlation function in terms of a bulk-to-boundary propagator which solves the linearized equations of motion for the transverse part of the axial vector field. For more details in the context of the present model, see Refs. [11, 12]. We summarize the results here.

The linearized equation of motion for the transverse part of the axial vector field $A_\mu^a(q, z)$ is given by,

$$\left[\partial_z\left(a\partial_z A_\mu^a\right) + \frac{q^2}{z}A_\mu^a - v^2 a^3 g_5^2 A_\mu^a\right]_\perp = 0.$$

(2.27)

The bulk-to-boundary propagator $A(q, z)$ describes the solution to (2.27) of the form $A_\mu^a(q, z) = A(q, z)A_{0\mu}^a(q)$, with boundary conditions $\partial_z A(q, z)|_{z_m} = 0$ and $A(q, \epsilon) = 1$. In terms of the bulk-to-boundary propagator the AdS/CFT prediction for the pion decay constant is

$$f_\pi^2 = -\frac{1}{g_5^2}\left.\frac{\partial_z A(0, z)}{z}\right|_{z=\epsilon}.$$

(2.28)

If $g_5 = 0$ then the bulk-to-boundary propagator at $q^2 = 0$ is uniform, $A(0, z) = 1$. To next order in g_5^2, we obtain

$$\frac{1}{z}\partial_z A(0, z) = -g_5^2 \int_z^{z_m} d\bar{z}\, v(\bar{z})^2/\bar{z}^3 + \mathcal{O}(g_5^4/z_m^4). \tag{2.29}$$

From (2.28) we obtain in the $g_5 \to 0$ limit,

$$\begin{aligned} f_\pi^2 &= \int_\epsilon^{z_m} dz\, v(z)^2/z^3 \\ &\approx \frac{\sigma^2 z_m^4}{4} + m_q \sigma z_m^2 + m_q^2 \log(z_m/\epsilon). \end{aligned} \tag{2.30}$$

Note that in the absence of boundary counterterms we must choose ϵ such that $\log(z_m/\epsilon) \ll \sigma z_m^2/m_q$ to respect the chiral limit. We choose $\epsilon = 1/(10^8 \text{ MeV})$. In that case the integral defining f_π^2 is dominated by the region where the pion wavefunction $\tilde{\pi}(z)$ is approximately constant. Comparing (2.30) with (2.23), we learn that the pion wavefunction $\tilde{\pi}(z) \approx 1/f_\pi$ except for a region of small z, as in Figure 2.1.
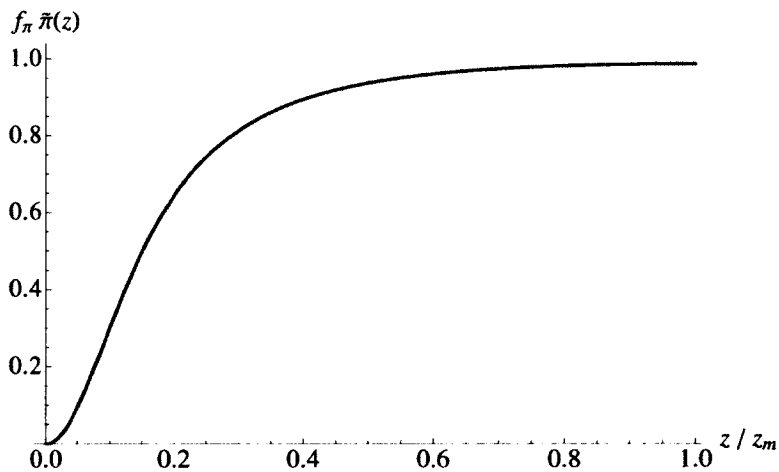
FIG. 2.1: Pion eigenfunction with $m_q = 4.25$ MeV, $\sigma = (263 \text{ MeV})^3$. and $z_m = 1/(323 \text{ Mev})$.

Similarly, from the integral defining $\tilde{\eta}$ we have

$$\tilde{\eta} \approx 1/f_\pi^2. \tag{2.31}$$

For a concrete example, fixing the mass of the lightest KK mode of the vector field V_μ^a to 776 MeV determines $z_m = 1/(323 \text{ MeV})$ [11]. Then with m_q=4.25 MeV and chiral condensate $\sigma = (263 \text{ MeV})^3$ we find physical values m_π=140 MeV and f_π=92 MeV in the $g_5 \to 0$ limit. With these values of the parameters, we find

$$\tilde{\eta} = \int_\epsilon^{z_m} dz\, v(z)^2 a(z)^3 \tilde{\pi}(z)^4 = 1/(91 \text{ MeV})^2, \tag{2.32}$$

which is approximately $1/f_\pi^2$ as expected. Note that the Gell-Mann-Oakes-Renner relation is approximately satisfied, $m_\pi^2 f_\pi^2/(2m_q\sigma) = 1.07 \approx 1$.

We now have the holographic prediction of the equation of state:

$$n_I \approx \frac{3}{4} f_\pi^2 \mu_I \left(1 - \frac{m_\pi^4}{\mu_I^4}\right). \tag{2.33}$$

For comparison, the corresponding prediction from the 4D chiral Lagrangian (2.17) is [68]

$$n_{4D} = f_\pi^2 \mu_I \left(1 - \frac{m_\pi^4}{\mu_I^4}\right), \tag{2.34}$$

which differs from the holographic prediction by an overall factor of 4/3. This overall factor drops out of the ratio of pressure to energy density and the speed of sound at zero temperature. The number densities are plotted in Figure 2.2. The model is not expected to be valid for $\mu_I \gtrsim m_\rho \approx 5.5 m_\pi$, but we plot the model prediction here and below over the entire range of μ_I.

The pressure p and energy density ε in the pion condensate medium are determined
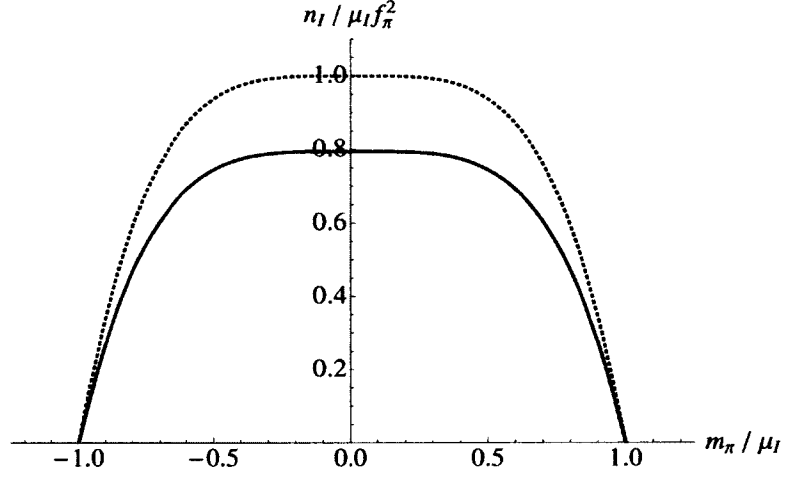
FIG. 2.2: Isospin number density. The bottom solid curve is the prediction of the hard-wall model with $m_q = 4.25$ MeV. $\sigma = (263 \text{ MeV})^3$ and $z_m = 1/(323 \text{ MeV})$. The top dotted curve is the result from Ref. [68] quoted in (2.34).

by $n_I(\mu_I)$ [68, 73]:

$$p(\mu_I) = \int_{m_\pi}^{\mu_I} n_I \, d\tilde{\mu} = \frac{3 f_\pi^2 \left(\mu_I^2 - m_\pi^2\right)^2}{8 \mu_I^2}, \tag{2.35}$$

$$\varepsilon(\mu_I) = \int_0^{n_I} \mu_I \, d\tilde{n} = \frac{3 f_\pi^2}{8 \mu_I^2} \left(\mu_I^2 - m_\pi^2\right) \left(\mu_I^2 + 3 m_\pi^2\right). \tag{2.36}$$

This gives

$$\frac{p}{\varepsilon} = \frac{\mu_I^2 - m_\pi^2}{\mu_I^2 + 3 m_\pi^2}, \tag{2.37}$$

and

$$c_s^2 = \frac{dp}{d\varepsilon} = \frac{\mu_I^4 - m_\pi^4}{\mu_I^4 + 3 m_\pi^4}. \tag{2.38}$$

The speed of sound violates the sound bound $c_s^2 < 1/3$ except near the phase transition boundary at $\mu_I = m_\pi$.

2.3.2 Including Dynamical 5D Gauge Bosons

Having understood how the $g_5 \to 0$ limit of holographic QCD reproduces the qualitative behavior of isospin matter at low temperature expected from the chiral Lagrangian,

we now consider the more general situation including couplings to the 5D gauge fields. In the calculations below we will take $g_5 = 2\pi$, which makes the holographic prediction of the vector current polarization at large momentum transfer agree with perturbative three-color QCD [11, 12] .

We first construct an approximate solution to (2.11) as an expansion in m_π, as in Ref. [11]. Combining the first two equations of (2.11) we get

$$m_\pi^2 \partial_z \phi^0 = v^2 a^2 g_5^2 \partial_z \pi^0. \tag{2.39}$$

Recalling the boundary conditions $\pi(\epsilon) = \phi(\epsilon) = \partial_z \phi|_{z_m} = 0$, to zeroth order in m_π the solution is $\pi^0 = 0$, and ϕ^0 satisfies the same equation as the bulk-to-boundary propagator in (2.27), so we set $\phi^0(z) = A(0, z) - 1$. Away from the boundary at $z = \epsilon$ consistency of the approximate solution with the first of the equations in (2.11) requires $\pi^0 \approx -1$. Recalling that the charged pions have the same wavefunction as the neutral pion, we temporarily normalize the fields so that $\pi^\pm(z) = \pi^0(z)$. Then $\phi^\pm = (1 \mp \mu_I/m_\pm) [A(0, z) - 1]$.

Integrating the action (2.10) by parts we get,

$$\begin{aligned}
S_\pi^{(2)} = \int d^4x\, dz \left\{ \left[v^2 a^3 \left(\pi^+\pi^- - \pi^+\phi^- - \pi^-\phi^+ + \phi^+\phi^- \right) - \frac{1}{g_5^2} \partial_z(a\partial_z\phi^-)\phi^+ \right] \right. \\
\times\, \partial_\mu \pi^+(x)\partial^\mu \pi^-(x) + \left[\partial_z \left(v^2 a^3 \partial_z \pi^+ \right) \pi^- + \mu_I^2 v^2 a^3 \pi^+\pi^- \right] \pi^+(x)\pi^-(x) \\
-\, i \left[v^2 a^3 \mu_I \left(\pi^-\pi^+ - \phi^-\pi^+ \right) \right] \partial_0 \pi^-(x)\pi^+(x) \\
\left. +\, i \left[v^2 a^3 \mu_I \left(\pi^+\pi^- - \phi^+\pi^- \right) \right] \partial_0 \pi^+(x)\pi^-(x) \right\}, \tag{2.40}
\end{aligned}$$

where functions without an argument are understood to be functions of z. Ignoring the π^0 terms, which can be obtained by taking $\mu_I \to 0$, we can use the third of Eqs. (2.11) to

solve for $\phi^\pm$ and obtain

$$\mathcal{S}_\pi^{(2)} = \int d^4x \left\{ \left[-\frac{\mu_I^2}{m_- m_+} \int dz\, v^2 a^3 \pi\pi - \frac{1}{g_5^2} \int dz\, \partial_z(a\partial_z\phi^-)\pi \right. \right.$$
$$\left. + \frac{\mu_I}{m_-} \frac{1}{g_5^2} \int dz\, \partial_z(a\partial_z\phi^+)\pi \right] \partial_\mu \pi^+(x)\partial^\mu \pi^-(x)$$
$$+ \left[\frac{m_+}{g_5^2} \int dz \partial_z(a\partial_z\phi^+)\pi + \mu_I^2 \int dz\, v^2 a^3 \pi\pi \right] \pi^+(x)\pi^-(x)$$
$$+ i\left[\frac{\mu_I}{m_-} \int dz\, v^2 a^3 \pi\pi + \frac{1}{g_5^2} \int dz\, \partial_z(a\partial_z\phi^-\pi) \right] \partial_0\pi^-(x)\pi^+(x)$$
$$\left. - i\left[-\frac{\mu_I}{m_+} \int dz\, v^2 a^3 \pi\pi + \frac{1}{g_5^2} \int dz\, \partial_z(a\partial_z\phi^+)\pi \right] \partial_0\pi^+(x)\pi^-(x) \right\}, \quad (2.41)$$

where we have used $\pi \equiv \pi^0(z) = \pi^\pm(z)$. We now use the approximate solutions for $\phi^\pm$ and make the approximation $\pi = -1$ in those integrals dominated by the region where the pion wavefunction is flat. Defining $\alpha \equiv \frac{1}{f_\pi^2} \int dz\, v^2 a^3 \pi\pi$ and making use of equation (2.28), we get

$$\mathcal{S}_\pi^{(2)} = \int d^4x \left\{ \left(\frac{m_\pi^2 - \alpha\mu_I^2}{m_\pi^2 - \mu_I^2} \right) f_\pi^2 \partial_\mu\pi^+(x)\partial^\mu\pi^-(x) - \left(m_\pi^2 - \alpha\mu_I^2 \right) f_\pi^2 \pi^+(x)\pi^-(x) \right.$$
$$\left. - 2i\mu_I f_\pi^2 \left(\frac{m_\pi^2 - \alpha\mu_I^2}{m_\pi^2 - \mu_I^2} \right) \partial_0\pi^+(x)\pi^-(x) \right\}. \quad (2.42)$$

The resulting Lagrangian after canonically normalizing the kinetic term is, transforming back to (π^1, π^2, π^3),

$$\mathcal{L}_{\text{eff.}} = \frac{1}{2}\partial_\mu\pi^a\partial^\mu\pi^a - \frac{1}{2}\left(m_\pi^2 - \mu_I^2 \right)\left(\pi^1\pi^1 + \pi^2\pi^2 \right)$$
$$- \frac{1}{2}m_\pi^2\pi^3\pi^3 + \mu_I \left(\partial_0\pi^2\pi^1 - \partial_0\pi^1\pi^2 \right). \quad (2.43)$$

This agrees with the leading order 4D chiral Lagrangian (2.18), and the earlier discussion which led to (2.15).

Having seen the instability to pion condensation, we now include the pion interactions

to quartic order, to determine the nature of the phase transition. The effective potential for static configurations of $\pi(x)$ takes the same form as (2.21) because the longitudinal gauge bosons are derivatively coupled. We make the ansatz that $n^3 = 0$; the pion expectation value is only in the (π^1, π^2) plane. With the approximate solutions for $\pi(z)$ and $\phi(z)$ described above, and applying the canonical rescaling of the kinetic term, the effective potential at $\mathcal{O}(b^4)$ becomes

$$V_{\text{eff.}}^{(4)}(b) = \frac{1}{2}\left(m_\pi^2 - \mu_I^2\right)b^2 + \frac{1}{6}\mu_I^2 f_\pi^{-2}\left(\frac{m_\pi^2 - \mu_I^2}{m_\pi^2 - \alpha\mu_I^2}\right)^2 \eta\, b^4, \qquad (2.44)$$

where $\eta = \frac{1}{f_\pi^2}\int dz\, v^2 a^3\, \pi\pi\pi\pi$, $\alpha = \frac{1}{f_\pi^2}\int dz\, v^2 a^3\, \pi\pi$, and f_π is given by (2.28). Note that $\pi(z)$ here is the approximate solution for small m_π described earlier, and is not the canonically normalized field. We can now solve for the minimum of the potential, $\partial V_{\text{eff.}}^{(4)}/\partial b = 0$:

$$b_0^2 = \frac{3}{2}\frac{f_\pi^2}{\eta\mu_I^2}\frac{(m_\pi^2 - \alpha\mu_I^2)^2}{(\mu_I^2 - m_\pi^2)}. \qquad (2.45)$$

The isospin number density is

$$n_I = -\frac{\partial V_{\text{eff.}}^{(4)}}{\partial\mu_I} = \mu_I f_\pi^2 \frac{1}{\eta}\frac{3}{4}\left(\alpha^2 - \frac{m_\pi^4}{\mu_I^4}\right). \qquad (2.46)$$

The phase transition is first order, with the order parameter jumping at the phase boundary $\mu_I = m_\pi$. The minimum value of the free energy $V_{\text{eff.}}$ at $\mathcal{O}(b^4)$ is discontinuous at the critical point $\mu_I = m_\pi$, but the perturbative expansion breaks down near the critical point and we expect a nonperturbative analysis to confirm continuity in the free energy across the phase boundary. However, we can say with confidence that the transition is not second order in this model, because if it were then the order parameter b would vary smoothly and we would expect a perturbative analysis to be valid. Although perturbation theory breaks down near the transition, we plot the perturbative prediction for the number density in

$$n_I \, / \, \mu_I f_\pi^2$$
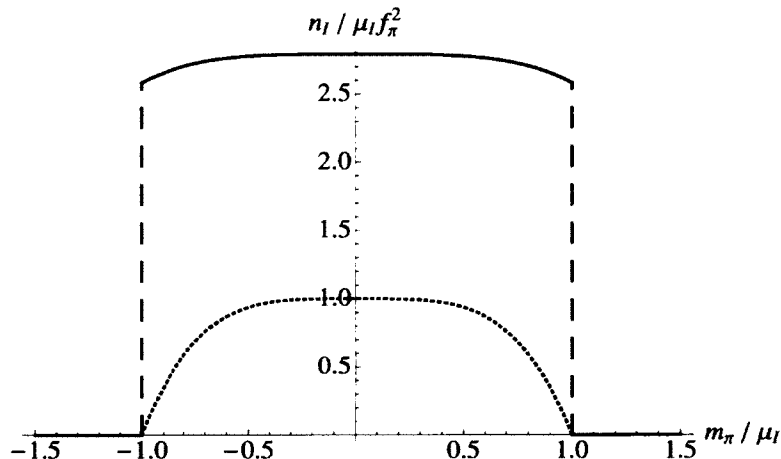
FIG. 2.3: Isospin number density. The top solid curve is the perturbative prediction of the hard-wall model with parameters fit to m_ρ, m_π and f_π: $m_q = 2.26$ MeV, $\sigma = (333 \text{ MeV})^3$, and $z_m = 1/(323 \text{ MeV})$. This set of parameters gives $\alpha = 3.66$ and $\eta = 3.60$, in (2.46). The bottom dotted curve is the result from Ref. [68] given in (2.34).

Figure 2.3.

The ratio of the pressure to energy density is now

$$\frac{p}{\varepsilon} = \frac{\alpha^2 \mu_I^2 - m_\pi^2}{\alpha^2 \mu_I^2 + 3m_\pi^2}, \tag{2.47}$$

and

$$c_s^2 = \frac{\alpha^2 \mu_I^4 - m_\pi^4}{\alpha^2 \mu_I^4 + 3m_\pi^4}. \tag{2.48}$$

This is plotted next to the chiral Lagrangian prediction in Figure 2.4. Note that the speed of sound exceeds the sound bound $c_s^2 = 1/3$ throughout the pion condensate phase at zero temperature.

2.4   A Comment on the Chiral Lagrangian

Leading order chiral perturbation theory predicts that the transition to the pion condensate phase is second order. We have learned that gauging the chiral symmetry in the
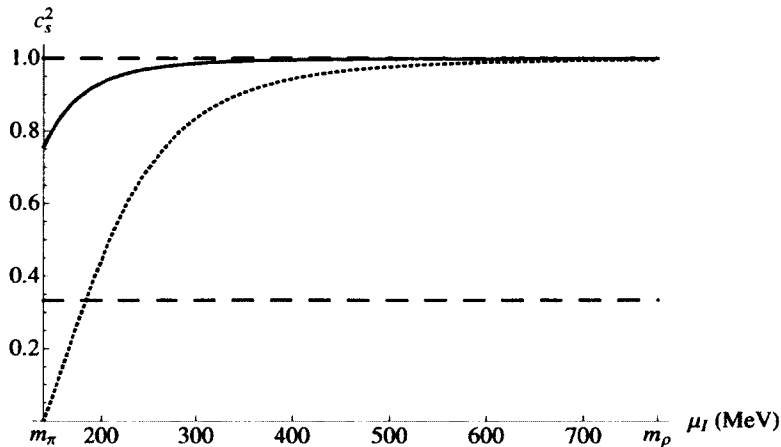
FIG. 2.4: Speed of Sound. The upper solid curve is the perturbative prediction of the hard-wall model for the speed of sound with $m_q = 2.26$ MeV. $\sigma = (333 \text{ MeV})^3$, and $z_m = 1/(323 \text{ MeV})$. This set of parameters gives the value $\alpha = 3.66$ in (2.48). The bottom dotted curve is the prediction based on (2.34). The top and bottom horizontal dashed lines represent the speed of light and the conformal limit $c_s^2 = 1/3$.

holographic model qualitatively modifies predictions for pion condensation at zero temperature. The transition becomes first order, and the medium becomes stiff immediately beyond the phase boundary. We note that the order of the transition is not determined entirely by the symmetry structure of the theory. Including higher derivative terms in the chiral Lagrangian, albeit with unphysically large coefficients, can have similar consequences, as we will now demonstrate. Consider the Lagrangian

$$\mathcal{L} = \frac{f_\pi^2}{4}\text{Tr}\left[D_\mu\Sigma D^\mu\Sigma^\dagger\right] + \frac{m_\pi^2 f_\pi^2}{4}\text{Tr}\left[\Sigma + \Sigma^\dagger\right] + \alpha_1\left(\text{Tr}\left[D_\mu\Sigma D^\mu\Sigma^\dagger\right]\right)^2$$
$$+ \alpha_2\text{Tr}\left[D_\mu\Sigma D_\nu\Sigma^\dagger\right]\text{Tr}\left[D^\mu\Sigma D^\nu\Sigma^\dagger\right], \tag{2.49}$$

where for this analysis α_1 and α_2 are arbitrary parameters. Once again we take the static part of the Lagrangian to get an expression for the effective potential. Defining

$\Sigma = \cos b + i\,(n^a \sigma^a)\sin b$, we have

$$V_{\text{eff.}}(\cos b) = -\frac{\mu_I^2 f_\pi^2}{2}\left(1 - \cos^2 b\right)\left(1 - n^3 n^3\right) - m_\pi^2 f_\pi^2 \cos b$$
$$- a_1 \frac{\mu_I^4 f_\pi^2}{4}\left(1 - \cos^2 b\right)^2 \left(1 - n^3 n^3\right)^2,$$

(2.50)

where $a_1 \equiv \frac{16}{f_\pi^2}(\alpha_1 + \alpha_2)$. At the minimum of $V_{\text{eff.}}$, $n^3 = 0$, and we find a region of a_1 parameter space where the phase transition is first order. That is, as a_1 increases past a critical value $a_1^{\text{crit.}} = 1/(2m_\pi^2)$, the phase transition changes from second to first order. This is illustrated in Figure 2.5 . However, $f_\pi^2 a_1^{\text{crit.}} = 0.22$ is much larger than the

(a) a_1 less than critical.

(b) a_1 critical.

(c) a_1 larger than critical.
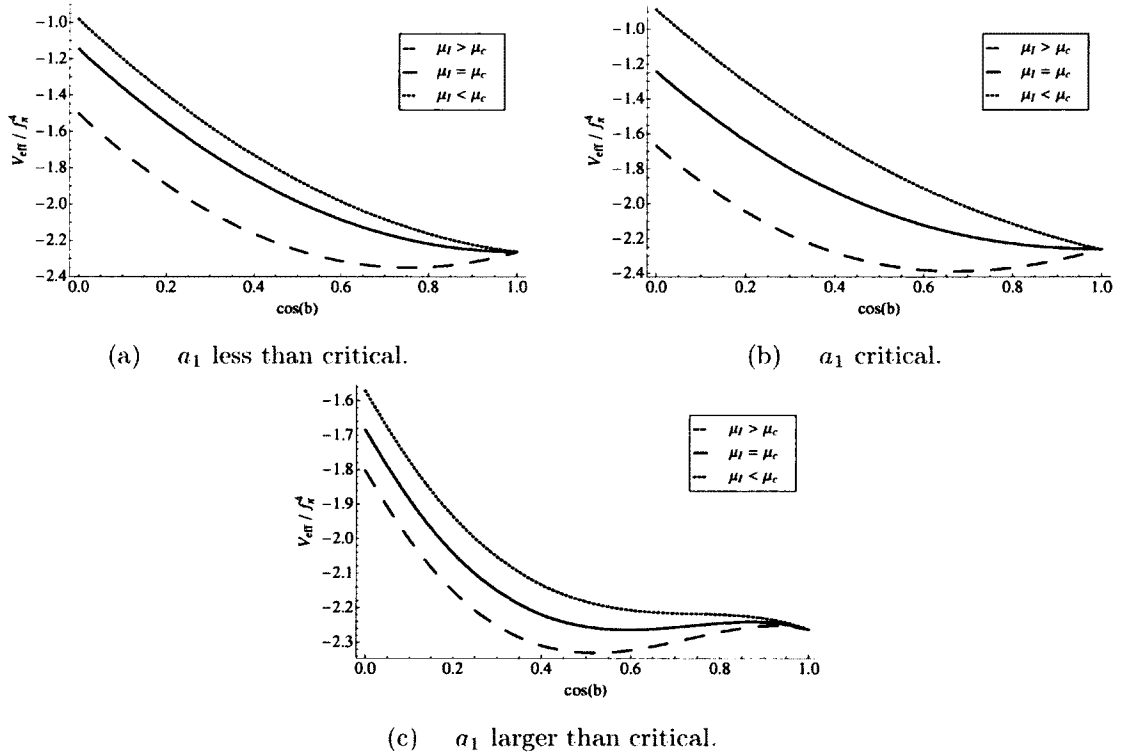
FIG. 2.5: Each plot shows the phase transition for a different value of the a_1 parameter. The critical value of μ_I for pion condensation depends on a_1. The three curves shown in each plot correspond to $\mu_I < \mu_c$, $\mu_I = \mu_c$, and $\mu_I > \mu_c$ (top dotted, middle solid, and bottom dashed curves, respectively). Plot (a) shows the transition for a_1 less than the critical value. Plot (b) is with a_1 the critical value, while a_1 of (c) is larger. These plots assumed $m_\pi = 139$ MeV and $f_\pi = 92.4$ MeV.

typical low energy coefficients in the chiral Lagrangian inferred by experiment ($l_1(m_\pi) = (-4 \pm 6) \times 10^{-4}$, $l_2(m_\pi) = (9.1 \pm 0.2) \times 10^{-3}$) [90, 91].

In summary, we have studied pion condensation at zero temperature and finite isospin chemical potential in a hard-wall model of holographic QCD with chiral symmetry breaking and massive pions. At the critical point $\mu_I = m_\pi$ the pion condenses, and our perturbative analysis suggests that the condensate creates a stiff medium approaching the Zel'dovich equation of state $p = \varepsilon$. Sound propagation exceeds the conformal sound bound $c_s^2 = 1/3$, except near the phase transition boundary if the 5D gauge coupling is small enough. The low-energy effective theory for pions as derived from the hard-wall model indicates that the transition from the hadronic phase to the condensate phase is first order, except in the limit of vanishing 5D gauge coupling. This is in contrast to leading order chiral perturbation theory, which predicts a second order transition [68], and lattice simulations which also seem to be consistent with a second order transition [74]. These results suggest possible improvements to the holographic model we've been working with, which will be the topic of the next chapter.

CHAPTER 3

Chiral Symmetry in Holographic QCD

Continuing with the model of Chapter 2, a hard-wall model of holographic QCD, we will find that nonlinear boundary dynamics are required in order to maintain the correct pattern of explicit and spontaneous chiral symmetry breaking beyond leading order in the pion fields. As a result, the pion condensate phase transition of this chirally improved model is second order. With the help of a field redefinition, we can relate the requisite nonlinear boundary conditions to a standard Sturm-Liouville system. Observables insensitive to the chiral limit receive only small corrections in the improved description, and classical calculations in the hard-wall model remain surprisingly accurate.

49

3.1 Background

The background spacetime is chosen to be a slice of Anti-de Sitter space (AdS$_5$), with metric

$$ds^2 = \frac{1}{z^2}\left(\eta_{\mu\nu}dx^\mu dx^\nu - dz^2\right), \quad \epsilon \leq z \leq z_{\mathrm{m}}, \tag{3.1}$$

The size of the extra dimension depends on z_{m}, which sets the Kaluza-Klein scale and is related holographically to the confining scale of QCD. Alternative spacetime backgrounds have been motivated by D-brane configurations in string theory which give rise to QCD-like theories with chiral symmetry breaking and confinement, as in the Sakai-Sugimoto model based on the D4-D8 system [10]. The established AdS/CFT dictionary between physics in 3+1 and 4+1 dimensions provides motivation for the model presented in Chapter 2, in which a complex scalar field in 4+1 dimensions, with the quantum numbers of the quark bilinears $q_{Li}\bar{q}_{Rj}$ with flavor labels $i.j$, transforms as a bifundamental under the SU(2)$_L \times$ SU(2)$_R$ gauge group. Again, the trace over the Lorentz structure of the operator $q\bar{q}$ is to be understood. As a demonstration of the pattern of chiral symmetry breaking in the model, the Gell-Mann-Oakes-Renner (GOR) relation for the pion mass was shown to be approximately satisfied [11, 92],

$$m_\pi^2 f_\pi^2 = 2m_q\sigma, \tag{3.2}$$

where m_π and f_π are the pion mass and decay constant calculated from the model, and m_q and σ are parameters in the scalar field background playing the role of the quark mass and chiral condensate, respectively. The GOR relation is also satisfied in an SU(3) extension of the hard-wall model with an independent strange quark mass parameter [93].

Classical calculations in the hard-wall model have reproduced a variety of QCD observables with surprising accuracy, generally at the 10-15% level [11, 12]. The hard-wall model fails at high energies [94] where the Kaluza-Klein spectrum diverges from the Regge

spectrum [95], a problem partially corrected in the soft-wall model [96]. More surprisingly, as we saw in the previous chapter, pion condensation in the hard-wall model has qualitatively different features from predictions of the chiral Lagrangian [97]. In chiral perturbation theory without unphysically large low-energy coefficients, the pion condensation transition is second order and approaches the Zel'dovich equation of state for stiff matter smoothly across the phase boundary [68]. However, in the hard-wall model the transition from the hadronic phase to the pion condensate phase was found to be first order, rapidly approaching the Zel'dovich equation of state across the phase boundary. Another subtle puzzle discovered in unpublished work [98] found that the GOR relation as derived in the hard-wall model with complex σ disagrees with the analogous prediction of the chiral Lagrangian. The holographic model takes as input the pattern of chiral symmetry breaking, so disagreement with lowest-order chiral perturbation theory is surprising.

In this chapter, we will see that the incorrect structure of pion interactions in the hard-wall model is a result of the choice of boundary conditions imposed on the 5D fields. Care must be taken in order that the boundary conditions respect the symmetry breaking structure. The subtlety compared with other extra-dimensional models is that here the background of a bulk field not only spontaneously breaks the gauge invariance in the bulk, but a non-normalizable term in the background also explicitly breaks the gauge invariance. In the hard-wall model the bulk gauge invariance is responsible for the global chiral symmetry of the effective 4D theory, so it is important that the explicit and spontaneous breaking be correctly accounted for at the boundary.

We will find that nonlinear boundary conditions on the bulk scalar field, or else nonlinear boundary terms in the action, may be consistently chosen so as to restore the proper pattern of chiral symmetry breaking in the hard-wall model. The nonlinear boundary dynamics we propose are an alternative to the description in Ref. [99], which also leads to acceptable symmetry structure (and also accommodates a bulk Chern-Simons term ab-

sent in the present model). The nonlinear boundary conditions relate the 5D σ-model scalars to products of pseudoscalars $\pi^a \pi^a$, $(\pi^a \pi^a)^2$, etc. In order to motivate these unusual boundary conditions and to demonstrate their relation to a Sturm-Liouville system, as required for consistency of the standard Kaluza-Klein decomposition of the fields and their interactions, we reparametrize the 5D fields by a nonlinear field redefinition. The reparametrization introduces a new surface term (i.e. a total derivative) involving the pions in the 5D action but replaces the nonlinear boundary conditions with ordinary linear boundary conditions consistent with the desired symmetry-breaking pattern. As opposed to the boundary conditions proposed to describe multitrace operators in the AdS/CFT correspondence [100, 101], the nonlinear boundary conditions in the hard-wall model arise away from the boundary of AdS, at the infrared boundary of the spacetime.

The modifications [102] of the hard-wall model [11] required to restore the structure of chiral symmetry breaking have a number of phenomenological consequences. The GOR relation for the pion mass, Eq. (3.2), is correctly normalized only after the quark mass and chiral condensate are rescaled. This same rescaling is consistent (up to a sign) with the AdS/CFT correspondence, and is a result of the modified boundary physics. The pion potential is modified so as to reconcile properties of the pion condensation transition with predictions of chiral perturbation theory. Most hadronic observables receive only small corrections which vanish in the chiral limit, so the hard-wall model remains surprisingly accurate in many of its predictions for low-energy QCD observables.

3.2 Features of the Hard-Wall Model

Starting with the action (2.3), we will point out some salient features of the hard-wall model. As before, the equations of motion have a solution with vanishing gauge fields and

scalar field profile (where we add a tilde because we will later rescale the quark mass),

$$X_0(z) = \frac{1}{2}(\tilde{m}_q z + \sigma z^3)\mathbf{1} \equiv \frac{\tilde{v}(z)}{2}\mathbf{1}, \tag{3.3}$$

where $\mathbf{1}$ is the 2×2 identity matrix. The fields X have the quantum numbers of the scalar quark bilinears, which are the operators that are effectively sourced in the Lagrangian of the 3+1 dimensional theory by quark masses. Again, the term in the solution Eq. (3.3) proportional to z is non-normalizable and is related by the AdS/CFT dictionary to the quark mass, which explicitly breaks the chiral symmetry; and the term in the solution proportional to z^3 is normalizable and is related to the condensate $\langle q_L \bar{q}_R \rangle$, which spontaneously breaks the chiral symmetry [53, 55].

The non-normalizable mode in the scalar field background explicitly breaks a bulk gauge invariance, but the presence of this mode is equivalent to spontaneous breaking due to a heavy Higgs field localized on the ultraviolet boundary $(z = \epsilon)$ in the decoupling limit. To see this, we write the Higgs doublet (ϕ^+, ϕ^0) as a matrix,

$$H = \begin{pmatrix} \overline{\phi^0} & \phi^+ \\ -\phi^- & \phi^0 \end{pmatrix}. \tag{3.4}$$

which transforms in the bifundamental representation of the chiral symmetry. The up and down quark Yukawa couplings enter the Lagrangian as $\mathcal{L}_{\text{Yuk.}} = \lambda \text{Tr}\left\{H^\dagger q_L \bar{q}_R + \text{h.c.}\right\}$. Replacing $q_L \bar{q}_R$ with the 5D field X, the localized Higgs field has boundary action

$$\mathcal{S}_\epsilon = \int_{z=\epsilon} d^4x \, \text{Tr}\left\{|\partial_\mu H|^2 - V(H) + \frac{\lambda}{\epsilon^3}\left(HX^\dagger + XH^\dagger\right)\right\}, \tag{3.5}$$

where $V(H)$ is the Higgs potential exhibiting spontaneous symmetry breaking. A similar coupling appears in bosonic technicolor models [103, 104]. The factor of $1/\epsilon^3$ in the last

term ensures the proper scaling with the field X near the UV boundary. We impose Neumann boundary conditions on X in the ultraviolet, modified by the presence of the boundary term (3.5). Replacing the Higgs field H by its vacuum expectation value $\langle H \rangle = \langle \phi^0 \rangle \mathbf{1}$, chosen real, the equations of motion and boundary condition for X are given by:

$$\partial_z \left(\frac{1}{z^3} \partial_z X \right) - \frac{1}{z^3} \Box X + \frac{3}{z^5} X = 0, \tag{3.6}$$

$$\partial_z X \big|_\epsilon = -\lambda \langle H \rangle, \tag{3.7}$$

where $\Box \equiv \eta^{\mu\nu} \partial_\mu \partial_\nu$. Greek indices will always refer to 3+1 dimensions, and capital Latin indices will refer to 4+1 dimensions.

By identifying the diagonal quark mass $M_q = \lambda \langle H \rangle$, the boundary condition becomes $\partial_z X \big|_\epsilon = -M_q$. Near the boundary as $\epsilon \to 0$, the solution for X consistent with this boundary condition takes the form $X \approx -M_q z$. Thus, the coupling of X to a Higgs field localized at the UV boundary gives rise to the appropriate non-normalizable background solution for X, which justifies the presence of the non-normalizable background and its AdS/CFT interpretation as the source for the operator $q\bar{q}$. However, the overall normalization of M_q in terms of the physical quark mass depends on the normalization of the field X. In Eq. (3.3) we have set $M_q = -\tilde{m}_q/2$. (Other normalizations may better match QCD predictions for correlators of products of scalar quark bilinears [105].)

The fluctuations of X, which contain scalars and pseudoscalars (pions), are typically decomposed as [11, 12, 106]:

$$X_{\text{old}}(x, z) = \left[\frac{1}{2} (\tilde{m}_q z + \sigma z^3) \mathbf{1} + \tilde{S}(x, z) \right] \tilde{U}(x, z), \tag{3.8}$$

where $\tilde{S}$ is a Hermitian matrix of scalars and $\tilde{U} = \exp[i\tilde{\pi}^a(x, z)\sigma^a]$ is unitary. Any matrix can be written as a product of a Hermitian and a unitary matrix, and any Hermitian

matrix function of x and z can be written as the term in parentheses in Eq. (3.8), so this ansatz is completely general up to a U(1) factor relevant for the chiral anomaly but which will not be discussed here.

The scalars and pseudoscalars decouple at quadratic order in the action, so we temporarily limit our attention to fluctuations with $\tilde{S} = 0$. In order to simplify the discussion we also temporarily decouple the vector fields by taking $g_5 = 0$. We will include the gauge couplings in Sec. 3.5, but they are an added complication which is not necessary to understand the main conclusions.

The lightest pion Kaluza-Klein mode, $\tilde{\pi}(x, z) = \tilde{\pi}^a(x, z)\sigma^a/2 = \tilde{\pi}^a(x)\psi(z)\sigma^a/2$, has action

$$
\begin{aligned}
\mathcal{S}_{g_5=0} &= \int d^5x \, \mathrm{Tr} \left\{ \frac{\tilde{v}(z)^2}{4z^3} (\partial_\mu \tilde{U} \partial^\mu \tilde{U}^\dagger - \partial_z \tilde{U} \partial_z \tilde{U}^\dagger) \right\} \\
&= \int d^5x \, \mathrm{Tr} \left\{ \frac{\tilde{v}(z)^2}{4z^3} \left(\partial_\mu \tilde{U} \partial^\mu \tilde{U}^\dagger - 4\psi'(z)^2 \, \tilde{\pi}(x)^2 \right) \right\}.
\end{aligned}
\tag{3.9}
$$

As explained in Ref. [11] and will also be explained in Sec. 3.3, the pion wavefunction is flat with $\psi(z) \approx 1$ except near $z = \epsilon$, so integrating over z yields the effective 4D action for the pions,

$$
\mathcal{S}_{\mathrm{eff.}} = \int d^4x \, \frac{f_\pi^2}{4} \mathrm{Tr} \left\{ \partial_\mu \tilde{U} \partial^\mu \tilde{U}^\dagger - 4m_\pi^2 \tilde{\pi}^2 \right\},
\tag{3.10}
$$

where m_π^2 is determined by the equations of motion and boundary conditions, and from the kinetic term we identify the pion decay constant

$$
\begin{aligned}
f_\pi^2 &\approx \int_\epsilon^{z_m} dz \, \sigma^2 z^3 \\
&= \frac{\sigma^2 z_m^4}{4}
\end{aligned}
\tag{3.11}
$$

as $\epsilon \to 0$. The expression (3.11) for f_π also follows from an AdS/CFT calculation of the transverse part of the axial vector current-current correlator [97].

3.3 Chiral Symmetry Breaking in the Hard-Wall Model

The structure of the pion effective action (3.10) demonstrates the discrepancy between the hard-wall model as defined above and chiral perturbation theory. The pion mass term in Eq. (3.10) does not include the higher-order pion interactions required for the chiral symmetry to be maintained while the quark mass matrix transforms in the bifundamental representation under the chiral symmetry (like a Higgs spurion). In the chiral Lagrangian the pion mass term is proportional to $\mathrm{Tr}\,(M_q U^\dagger + M_q^\dagger U)$, which displays the proper pattern of explicit and spontaneous chiral symmetry breaking. Beyond quadratic order in the pion fields, the hard-wall model as described above disagrees with the chiral Lagrangian, leading to unusual pion phenomenology inconsistent with chiral perturbation theory. The absence of quartic terms in the pion potential in this context was also noted in Ref. [107].

Restoration of the correct pattern of chiral symmetry breaking may be achieved by modifying the boundary conditions in a nonlinear way which mixes the scalar modes $\tilde{S}$ and products of pseudoscalars $\tilde{\pi}^a \tilde{\pi}^a$, as we discuss below. It will be convenient to rescale the quark mass parameter $\tilde{m}_q = -2m_q$, so that the background profile of the field X takes the form

$$X_0(z) = -m_q z + \frac{\sigma z^3}{2} \equiv \frac{v(z)}{2}\mathbf{1}. \tag{3.12}$$

We then consider a nonlinear redefinition of the 5D fields as follows:

$$X(x,z) = -m_q z + \left[\frac{\sigma}{2}z^3 + S(x,z)\right] U(x,z). \tag{3.13}$$

which is to be compared with Eq. (3.8). We write $U(x,z) = \exp[i\pi^a(x,z)\sigma^a]$. Now the pseudoscalar fluctuations in $U(x,z)$ multiply the term in the background responsible for the spontaneous breaking of the chiral symmetry, but not the term responsible for the

explicit breaking. We also add to the action a counterterm localized in the UV,

$$\mathcal{S}_{\rm ct.} = -\int_\epsilon d^4x \, \frac{|X|^2}{\epsilon^4},$$ (3.14)

to cancel off the divergent term m_q^2/ϵ^2. The finite part of this counterterm $m_q\sigma$ has the consequence of modifying the AdS/CFT calculation of $\langle q\bar{q}\rangle$ in terms of σ such that the normalization of m_q and σ in Eq. (3.12) is consistent with the AdS/CFT correspondence. We note that this normalization of m_q and σ agrees up to a sign with the normalization of the tachyon background in a string-motivated holographic QCD model, in which chiral symmetry is broken by tachyon condensation [108]. It seems that the origin of the sign is entirely due to the boundary term (discussed below) appearing on the IR brane, and if we were to shift the boundary contribution to the UV brane we would have the canonical AdS/CFT sign, but we will not pursue this line of reasoning further.

With boundary conditions $S(x, \epsilon) = \pi^a(x, \epsilon) = S(x, z_{\rm m}) = 0$, and a Neumann condition on π^a at $z_{\rm m}$, the scalar and pseudoscalar modes again decouple and the pion action takes the form

$$\mathcal{S}_{g_5=0} = \int d^5x \, {\rm Tr}\left\{\frac{\sigma^2 z^3}{4}(\partial_\mu U \partial^\mu U^\dagger - \partial_z U \partial_z U^\dagger)\right\}$$
$$+ \int d^4x \, {\rm Tr}\left\{\frac{m_q\sigma}{2}(U + U^\dagger)\big|_{z_{\rm m}}\right\},$$ (3.15)

where the last term is an IR localized boundary term due to a total derivative in the action, and we have discarded some irrelevant constants. Although we focus in this paper on the leading terms in the chiral Lagrangian, we note that at higher-order there are two terms in the 5D Lagrangian (with structure ${\rm Tr}\, S^2 \partial_z U \partial_z U^\dagger$ and ${\rm Tr}\, S \partial_z U \partial_z U^\dagger$) which could damage the chiral symmetry. We suggest that nonlinear modification of the boundary conditions may be introduced to modify these terms, but we will not pursue this issue further here.

The field parametrization Eq. (3.13) is an alternative to those of Refs. [109, 99] which also lead to an acceptable model, but with a nonlinear term at the UV boundary $z = \epsilon$ rather than at the IR boundary $z = z_\mathrm{m}$. The Kaluza-Klein modes are solutions to the linearized equations of motion, which follow from the quadratic part of the action:

$$\mathcal{S}^{(2)}_{g_5=0} = \int d^5x \, \frac{\sigma^2 z^3}{2} (\partial_\mu \pi^a \partial^\mu \pi^a - \partial_z \pi^a \partial_z \pi^a) - \int d^4x \, m_q \sigma (\pi^a \pi^a)\big|_{z_\mathrm{m}}, \tag{3.16}$$

where $\pi^a(x, z) = \pi^a(x)\psi(z)$. The linearized equation of motion for the pion wavefunction is

$$\partial_z(z^3 \partial_z \psi) = -m_\pi^2 z^3 \psi. \tag{3.17}$$

The Neumann boundary condition in the IR is modified by the boundary term in the action, with the result

$$\partial_z \psi(z)\big|_{z_\mathrm{m}} = -\frac{2m_q}{\sigma z_\mathrm{m}^3} \psi(z_\mathrm{m}). \tag{3.18}$$

Note that the boundary conditions here are linear, and the nonlinear boundary terms in the action are treated as interactions. In this form, the pions are described by a standard Sturm-Liouville system. The solutions are in terms of Bessel functions and the normalizable solution has the expansion

$$\psi(z) = \left(1 - \frac{m_\pi^2 z^2}{8} + \text{higher order in } m_\pi z\right). \tag{3.19}$$

If $m_\pi z_\mathrm{m} \ll 1$ then $\psi(z) \approx 1$ in the entire interval $\epsilon < z < z_\mathrm{m}$. Substituting the expansion of $\psi(z)$ into the boundary condition Eq. (3.18), we find to leading order in m_q,

$$m_\pi^2 \frac{\sigma^2 z_\mathrm{m}^4}{4} = 2m_q \sigma. \tag{3.20}$$

Using Eq. (3.11), which is not affected by the field redefinition, Eq. (3.20) is just the

Gell-Mann-Oakes-Renner relation

$$m_\pi^2 f_\pi^2 = 2m_q\sigma. \tag{3.21}$$

justifying the interpretation of m_q and σ as the quark mass and chiral condensate, respectively, up to a simultaneous rescaling of m_q and σ as in Ref. [105]. Note that the quark mass, and in particular the product $m_q\sigma$, is rescaled from the old parameter $\tilde{m}_q$ and even has a different sign. This rescaling is required in order to obtain the correct normalization in the GOR relation, but is also consistent with the AdS/CFT interpretation of m_q as the source for the operator $q_L\bar{q}_R$ whose expectation value is the chiral condensate. The condensate is obtained by varying the action with respect to the source m_q. Because of the additional boundary term, which scales as m_q, the quark mass needs to be rescaled with respect to the chiral condensate as above.

We now derive the 4D effective Lagrangian for the redefined pions. Let us first focus on the z-derivative piece. Ignoring the higher KK modes and writing $U = \exp[i\pi^a(x)\psi(z)\,\sigma^a]$, we find

$$\int d^5x\,\mathrm{Tr}\left(\frac{\sigma^2 z^3}{4}\partial_z U\partial_z U^\dagger\right) = \int d^4x\left[\int dz\,\frac{\sigma^2 z^3}{2}\psi'(z)^2\right]\pi^a(x)\pi^a(x). \tag{3.22}$$

as before. Integrating by parts and using the equations of motion and the boundary condition for ψ we arrive at:

$$\mathcal{S}_{g_5=0}^{(2)} \supset \int d^4x\left[\int dz\,(-m_\pi^2\sigma^2 z^3)\psi(z)^2 + 2m_q\sigma\right]\frac{1}{2}\pi^a(x)\pi^a(x). \tag{3.23}$$

Using the flatness of the $\psi(z)$ profile, the expression for f_π^2 in Eq. (3.11), and the GOR relation, the above expression in brackets vanishes. Evaluating the rest of the pion action (3.15) on the bulk linearized equations of motion and integrating over the extra dimen-

sion, we obtain the approximate 4D effective action, $\mathcal{S}_{\text{eff}}$. Including the boundary term in Eq. (3.15), the approximate 4D effective Lagrangian is equivalent to the lowest-order[1] chiral Lagrangian:

$$\mathcal{S}_{\text{4D}} = \int d^4x \, \text{Tr} \left\{ \frac{f_\pi^2}{4} \partial_\mu U \partial^\mu U^\dagger + \frac{m_\pi^2 f_\pi^2}{4} (U + U^\dagger) \right\}. \tag{3.24}$$

As a consequence, the properties of the pion condensate phase and other aspects of pion physics now agree with the predictions of chiral perturbation theory thanks to the modified boundary dynamics.

3.4   Nonlinear Boundary Conditions

The nonlinear reparametrization of the bulk field X in Eq. (3.13) allows for independent linear boundary conditions on the scalar and pseudoscalar modes while maintaining the proper pattern of chiral symmetry breaking. In terms of the original decomposition of X as per Eq. (3.8), the boundary conditions required to maintain the pattern of chiral symmetry mix the scalar and pseudoscalar fields in a nonlinear way. To understand the structure of the nonlinear boundary conditions we can expand the two field decompositions, Eqs. (3.8) and (3.13):

$$\begin{aligned}
X &= \left[\frac{1}{2}(\tilde{m}_q z + \sigma z^3) + \tilde{S} \right] \left(1 + 2i\tilde{\pi} - 2\tilde{\pi}^2 + \ldots \right) \\
&= -m_q z + \left(\frac{\sigma z^3}{2} + S \right) \left(1 + 2i\pi - 2\pi^2 + \ldots \right),
\end{aligned} \tag{3.25}$$

---

[1] By "lowest-order" here we are referring to the energy expansion of the chiral Lagrangian, which is an expansion in ∂_μ and m_π^2.

where $\tilde{\pi} = \tilde{\pi}^a \sigma^a / 2$, and similarly for π. Equating the anti-Hermitian parts of the two descriptions gives, to quadratic order in the fields,

$$
\begin{aligned}
\pi &= \tilde{\pi}\left(1 + \frac{\tilde{m}_q}{\sigma z^2}\right) + \frac{1}{\sigma z^3}\left[(\tilde{S}\tilde{\pi} - S\pi) + (\tilde{\pi}\tilde{S} - \pi S)\right] + \ldots \\
&= \tilde{\pi}\left(1 + \frac{\tilde{m}_q}{\sigma z^2}\right) + \frac{1}{\sigma z^3}\left\{\left[\tilde{S}\tilde{\pi} - \tilde{S}\tilde{\pi}\left(1 + \frac{\tilde{m}_q}{\sigma z^2}\right)\right] + \text{h.c.}\right\} + \ldots \qquad (3.26) \\
&= \tilde{\pi}\left(1 + \frac{\tilde{m}_q}{\sigma z^2}\right) - \frac{\tilde{m}_q}{\sigma^2 z^5}\left(\tilde{S}\tilde{\pi} + \tilde{\pi}\tilde{S}\right) + \ldots .
\end{aligned}
$$

Similarly, the Hermitian parts give,

$$
\begin{aligned}
S &= \tilde{S} - \tilde{m}_q z\,\tilde{\pi}^2 - \sigma z^3\left(\tilde{\pi}^2 - \pi^2\right) + i\left[\tilde{S}\left(\tilde{\pi} - \pi\right) - \text{h.c.}\right] + \ldots \\
&= \tilde{S} + \tilde{m}_q z\,\tilde{\pi}^2 - i\frac{\tilde{m}_q}{\sigma z^2}\left(\tilde{S}\tilde{\pi} - \tilde{\pi}\tilde{S}\right) + \ldots .
\end{aligned} \qquad (3.27)
$$

These expressions have been left in terms of the old mass parameter $\tilde{m}_q$, which is equivalent to $-2m_q$, and terms higher order in $\tilde{m}_q$ have been dropped.

In the new decomposition of the field X, the boundary conditions consistent with the chiral symmetry breaking structure are:

$$
S(x, \epsilon) = S(x, z_{\mathrm{m}}) = 0 = \pi(x, \epsilon) = 0, \quad \partial_z \pi(x, z)|_{z_{\mathrm{m}}} = \frac{\tilde{m}_q}{\sigma z_{\mathrm{m}}^3}\pi. \qquad (3.28)
$$

In terms of the original decomposition of the field X, the boundary conditions are,

$$
S = 0 \;\rightarrow\; \tilde{S} = -\tilde{m}_q z\,\tilde{\pi}^2 + \ldots . \qquad (3.29)
$$

$$
\partial_z \pi = \frac{\tilde{m}_q}{\sigma z^3}\pi \;\rightarrow\; \partial_z \tilde{\pi} = \frac{3\tilde{m}_q}{\sigma z^3}\tilde{\pi} + \ldots . \qquad (3.30)
$$

where the ellipses include terms higher order in the fields and in $\tilde{m}_q$, and terms that vanish when traced over.

For these boundary conditions to be physically acceptable, the boundary variation of the action must vanish. Expanding the action (2.3) with $g_5 = 0$ about the background as in Eq. (3.8), we obtain

$$\mathcal{S}_{g_5=0} = \int d^5x\, \mathrm{Tr}\left\{ \frac{1}{z^3}\partial_\mu X \partial^\mu X^\dagger - \frac{1}{z^3}(\partial_z \tilde{S})^2 - \frac{\tilde{v}'(z)}{z^3}\partial_z \tilde{S} \right.$$
$$\left. - \frac{1}{z^3}\left(\frac{\tilde{v}}{2} + \tilde{S}\right)^2 \partial_z \tilde{U}\partial_z \tilde{U}^\dagger + \frac{3}{z^5}\left(\tilde{v}\tilde{S} + \tilde{S}^2\right) \right\} + \text{constant}. \quad (3.31)$$

where $\tilde{v}(z) = \tilde{m}_q z + \sigma z^3$ as in Eq. (3.3). The terms in Eq. (3.31) with z-derivatives lead to boundary terms in the variation of the action. Expanding to quadratic order in $\tilde{S}$ and $\tilde{\pi}$, we find for the boundary variation of $\mathcal{S}_{g_5=0}^{(2)}$:

$$\delta\mathcal{S}_{g_5=0}^{(2)} = \int_{\epsilon, z_m} d^4x\, \mathrm{Tr}\left\{ \left[-\frac{2}{z^3}\partial_z \tilde{S} - \frac{1}{z^3}\left(\tilde{m}_q + 3\sigma z^2\right) \right]\delta\tilde{S} \right.$$
$$\left. - \left[\frac{2(\tilde{m}_q z + \sigma z^3)^2}{z^3}\partial_z \tilde{\pi} \right]\delta\tilde{\pi} \right\}. \quad (3.32)$$

To leading order in $\tilde{m}_q$ and in the fields, using

$$\delta\tilde{S} = -\tilde{m}_q z\left(\tilde{\pi}\,\delta\tilde{\pi} + \delta\tilde{\pi}\,\tilde{\pi}\right) + \ldots \quad (3.33)$$

from Eq. (3.29), we find that the boundary variation $\delta\mathcal{S}_{g_5=0}^{(2)}$ indeed vanishes. The cancellation of boundary variations in this nonlinear fashion is novel in the context of extra-dimensional models, though it is reminiscent of the mixed boundary conditions of certain Higgsless models [110] in which the contributions to the boundary variation of the action from different fields cancel one another.

In Kaluza-Klein theories an effective description of the lightest modes is often derived by simply neglecting the heavier modes and integrating the action over the extra

dimension. Indeed, that is how we derive the pion effective action in this paper. However, consistency of this approach relies on orthogonality and completeness relations dependent on the Sturm-Liouville structure of the equations of motion and boundary conditions. It is a mathematical question which classes of systems of differential equations with nonlinear boundary conditions satisfy the completeness and orthogonality theorems of Sturm-Liouville systems. In holographic QCD we have seen that there is a nonlinear field redefinition after which the boundary conditions are of the linear Sturm-Liouville form. This justifies the effective description obtained by keeping only the lightest modes.

3.5 Couplings to Vector and Axial-Vector Fields

Having derived the chiral Lagrangian in the $g_5 \to 0$ limit, we turn to the case of nonzero 5D gauge couplings with dynamical gauge bosons representing the vector and axial vector mesons. Including the gauge fields, the action takes the form of Eq. (2.3). The field X transforms as a bifundamental under the gauge group $SU(2)_L \times SU(2)_R$ and we will use the gauge fixing condition $L_z^a = R_z^a = 0$. We will also be working mainly with the linear combinations $A_\mu^a = (L_\mu^a - R_\mu^a)/2$, the axial vector field, and $V_\mu^a = (L_\mu^a + R_\mu^a)/2$, the vector field. The normalization of these combinations by a factor of 2 (rather than $\sqrt{2}$) is so that their kinetic terms are canonically normalized given the unconventional normalization of the gauge fields in Eq. (2.3).

We parameterize the fluctuations of the field X as in Eq. (3.13). To leading order the scalars and pseudoscalars are decoupled, so we focus only on the pseudoscalars and set $S = 0$ for the present discussion. As in the previous section, the boundary condition on the pion is modified as in Eq. (3.18).

We will determine the pion decay constant as in Refs. [11, 12] by the residue of the axial current two-point correlator at $q^2 = 0$. The AdS/CFT calculation of the correlator

is performed by taking two functional derivatives, with respect to the source of the axial current operator, of the action evaluated on the classical solution to the linearized equation of motion for the transverse part of A_μ^a. The resulting correlator is in terms of the bulk-to-boundary propagator for A_μ^a, which is a particular solution to the transverse-projected linearized equation of motion. This equation of motion for $A_\mu^a(q, z)_\perp$ is

$$\left[\partial_z\left(\frac{1}{z}\partial_z A_\mu^a\right) + \frac{q^2}{z}A_\mu^a - \frac{v^2 g_5^2}{z^3}A_\mu^a\right]_\perp = 0. \tag{3.34}$$

If we have a solution to Eq. (3.34) of the form $A_\mu^a(q, z) = A(q, z)A_{0\mu}^a(q)$, with boundary conditions $\partial_z A(q, z)|_{z_m} = 0$ and $A(q, \epsilon) = 1$, then $A(q, z)$ is identified as the bulk-to-boundary propagator and $A_{0\mu}^a(q)$ is the source for the axial current. The AdS/CFT prediction for the pion decay constant is then,

$$f_\pi^2 = -\frac{1}{g_5^2}\left.\frac{\partial_z A(0, z)}{z}\right|_{z=\epsilon}. \tag{3.35}$$

In order to study the pions we note that the pion fluctuations identified in the field X mix with the longitudinal part of the axial vector field $A_\mu^a \to \partial_\mu \phi^a$, which has the same quantum numbers. The pions will be identified as the lowest mode of this coupled system. Since we have in mind a Kaluza-Klein decomposition of the fields and since, for the purposes of deriving the low energy theory, we are only interested in the lowest mode, we will make the substitutions $\pi^a(x, z) \to \pi^a(x)\psi(z)$ and $\phi^a(x, z) \to \pi^a(x)\phi(z)$. The linearized equations of motion for $\psi(z)$ and $\phi(z)$ are

$$v\phi - \sigma z^3 \psi = \frac{z^3}{v g_5^2}\partial_z\left(\frac{1}{z}\partial_z \phi\right).$$
$$m_\pi^2(v\phi - \sigma z^3 \psi) = \partial_z\left(\sigma z^3 \partial_z \psi\right), \tag{3.36}$$

where the fields satisfy the boundary conditions $\partial_z \phi(z)|_{z_m} = \phi(\epsilon) = \psi(\epsilon) = 0$, and

Eq. (3.18).

3.5.1   Approximate Analytic Results

We can obtain an approximate solution to the equations of motion, Eqs. (3.36), in the chiral limit, in a similar fashion to Ref. [11]. We find that the approximate solutions near the ϵ boundary are $\phi(z) = 1 - A(0, z)$ and $\psi(z) = 0$, while those away from the ϵ boundary are $\phi(z) = 1 - A(0, z)$ and $\psi(z) \approx 1$. Plugging the first equation of Eq. (3.36) into the second, approximating $v(z) \approx \sigma z^3$, and integrating once we arrive at

$$\frac{m_\pi^2}{\sigma g_5^2} \left(\frac{1}{z} \partial_z \phi - \frac{1}{z} \partial_z \phi \bigg|_\epsilon \right) = \sigma z^3 \partial_z \psi. \tag{3.37}$$

Now if we evaluate this expression on the IR boundary, using our approximate solution for $\phi(z)$ and recalling the boundary conditions, we find

$$m_\pi^2 \left(-\frac{1}{g_5^2} \frac{\partial_z A(0, z)}{z} \bigg|_\epsilon \right) = 2 m_q \sigma \psi(z_m). \tag{3.38}$$

By utilizing Eq. (3.35) and the fact that $\psi(z_m) \approx 1$, we have once again derived the GOR relation.

The derivation of the chiral Lagrangian mass term is similar to that of previous sections. The only contributions come from the term proportional to $\partial_z U \partial_z U^\dagger$ and the boundary term proportional to $U + U^\dagger$. In particular we have, upon integration by parts,

$$\mathcal{S} \supset \int d^4x \left[\int dz\, \partial_z \left(\sigma z^3 \partial_z \psi \right) \psi + 2 m_q \sigma \psi(z_m)^2 \right] \frac{1}{2} \pi^a(x) \pi^a(x)$$
$$+ \int d^4x\, \mathrm{Tr} \left\{ \frac{m_q \sigma}{2} (U + U^\dagger) \big|_{z_m} \right\}. \tag{3.39}$$

If we make use of the equations of motion, Eq. (3.36), and substitute our approximate

solutions for ϕ and ψ, we find that the two terms in the square brackets cancel, to first order in m_q. Thus, to this order in m_q, we are left with the mass term of the chiral Lagrangian:

$$\mathcal{S}_{4D} \supset \int d^4x \, \mathrm{Tr} \left\{ \frac{m_\pi^2 f_\pi^2}{4} (U + U^\dagger) \right\}. \tag{3.40}$$

3.5.2 Numerical Results

We will now present a numerical analysis of the equations of motion, Eqs. (3.36). We choose a value $\epsilon = 10^{-7}$ MeV for the UV cutoff, and determine the location of the IR boundary to be $z_m = 1/(323 \text{ MeV})$, by setting the rho mass to 776 MeV [11]. We take $g_5 = 2\pi$ as in Ref. [11], noting that the derivation of this assignment is unaffected by our new choice for the form of the field $X(x, z)$, with different background. With the values $m_q = 2.36$ MeV for the quark mass and $\sigma = (333 \text{ MeV})^3$ for the condensate, we have $m_\pi = 140$ MeV for the pion mass and $f_\pi = 92.0$ MeV for the pion decay constant. The solutions for $\psi(z)$ and $\phi(z)$ are plotted in Fig. 3.1, along with their approximate solutions, namely $\psi(z) = 1$ and $\phi(z) = 1 - A(0, z)$. The functions $\psi(z)$ and $\phi(z)$ are

(a)   (b)
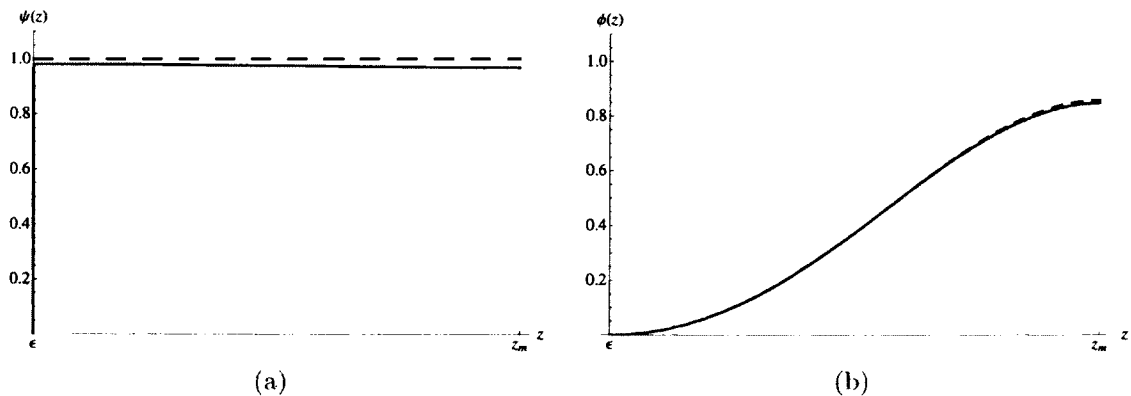
FIG. 3.1: Figures (a) and (b) display the numerical solutions to Eq. (3.36) for $\psi(z)$ and $\phi(z)$, respectively. In both figures there are two curves plotted: the blue curves are the numerical solutions and the red, dashed curves are the approximate solutions (in figure (a), $\psi(z) = 1$ and in figure (b), $\phi(z) = [1 - A(0, z)]$). These plots were made with $m_q = 2.36$ MeV and $\sigma = (333 \text{ MeV})^3$.

normalized to obtain a canonically normalized kinetic term in the low energy theory. The plotted numerical solutions illustrate the extent to which the approximations of the previous section are valid.

We would also like to understand numerically how robust the GOR relation is in this model, with respect to varying some of the parameters. In particular, fixing $m_\pi = 140$ MeV (by adjusting m_q for fixed values of σ) we would like to see what happens for different values of σ. Varying the condensate by sampling a discrete number of points from $(290 \text{ MeV})^3$ to $(360 \text{ MeV})^3$, the pion decay constant takes values ranging from 79 MeV to 102 MeV and the quark mass goes from 2.52 MeV down to 2.21 MeV. In Fig. 3.2, we plot the ratio $(m_\pi^2 f_\pi^2)/(2m_q\sigma)$ for the above specified range of values for the condensate. If the GOR relation holds, the ratio should be approximately 1 and we can see that the plot shows good agreement over the entire region.
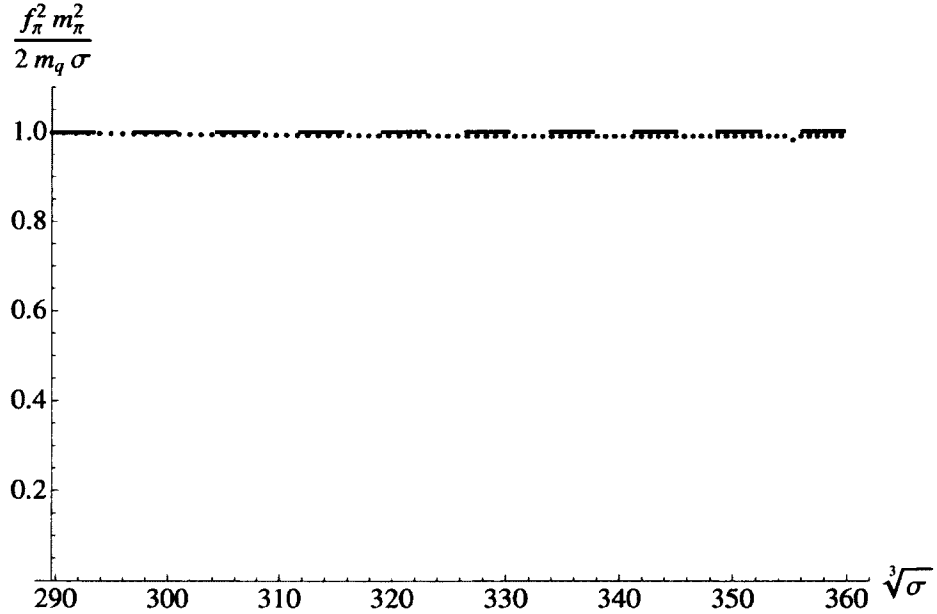
FIG. 3.2: The red long-dashed line is a horizontal line at 1. The blue dots are the values of the function, $(m_\pi^2 f_\pi^2)/(2m_q\sigma)$. For this plot, the quark mass is adjusted to fix $m_\pi = 140$ MeV at each point.

3.6   Consequences for Holographic QCD

We check that the change of background does not adversely affect some standard predictions of the hard-wall model; that is, we will compare our predictions with those of "Model A" in Ref. [11]. We might expect the modifications to be marginal because only the pion physics should be sensitive to changes in m_q, but we have also changed a sign. Aside from the substitution $\tilde{m}_q \to -2m_q$, the derivations of the equations of motion for the gauge fields and of the vector current correlators are unaffected by the new form of the X-field. Since the expressions for the related observables we compute are likewise unchanged, we refer the reader to Ref. [11], for more detail. In the following, we summarize the methods for obtaining the results. To calculate the mass of the a_1, we solve Eq. (3.34) for the normalizable mode $\psi_{a_1}(z)$ with boundary conditions $\psi_{a_1}(\epsilon) = \partial_z \psi_{a_1}(z_{\mathrm{m}}) = 0$. The wavefunction ψ_{a_1} is normalized such that $A_\mu(x)$ has a canonical kinetic term, where $A_\mu(x,z) = \psi_{a_1}(z)A_\mu(x)$. As derivable from the two-point vector current correlator, we use the following expression to calculate the decay constants in terms of the profile in the extra dimension: $F^{1/2} = \sqrt{\psi''(0)/g_5}$. And finally, by looking at the terms cubic in the fields, coupling $V\pi\pi$, we make a prediction for $g_{\rho\pi\pi}$. All relevant cubic terms are the following:

$$\mathcal{S} \supset \epsilon^{abc} \int d^5x \; V_\mu^b \left[\frac{1}{zg_5^2} \partial_z \partial^\mu \phi^a \partial_z \phi^c + \frac{1}{z^3} \partial^\mu \left(v\phi^a - \sigma z^3 \pi^a \right) \left(v\phi^c - \sigma z^3 \pi^c \right) \right], \qquad (3.41)$$

where we have used the equations of motion for the vector field to obtain this expression. In order to calculate the on-shell $g_{\rho\pi\pi}$ from the effective 4D theory, we integrate out the extra dimension and identify $g_{\rho\pi\pi}$ as the coefficient of $\epsilon^{abc}\partial^\mu\pi^a(x)\rho_\mu^b(x)\pi^c(x)$, where ρ_μ^b is the lowest mode in the vector field KK decomposition. Extracting this coefficient from

Eq. (3.41) we find

$$g_{\rho\pi\pi} = \frac{g_5}{f_\pi^2} \int dz \; \psi_\rho(z) \left[\frac{1}{z g_5^2}(\partial_z \phi)^2 + \frac{1}{z^3}\left(v\phi - \sigma z^3 \psi\right)^2 \right], \qquad (3.42)$$

where the z-integral of the expression in brackets is normalized to f_π^2. The results are presented in Table 3.1 and we find that the new predictions have not changed significantly compared to "Model A" – they are still on the 10% level, with the exception of $g_{\rho\pi\pi}$.

Observable	Measured (MeV)	Model (MeV)	Model A (MeV)[11]
m_π	140	140	140
m_ρ	776	776	776
m_{a_1}	1230	1370	1360
f_π	92.4	92.0	92.4
$F_\rho^{1/2}$	345	329	329
$F_{a_1}^{1/2}$	433	493	486
$g_{\rho\pi\pi}$	6.03	4.44	4.48

TABLE 3.1: The predictions of the model as compared with "Model A" and experimental values [11]. The results are based on fitting to m_π, f_π, and m_ρ, leading to the parameter choice $m_q = 2.36$ MeV. $\sigma = (333 \text{ MeV})^3$. and $z_m = 1/(323 \text{ MeV})$.

3.7   In Summary

Holographic QCD models are surprisingly successful in their predictions of low-energy QCD observables. However, it was discovered in earlier work that the pion condensation transition in one version of the hard-wall model has qualitatively different features than the predictions of chiral perturbation theory and other approaches. We have shown that this disagreement is due to a boundary effect related to the explicit breaking of the gauged chiral symmetry by the non-normalizable background of a 5D scalar field. To restore agreement with the chiral Lagrangian we modified the boundary dynamics. either by introducing nonlinear boundary conditions on the fields, or by performing a nonlinear field

redefinition which induced an infrared boundary term in the action. The field redefinition allowed us to relate the system with nonlinear boundary conditions to a standard Sturm-Liouville system which manifestly maintains the proper symmetry structure, justifying the subsequent Kaluza-Klein decomposition of the fields. The chirally improved hard-wall model makes predictions for low-energy QCD observables that agree with the original model to within 1-2%.

It would be useful to further explore the consequences of the modified boundary physics with regard to pion observables. It would also be interesting to find additional applications of nonlinear boundary conditions to extra-dimensional model building, for example to Higgsless models and holographic technicolor models. Finally, the necessity for nonlinear boundary dynamics in the hard-wall model provides motivation for further study of the mathematical problem of differential equations with nonlinear boundary conditions. In particular, it might be useful to classify those systems of equations and boundary conditions that can be related to a Sturm-Liouville system by a change of variables.

CHAPTER 4

Deconstructing Holographic Superconductors

We will now shift gears, focusing on models with potential application to condensed matter physics. We briefly review some properties of the earliest holographic models of superconductivity. Then we will present a dimensionally deconstructed model of an s-wave holographic superconductor. The 2+1 dimensional model includes multiple charged Cooper pair fields and neutral exciton fields that have interactions governed by hidden local symmetries. We will analyze properties of the Cooper pair condensates and the complex conductivity. We will also see that there are AdS/CFT-like relations for the current and charge density in the model.

4.1 Introduction

High-T_c superconductors continue to fascinate physicists, both for their technological prospects and for their unconventional physical properties. Discovered in 1986 [111],

high-T_c superconductors have superconducting transition temperatures T_c higher than the upper limit of around 30 K suggested by the BCS theory [112], and the mechanism of superconductivity in these materials remains uncertain. High-T_c superconductors are Type II, allowing magnetic fields to penetrate in conjunction with Abrikosov vortex currents which maintain localized magnetic fluxes. A number of features of high-temperature superconductors remain poorly understood, including the existence of a pseudogap phase in which a gap in the excitation spectrum opens up at temperatures above the superconducting transition [113], and a thermoelectric Nernst effect that occurs in both the superconducting and pseudogap phases [114]. A few additional classes of exotic high-T_c superconductors have recently been discovered, including the iron pnictides [115], and research into their properties is ongoing.

In the absence of a clear theoretical understanding of high-T_c superconductors and other systems with strongly correlated electrons, it is useful to explore simplified models which describe similar phenomenology. It has long been understood that certain relativistic field theories describe a variety of phenomena typical of superconductors. In the Abelian Higgs model, a charged scalar field condenses while the photon becomes massive, in analogy to the condensation of Cooper pairs and the consequent expulsion of magnetic fields from superconducting materials. The Abelian Higgs model also has Nielsen-Olesen vortex solutions which maintain localized magnetic flux tubes [116], much like the Abrikosov vortices in Type II superconductors.

One approach that has stimulated much effort especially from the string theory community is the use of the AdS/CFT correspondence. The particular model that we will examine is one of the first holographic superconductors [15]. Our approach will make use of an idea called dimensional deconstruction. In parallel to the development of the AdS/CFT correspondence in string theory, extra-dimensional model building has led to the discovery of new paradigms for gravitational physics [117, 118], electroweak symme-

try breaking [119], grand unification [120], and other possible new physics. Notably, in order to define these otherwise nonrenormalizable extra-dimensional gauge theories, a procedure was developed for dimensionally "deconstructing" extra-dimensional theories into renormalizable field theories defined in the natural (lower) dimension of the system of interest [121]. At long distances, a deconstructed model is effectively described by the corresponding extra-dimensional theory, latticized in the extra dimension(s). In some models the number of effective lattice sites can be taken as small as just two or three while retaining the desirable features of the extra-dimensional theory. Deconstruction provides a systematic procedure for finding relatively simple, weakly coupled models of interesting physical systems, in the number of dimensions that naturally characterizes the system of interest [122].

In this chapter, we will study a deconstructed model of the simplest holographic superconductor, the Abelian Higgs model in 3+1 dimensional Anti-de Sitter-Schwarzschild spacetime (AdS_4-Schwarzschild), which is intended to model s-wave superconductors in 2+1 dimensions [15]. Superconductivity in the cuprates is along two-dimensional CuO_2 planes, so the hope is that a model with two spatial dimensions will capture some of the relevant physics in these systems. The deconstructed model is a 2+1 dimensional model in which Maxwell's electrodynamics is replicated a number of times. Fields charged under pairs of the electromagnetic U(1) gauge groups condense, giving rise to the latticized extra-dimensional structure of the model. The temperature-dependent couplings of the Maxwell fields are rotationally invariant but not Lorentz invariant. Additional charged fields representing Cooper pair operators condense in the superconducting phase, and the combined effects of the multiple condensates determine the properties of the superconductor. The electron pair wavefunctions in high-T_c superconductors are thought to have more complicated symmetry than the s-wave described by scalar Cooper pair fields, so the present model is not expected to capture features sensitive to the symmetry of the

wavefunctions.

The deconstructed model helps to elucidate certain aspects of holographic supercon-ductivity and suggests the relevant effective degrees of freedom in physical realizations of these superconductors. One generic feature of this class of models is the existence of hidden local symmetries [123] and corresponding neutral excitations, much like the vector mesons of Quantum Chromodynamics. Such excitations in the superconductor may be interpreted as excitons[1], electron-hole bound states which can be created when a photon is absorbed by certain materials [124]. In analogy to a deconstructed holographic model of hadrons [125], we derive discretized AdS/CFT relations between bulk and boundary observables. We analyze properties of the superconducting transition and the frequency-dependent conductivity as the number of extra-dimensional lattice sites, and correspond-ingly the number of pair condensates and exciton fields, is reduced.

In Sec. 4.2, we review the Abelian Higgs model in the AdS_4-Schwarzschild spacetime as a model of superconductivity in two spatial dimensions. In Sec. 4.3, we describe the deconstructed model and explain the calculation of observables of interest. In Sec. 4.4, we present numerical results. We conclude with a discussion and suggestions for future research in Sec. 4.5.

4.2 Continuum Holographic Model

In this section we review the holographic model that will be deconstructed in Sec. 4.3. Much of the content of this section is a summary of results contained elsewhere, for example in Ref. [15], though we generalize certain results for the sake of comparison with the deconstructed model.

---

[1] The neutral, spin-1 excitations might more appropriately be identified with polaritons, if there were a dynamical photon in the deconstructed theory that mixed strongly with these excitons.

The starting point is a vacuum solution to Einstein's equations with negative cosmological constant in 3+1 dimensions, namely the AdS_4-Schwarzschild solution. The spacetime is described by a metric of the form

$$ds^2 = F(r)dt^2 - r^2(dx^2 + dy^2) - \frac{1}{F(r)}dr^2.$$
(4.1)

where

$$F(r) = \frac{r^2}{L^2}\left(1 - \frac{r_H^3}{r^3}\right).$$
(4.2)

The constant L is the Anti-de Sitter scale, which we will often set to 1. We refer to coordinates in which the metric takes the form of Eq. (4.1) as r-coordinates, and the coordinate r runs from r_H to ∞. The 2+1 dimensional surface at $r = \infty$ is referred to as the ultraviolet (UV) boundary, and the surface at $r = r_H$ is the horizon. The AdS/CFT correspondence suggests the identification of the temperature of the material with the Hawking temperature of the AdS black hole, namely

$$T = 3r_H/(4\pi L^2).$$
(4.3)

With nonvanishing charge density the relevant background spacetime is instead the AdS-Reissner-Nordstrom spacetime, a charged solution to the Einstein-Maxwell equations with a negative cosmological constant. However, in this paper we neglect the backreaction of the charge density on the geometry. In this approximation the spacetime metric continues to take the form of Eqs. (4.1) and (4.2), even when the solutions of interest have nonvanishing charge density.

The holographic model contains a U(1) gauge field corresponding to electromagnetism, and a charged scalar field corresponding to the Cooper pairs. The model is translationally invariant in 2 spatial dimensions, and is therefore not expected to reproduce phenomena

that are sensitive to the atomic lattice.

The action for the model is given by

$$S = \int d^4x \sqrt{g} \left\{ -\frac{1}{4} F_{MN} F^{MN} + |(\partial_M - iA_M)\psi|^2 - m^2|\psi|^2 \right\}, \tag{4.4}$$

where index contractions are with the 4D metric g_{MN}, and $g = |\det g_{MN}|$. This is probe limit of the model in Ref. [14], as we discussed in the Introduction.

The action in r-coordinates has the form

$$S = \int d^3x\, dr\, r^2 \left\{ \frac{1}{2r^2 F(r)} (F_{0a})^2 - \frac{1}{4} r^{-4}(F_{ab})^2 + \frac{1}{2}(F_{0r})^2 - \frac{F}{2r^2}(F_{ar})^2 \right.$$
$$+ \frac{1}{F(r)} |(\partial_0 - iA_0)\psi|^2 - r^{-2}|(\partial_a - iA_a)\psi|^2$$
$$\left. - F(r)|(\partial_r - iA_r)\psi|^2 - m^2|\psi|^2 \right\}. \tag{4.5}$$

Here $F_{MN} = \partial_M A_N - \partial_N A_M$ is the field strength of the U(1) gauge field, and the charge of the field ψ is normalized to 1. Our convention is that Latin indices a, b, etc., represent spatial components x or y. We have explicitly shown the metric factors in Eq. (4.5), so remaining index contractions are taken with the Kronecker delta δ_{MN}. According to the AdS/CFT correspondence the mass m is related to the scaling dimension of the operator related to ψ, and for definiteness we will assume $m^2 = -2/L^2$ as in Ref. [15], corresponding to a Cooper pair operator of dimension 2 (or 1, as discussed below).

Defining $\phi \equiv A_0$ as in Ref. [15], and considering solutions with $\psi = \psi(r)$, $\phi = \phi(r)$ and $A_a = 0$, the coupled equations of motion for ψ and ϕ in the gauge where $A_r = 0$ are

$$\psi'' + \left(\frac{F'(r)}{F(r)} + \frac{2}{r} \right) \psi' + \frac{\phi^2}{F(r)^2}\psi - \frac{m^2}{F(r)}\psi = 0, \tag{4.6}$$

$$\phi'' + \frac{2}{r}\phi' - \frac{2|\psi|^2}{F(r)}\phi = 0. \tag{4.7}$$

Near the UV boundary, the solutions behave as [15],

$$\psi = \frac{\psi^{(1)}}{r} + \frac{\psi^{(2)}}{r^2} + \cdots , \tag{4.8}$$

$$\phi = \mu - \frac{\rho}{r} + \cdots . \tag{4.9}$$

The time component of the gauge field couples to the charge density, so the AdS/CFT correspondence identifies μ with the electric chemical potential and ρ with the charge density. For the Cooper pair operator there are two choices: either $\psi^{(1)}$ acts as a source and $\psi^{(2)}$ corresponds to the expectation value of the Cooper pair operator, or *vice versa*. This choice determines the scaling dimension of the Cooper pair operator according to the AdS/CFT correspondence, as discussed in the Introduction. For definiteness we will choose to take $\psi^{(1)}$ as the source of the Cooper pair operator O_2, which then has mass dimension two; the other choice would correspond to an operator of dimension 1. The Cooper pair operator should only be turned on dynamically, so vanishing of its source becomes a UV boundary condition, $\psi^{(1)} = 0$. Additional boundary conditions are $\phi(r_H) = 0$ for regularity of the solution and $\phi(\infty) = \mu$. The equations of motion enforce the condition $F'(r)\psi'(r) = m^2\psi(r)$ at the horizon if $\psi(r)$ is finite, so the additional boundary condition on ψ at the horizon is replaced with a regularity condition.

In order to study the response of our system to an oscillating electric field, we consider solutions for which A_x oscillates in time, $A_y = A_r = 0$ and A_0 behaves as in Eq. (4.9). Assuming the form

$$A_x(t, r) = e^{-i\omega t}A(r), \tag{4.10}$$

the bulk equation of motion for A_x has the form,

$$-\frac{\omega^2}{F(r)}A(r) - \frac{d}{dr}\left[F(r)A'(r)\right] + 2A(r)|\psi(r)|^2 = 0. \tag{4.11}$$

For large r the solutions for A_x have the form

$$A_x = A_x^{(0)} + A_x^{(1)}/r + \cdots . \tag{4.12}$$

According to the AdS/CFT correspondence, $A_x^{(0)}$ acts as the source for the current j^x and hence corresponds to a background electric field $E_x = \partial_t A_x^{(0)}$. The AdS/CFT correspondence also suggests an identification of the normalizable component $A_x^{(1)}$ with (minus) the current j^x in the given background state [55, 53]. In Sec. 4.3, we explain how this identification arises in the deconstructed model. Hence, we can write[2]

$$E_x = \partial_t A_x|_{r\to\infty} = -i\omega A_x|_{r\to\infty}.$$
$$j^x = -A_x^{(1)} = r^2\partial_r A_x|_{r\to\infty}. \tag{4.13}$$

The conductivity σ is therefore determined in the holographic model by

$$\sigma = \frac{j^x}{E_x} = \left.\frac{r^2 A'(r)}{-i\omega A(r)}\right|_{r\to\infty}, \tag{4.14}$$

---

[2]The sign differences in these expressions compared with Ref. [15] are due to differences in convention related to the signature of the metric. We follow the conventions of Jackson's *Classical Electrodynamics* [126].

4.2.1 The Normal Phase

At temperatures greater than T_c the charged field ψ vanishes, in which case solutions of the following first order equations also solve Eq. (4.11):

$$A'_\pm(r) = \pm\frac{i\omega}{F(r)}A_\pm(r). \tag{4.15}$$

The solutions are

$$\begin{aligned}
A_\pm(r) &= \exp\left\{\pm i\omega \int \frac{dr}{F(r)}\right\}\\
&= \exp\left\{\pm\frac{i\omega}{6r_H}\left(2\sqrt{3}\tan^{-1}\left[\frac{2r+r_H}{\sqrt{3}\,r_H}\right] + \log\left[\frac{(r-r_H)^2}{r^2+rr_H+r_H^2}\right]\right)\right\}.
\end{aligned} \tag{4.16}$$

and the generic solution to Eq. (4.11) is a linear combination $A(r) = c_+A_+(r) + c_-A_-(r)$ with constants c_+ and c_-. The choice of branch of the inverse tangent and the logarithm in Eq. (4.16) determines an ω-dependent constant multiplying each of the two solutions, which can be absorbed in the coefficients c_+ and c_-. The solution $A_-(r)$ describes a wave flowing into the black hole horizon, and $A_+(r)$ describes an outgoing wave. Son and Starinets have advocated the choice of ingoing-wave solution as a boundary condition at the horizon, based on the requirement of causality of correlators calculated by the AdS/CFT correspondence [58]. For now, we explore the consequences of the generic solution, for guidance as to what to expect from the deconstructed model. A natural choice for the boundary condition in the discretized theory is more ambiguous because causality may be imposed at the level of the lower-dimensional theory, without regards to the effective higher-dimensional description.

The complex conductivity as a function of frequency distinguishes the normal and superconducting phases. A hallmark of perfect conductivity is a delta function in the real part of the conductivity at zero frequency which, by the Kramers-Kronig relation

for the conductivity, is tantamount to a zero-frequency pole in the imaginary part. The Kramers-Kronig relation follows from the assumption that correlations are causal. As a consequence, the conductivity $\sigma(\omega)$, which by definition is the Fourier transform of the response function relating the current to a background electric field, is analytic in the upper half plane. The Kramers-Kronig relation is then the statement of Cauchy's integral theorem for the following integral:

$$\oint_C \frac{\sigma(\omega')}{\omega' - \omega} d\omega' = \mathcal{P} \int_{-\infty}^{\infty} \frac{\sigma(\omega')}{\omega' - \omega} d\omega' - i\pi\,\sigma(\omega) = 0, \qquad (4.17)$$

where the contour C spans the real axis above the pole at $\omega' = \omega$ and closes in the upper half plane, and $\mathcal{P}$ represents the principal value of the integral. The conductivity $\sigma(\omega)$ is assumed to fall off in the upper half plane faster than $1/|\omega|$, so that that integral over the contour at infinity vanishes. As a consequence of Eq. (4.17), if the real part of $\sigma(\omega)$ has a delta-function at $\omega = 0$ then the imaginary part has a pole at $\omega = 0$, and *vice versa*.

It follows from Eqs. (4.14) and (4.15) that when ψ vanishes, the zero-frequency pole in $\mathrm{Im}[\sigma(\omega)]$ is generically absent; the holographic description indeed describes a non-superconducting phase when the condensate vanishes, for a generic choice of boundary condition at the horizon. Note that for both the ingoing-wave and outgoing-wave solutions, the normal-phase conductivity is independent of ω: $\sigma = +1$ for the ingoing wave, and $\sigma = -1$ for the outgoing wave. This result provides a phenomenological motivation for the ingoing-wave boundary conditions: the outgoing-wave solution would describe an unusual situation in which the current produced by an electric field points in the direction opposite to the electric field. Note also that the conductivity in this model does not indicate the existence of a pseudogap phase, and does not fall off at large ω due to relaxation as in ordinary materials.

For the generic solution for A_r with vanishing ψ and with the identification $r_{\mathrm{H}} =$

$4\pi T/3$, Eq. (4.14) gives the normal-phase conductivity:

$$\sigma(\omega) = \frac{c_- \exp\left(\frac{-i\sqrt{3}\omega}{8T}\right) - c_+ \exp\left(\frac{i\sqrt{3}\omega}{8T}\right)}{c_- \exp\left(\frac{-i\sqrt{3}\omega}{8T}\right) + c_+ \exp\left(\frac{i\sqrt{3}\omega}{8T}\right)}.$$ (4.18)

The real part of the conductivity is then,

$$\mathrm{Re}[\sigma(\omega)] = \frac{|c_-|^2 - |c_+|^2}{|c_-|^2 + |c_+|^2 + c_- c_+^* e^{\frac{-i\sqrt{3}\omega}{4T}} + c_+ c_-^* e^{\frac{i\sqrt{3}\omega}{4T}}},$$ (4.19)

which oscillates as a function of ω/T around $\sigma = 1$ for constant $|c_+| \ll |c_-|$.

4.2.2 The Superconducting Phase

For small enough T, the coupling between ϕ and ψ leads to an instability which turns on the Cooper pair condensate $\langle O_2 \rangle$. The condensate depends on the chemical potential μ and the charge density ρ determined by the solution to the coupled equations of motion. As argued in Ref. [15], the critical temperature scales as $\rho^{1/2}$. Near T_c the condensate behaves as $\langle O_2 \rangle \propto (1 - T/T_c)^{1/2}$. The complex conductivity for generic $T < T_c$ has a delta function at $\omega = 0$ and a gap ω_g, as expected for typical superconductors, but with $\omega_g/T_c \approx 8$ [15], significantly larger than the BCS prediction $\omega_g/T_c \approx 3.5$. The phenomenology of the deconstructed model has similarities to that of the continuum theory, even with only a few lattice sites, as we will see in Sec. 4.4.

4.3 Deconstructed Model

We will now develop a dimensionally deconstructed version of the continuum holographic model of the previous section. We will identify, in an analogous fashion to the continuum case, a charged condensate and determine its near-T_c temperature dependence;

and we will calculate the frequency dependent conductivity.

In the deconstructed model we will define coordinates differently, replacing r with a new coordinate $z = 1/r$. In z-coordinates, the extra dimension corresponds to a finite coordinate interval. The metric in z-coordinates has the form

$$ds^2 = \frac{1}{z^2} \left[f(z)dt^2 - \frac{1}{f(z)}dz^2 - (dx^2 + dy^2) \right], \qquad (4.20)$$

where

$$f(z) = \frac{1}{L^2} \left(1 - \frac{z^3}{z_{\mathrm{H}}^3} \right), \qquad (4.21)$$

and z runs from 0 to z_{H}. The surface $z = 0$ is the ultraviolet boundary, and $z = z_{\mathrm{H}}$ is the horizon. One should keep in mind that results are coordinate independent in the continuum model, but away from the continuum limit, deconstructed models depend on the choice of coordinates in which their extra-dimensional parent model is defined.

In z-coordinates, the action in the continuum theory takes the form

$$\begin{aligned}
\mathcal{S} &= \int d^4 x \left\{ \frac{1}{2}F_{0z}^2 + \frac{1}{2f}F_{0a}^2 - \frac{f}{2}F_{za}^2 - \frac{1}{4}F_{ab}^2 + \frac{1}{z^2 f}|\partial_0\psi - iA_0\psi|^2 \right. \\
&\qquad \left. - \frac{f}{z^2}|\partial_z\psi - iA_z\psi|^2 - \frac{1}{z^2}|\partial_a\psi - iA_a\psi|^2 - \frac{1}{z^4}m^2|\psi|^2 \right\}.
\end{aligned} \qquad (4.22)$$

where repeated a or b indices are summed over the spatial coordinates x and y. As before, we use the notation of Ref. [15], where we define $\phi \equiv A_0$. We replace the z axis by a lattice of N points,

$$z_j = \begin{cases} \epsilon + (j-1)a & \text{for } j = 1 \ldots N-1 \\ \epsilon + (N-2)a + a_{\mathrm{H}} & \text{for } j = N . \end{cases} \qquad (4.23)$$

where $z_N = z_{\mathrm{H}}$ and ϵ is a UV cutoff. The lattice spacing a_j between the j and $j+1^{\mathrm{th}}$ lattice sites is therefore a for $j = 1 \ldots N-2$ and a_{H} for $j = N-1$. We give ourselves the
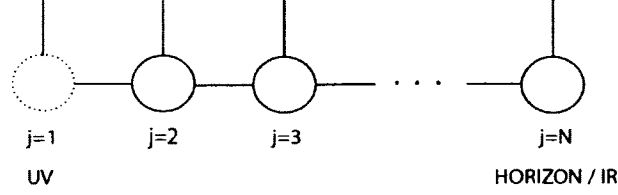
FIG. 4.1: Moose diagram representation of the deconstructed theory.

freedom to vary a_H away from a to test the sensitivity of our results to the density of sites nearest to the horizon. The discretized action is given by

$$
\begin{aligned}
S = \sum_{j=1}^{N-1} a_j \int d^3x \left\{ \frac{1}{2}(\partial_0 A_{zj} - \phi_j')^2 + \frac{1}{2f_j}(F_{0a})_j^2 - \frac{f_j}{2}(\partial_a A_{zj} - A_{aj}')^2 \right. \\
- \frac{1}{4}(F_{ab})_j^2 + \frac{1}{z_j^2 f_j}|\partial_0 \psi_j - i\phi_j \psi_j|^2 - \frac{f_j}{z_j^2}|\psi_j' - iA_{zj}\psi_j|^2 \\
\left. - \frac{1}{z_j^2}|\partial_a \psi_j - iA_{aj}\psi_j|^2 - \frac{1}{z_j^4}m^2|\psi_j|^2 \right\} ,
\end{aligned}
\tag{4.24}
$$

where $f_j \equiv f(z_j)$. We define derivatives in the discretized action such that

$$
\phi_j' \equiv (\phi_{j+1} - \phi_j)/a_j ,
\tag{4.25}
$$

and similarly for the other fields in the theory. We now construct a 3D theory that reproduces Eq. (4.24), up to differences at the $j = 1$ and N boundaries. These differences will be required for a proper holographic interpretation of the deconstructed theory.

Consider a 3D theory with N global U(1) symmetries of which $N - 1$ are gauged. We label the $N - 1$ gauge factors by the index $j = 2 \ldots N$. We introduce a set of bifundamental complex scalar fields Σ_j, $j = 1 \ldots N - 1$, where Σ_j transforms under the jth and $(j + 1)^{\text{th}}$ U(1) factors, with charges -1 and $+1$, respectively. In addition, we introduce N complex scalar fields ψ_j, $j = 1 \ldots N$, where ψ_j transforms under the jth U(1) factor, with charge $+1$. The particle content and charge assignments of this theory are conveniently summarized

by the moose diagram shown in Fig. 4.1. The solid circles represent U(1) gauge groups. while each line connecting to a given circle represents a complex scalar field that transforms under that group. The global U(1) symmetry is represented by the dotted circle at the left end of the moose.

We assume that the bifundamental fields develop vacuum expectation values (vevs) $\langle \Sigma_j \rangle \equiv v_j$. Although the first link field Σ_1 is charged under the global U(1) factor, the global symmetry nevertheless remains unbroken if the ψ_j have vanishing expectation values. This can be seen by noting that the effect of a global phase rotation on $\langle \Sigma_1 \rangle$ can be undone by a (constant and spatially uniform) U(1) gauge transformation at the $j = 2$ site. The effect of this phase rotation on $\langle \Sigma_2 \rangle$ can then be undone by a U(1) gauge transformation at the $j = 3$ site, and so on. In this way, one sees that the global symmetry of the first site remains an invariance of the vacuum, even when the link field vevs assume a nonvanishing profile. We therefore identify the current associated with the global symmetry of the first site as the QED current j^μ. As has been discussed in the literature [15], even though the U(1) symmetry associated with QED is not gauged, the model still describes aspects of superconductivity to the extent that a treatment of electromagnetic fields as external backgrounds is appropriate. In the deconstructed model we could simply add a kinetic term for the associated U(1) gauge field to describe a fully dynamical electromagnetism. but in order to match the AdS/CFT description we will not do that here.

In order to compute expectation values of j^μ, we will turn on a non-propagating gauge field at the first site, A_1^μ, that couples to this current. We will also assume that the gauge field at the last site A_N^μ is non-propagating and assumes a specified background configuration; this will allow us to impose incoming-wave boundary conditions near the horizon. The boundary fields ψ_1 and ψ_N are also assumed to be non-propagating below, but only to simplify the discussion. The case in which all the ψ_j are dynamical is discussed

in an appendix.

The Lagrangian for the 3D theory in Fig. 4.1 is of the form

$$\mathcal{L} = \sum_{j=2}^{N-1} \left[-\frac{1}{4}(F_{\mu\nu})_j (F^{\mu\nu})_j + Z_j |D_\mu \psi_j|^2 \right] + \sum_{j=1}^{N-1} \left[|D_\mu \Sigma_j|^2 - Z_j V_j \right] \qquad (4.26)$$

where V_j determines the scalar potential at the jth site. The coefficients Z_j and the 3D metric $g_j^{\mu\nu}$ vary from site to site. Although we use the term "metric" to refer to $g_j^{\mu\nu}$, the $g_j^{\mu\nu}$ simply encode the Lorentz-violating couplings of the theory. The covariant derivative is given by

$$D^\mu \Sigma_j = \partial^\mu \Sigma_j + iA_j^\mu \Sigma_j - iA_{j+1}^\mu \Sigma_j \,, \qquad (4.27)$$

and

$$D^\mu \psi_j = \partial^\mu \psi_j - iA_j^\mu \psi_j \,. \qquad (4.28)$$

Notice the absence of ψ_j and A_j kinetic terms for $j = 1$ and $j = N$ in Eq. (4.26). We identify the non-propagating fields that appear at the ends of the moose with fixed backgrounds in the ultraviolet (UV) and the infrared (IR):

$$\begin{aligned} A_1^\mu &\equiv A_{\text{UV}}^\mu(x^\nu)\,, & \psi_1 &\equiv \psi_{\text{UV}}(x^\nu)\,, \\ A_N^\mu &\equiv A_{\text{IR}}^\mu(x^\nu)\,, & \psi_N &\equiv \psi_{\text{IR}}(x^\nu)\,. \end{aligned} \qquad (4.29)$$

We can now compare Eq. (4.26) to the Lagrangian obtained by latticizing the z coordinate of the continuum theory, Eq. (4.24). Up to differences that vanish in the $a \to 0$ limit, one finds after some algebra that the latticized theory is recovered if one chooses

$$g_j^{00} = \frac{1}{f_j}\,, \qquad g_j^{ab} = -\delta^{ab}\,, \qquad Z_j = \frac{1}{z_j^2} \qquad \text{and} \qquad v_j = \frac{1}{a_j}\sqrt{\frac{f_j}{2}}\,, \qquad (4.30)$$

the scalar potential

$$
V_j = \begin{cases} 2|v_j\psi_{j+1} - \psi_j\Sigma_j|^2 & \text{for} \quad j = 1 \\ 2|v_j\psi_{j+1} - \psi_j\Sigma_j|^2 + m^2|\psi_j|^2/z_j^2 & \text{for} \quad j = 2\ldots N-1 \end{cases}
\tag{4.31}
$$

and the identification

$$
\Sigma_j = v_j \exp[ia_j A_{zj}] \approx v_j(1 + ia_j A_{zj}) \, .
\tag{4.32}
$$

The potential is not the most general one consistent with the symmetries of the theory; as in any deconstructed model, the form of the action is dictated by the requirement that it reproduce the latticized action obtained from the continuum theory. For example, Eq. (4.31) is fine-tuned so that the $(\psi_i')^2$ term in Eq. (4.24) is reproduced when Σ_j is set equal to its vev. For definiteness, we fix the mass parameter m^2 to its holographically motivated value $m^2 = -2$. One could allow m to deviate from this choice in more general theories, but we will not consider that possibility here. The temperature dependence of terms in the action is inferred from the form of f_j, which depends on temperature via $z_H = 3/(4\pi T)$. One could also imagine more general moose models in which the temperature dependence of the f_j is determined directly from the microscopic properties of the system. Here we will strictly consider the f_j that follow from discretizing the continuum holographic theory.

In what follows, we work in unitary gauge, corresponding to the gauge $A_z = 0$ in the four-dimensional theory. As in Eq. (4.32), we ignore the physical fluctuations of the link fields about their vevs. Then, the Lagrangian of the moose model may be written

$$
\mathcal{L} = \sum_{j=1}^{N-1} a_j \left[\frac{1}{2}(\phi_j')^2 - \frac{f_j}{2}(A_{aj}')^2 - \frac{f_j}{z_j^2}|\psi_j'|^2 \right] + \sum_{j=2}^{N-1} a_j \left[\frac{1}{2f_j}(F_{0a})_j^2 - \frac{1}{4}(F_{ab})_j^2 \right]
$$

$$
+ \sum_{j=2}^{N-1} a_j \left[\frac{1}{z_j^2 f_j}|\partial_0\psi_j - i\phi_j\psi_j|^2 - \frac{1}{z_j^2}|\partial_a\psi_j - iA_{aj}\psi_j|^2 - \frac{1}{z_j^4}m^2|\psi_j|^2 \right] \, .
\tag{4.33}
$$

One may now derive the equations of motion for the dynamical fields ($j = 2 \ldots N - 1$), assuming the same ansatz applied in the continuum theory. For ϕ_j that are time-independent and spatially constant, the equations of motion for the dynamical fields are given by

$$\phi_j'' - \frac{2}{z_j^2 f_j} \phi_j \, \psi_j^2 = 0 \,, \qquad (4.34)$$

where $\phi_j'' \equiv (\phi_{j+1} - 2\phi_j + \phi_{j-1})/a^2$, for $j = 2 \ldots N - 2$ and $\phi_{N-1}'' \equiv [(\phi_N - \phi_{N-1})/a_H - (\phi_{N-1} - \phi_{N-2})/a]/a_H$. For the same ansatz, the equations of motion for the ψ_j are given by

$$\psi_j'' + \frac{1}{a_j} \left(1 - \frac{z_j^2}{z_{j-1}^2} \frac{f_{j-1}}{f_j} \right) \psi_{j-1}' + \frac{1}{f_j^2} \phi_j^2 \psi_j - \frac{m^2}{z_j^2 f_j} \psi_j = 0 \,, \qquad (4.35)$$

where ψ_j'' is defined analogously to ϕ_j'' and $\psi_j' \equiv (\psi_{j+1} - \psi_j)/a_j$. When ϕ_j is nonvanishing, corresponding to a nonvanishing chemical potential and charge density, the coupling between ϕ_j and ψ_j in Eq. (4.35) acts as a negative squared mass term for each Cooper pair field ψ_j, creating an instability that is enhanced for z_j near z_H by the temperature-dependent factor of $1/f_j^2$.

Finally, we will require the equation of motion for the spatial components of the gauge field, assuming spatially constant fields and the time dependence

$$A_{aj}(x^\mu) \equiv A_{aj} e^{-i\omega t} \,. \qquad (4.36)$$

Again for $j = 2 \ldots N - 1$, one finds

$$A_{aj}'' + \frac{1}{a_j} \left(1 - \frac{f_{j-1}}{f_j} \right) A_{aj-1}' + \left(\frac{\omega^2}{f_j^2} - 2 \frac{\psi_j^2}{z_j^2 f_j} \right) A_{aj} = 0 \,, \qquad (4.37)$$

where A_j'' and A_j' are defined analogously to ψ_j'' and ψ_j'. The exciton fields $(A_a)_j$ are excited collectively by the external electromagnetic field $(A_a)_1$.

The horizon boundary condition on Eqs. (4.34) and (4.35) that correspond to those of the continuum theory are

$$\phi_N = 0 \quad \text{and} \quad \psi'_{N-1} = \frac{2}{3z_N}\psi_N \,. \tag{4.38}$$

If the ψ_N field were dynamical at the last site, it turns out that the same boundary condition on ψ would follow from the ψ_N equation of motion in the continuum limit, as we discuss in the Appendix. The boundary condition on the spatial components of A_N can be chosen to reproduce the incoming-wave boundary conditions in the continuum limit, as we discuss in more detail below.

In the continuum holographic theory, physical quantities of interest are related to the values and derivatives of the fields at the UV boundary. In the deconstructed theory, we find that similar relations apply to the expectation value of the charge density ρ and the current density j^a, which are identified via their coupling to the background field A_{UV}^μ:

$$j^\mu = i\frac{\delta}{\delta A_{UV\mu}} \ln\left\{ \int \prod_{j=2}^{N-1} \mathcal{D}A_j \mathcal{D}\psi_j \, e^{iS} \right\} \,. \tag{4.39}$$

This reduces at tree-level to

$$j^\mu = -\frac{\delta}{\delta A_{UV\mu}} S_{cl}[A_{UV}] \,, \tag{4.40}$$

where the dependence on A_{UV} arises since the fields are evaluated on their classical equations of motion. In the linearized theory, one finds algebraically that S_{cl} evaluates to a sum of surface terms

$$S_{cl} = \int d^3x \, [\mathcal{L}_{UV} + \mathcal{L}_{IR}] \,, \tag{4.41}$$

where the terms involving the exciton fields are given by

$$\mathcal{L}_{\text{UV}} = -\frac{1}{2a}\,\phi_1(\phi_2 - \phi_1) + \frac{1}{2a}f_1\,A_{a1}(A_{a2} - A_{a1}) \qquad (4.42)$$

and

$$\mathcal{L}_{\text{IR}} = -\frac{1}{2a_{\text{H}}}f_{N-1}\,A_{aN}(A_{aN} - A_{a\,N-1})\,, \qquad (4.43)$$

using the boundary condition $\phi_N = 0$. Before evaluating Eq. (4.40), we first arrange that the IR surface term vanishes. This is consistent with the approach in the continuum holographic theory, where the IR surface term is also present, but is simply discarded [58]. To eliminate Eq. (4.43), we can add an *ad hoc* term to the Lagrangian such that the desired IR boundary condition is consistent with vanishing IR surface term. Near the horizon, the ingoing-wave solution satisfies Eq. (4.15), which can be imposed as a boundary condition in the deconstructed model in a number of ways. We choose to approximate the ingoing-wave boundary condition as

$$A'_{a\,N-n-1} = \frac{i\omega}{f_{N-n-1}}A_{a\,N-n} \qquad (4.44)$$

for some n, with $n \ll N$ in the continuum limit $N \to \infty$. If n is taken too small, the factor of $1/f$ in Eq. (4.44) is large and magnifies the discrepancy between the discretized and continuum boundary conditions. Integrating from $j = n$ towards the horizon and solving the ω^2-dependent equations of motion, one obtains a relation between $A_{a\,N}$ and $A_{a\,N-1}$ that generally leads to a nonvanishing surface term. However, if we add a new term to the Lagrangian of the form

$$\mathcal{L}_{\text{H}} = \xi\left[c(\omega^2)A_{a\,N} - A_{a\,N-1}\right]^2\,, \qquad (4.45)$$

then the new IR surface term, evaluated on the solution to the equations of motion, becomes a function of $c(\omega^2)$. This function can be chosen so that the surface term vanishes. Eq. (4.45) can be expressed as a function of the gauge-invariant field strength tensors

$F_{rz\,N-1}$ and $F_{0r\,N-1}$. and the function $c(\omega^2)$ may be interpreted as a function of $-\partial_t^2$, which ultimately acts on the non-dynamical field A_{aN}. The function $c(\omega^2)$ may be replaced by a polynomial approximation, valid at least over some finite range in ω. In this way, our discrete approximation to the ingoing-wave boundary condition. Eq. (4.44). can be imposed n sites away from the IR boundary, while the IR surface term is arranged to vanish.

The expectation value of the current thus depends only on the UV surface terms, as in the continuum holographic theory. Each $j = 2$ field in Eq. (4.42) can be related to the corresponding boundary field by the discrete version of a bulk-to-boundary propagator. For example, we could write $\phi_j = B_{j1}\phi_1$, for some bulk-to-boundary propagator B_{j1}. Then the charge density is found by computing

$$\rho = \frac{\delta}{\delta\phi_1}\left[-\frac{1}{2a}\phi_1^2\,(B_{21} - 1)\right] = -\frac{1}{a}\phi_1\,(B_{21} - 1)\,. \tag{4.46}$$

The quantity $\phi_1(B_{21} - 1)/a$ is nothing more than what we would find by numerically solving the ϕ equation of motion and evaluating ϕ_1' as we defined it previously. Hence, we conclude

$$\rho = -\phi_1'\,, \tag{4.47}$$

in agreement with the holographic prescription for computing the charge density in the continuum theory. By the same reasoning. the current density following from Eq. (4.42) is given by

$$j^a = -f_1 A_{a1}'\,, \tag{4.48}$$

which also agrees with the usual holographic prescription in the continuum, where $f_1 \to 1$. Since j^0 is proportional to the charge density operator. we identify ϕ_1 with the chemical

potential

$$\mu = \phi_1 \,. \tag{4.49}$$

The transition to the superconducting phase occurs when the ψ_j develop a nonvanishing profile. In the continuum limit, $\psi(z)$ takes the form $\psi(z) = \psi^{(1)}z + \psi^{(2)}z^2$ near the UV boundary, so that the existence of the condensate is determined by nonvanishing first or second derivatives:

$$\psi^{(1)} \equiv \psi'(z = 0) \neq 0 \quad \text{or} \quad \psi^{(2)} \equiv \frac{1}{2}\psi''(z = 0) \neq 0 \,. \tag{4.50}$$

In the discretized theory, we use the analogous expression $\psi_j = \psi^{(1)}z_j + \psi^{(2)}z_j^2$ evaluated at the first two lattice sites ($z_1 = \epsilon$ and $z_2 = \epsilon + a$) to define the operators $\psi^{(1)}$ and $\psi^{(2)}$,

$$\psi^{(1)} = \frac{\psi_2\,\epsilon^2 - \psi_1(\epsilon + a)^2}{\epsilon^2(\epsilon + a) - \epsilon(\epsilon + a)^2} \quad \text{and} \quad \psi^{(2)} = \frac{\psi_2\,\epsilon - \psi_1(\epsilon + a)}{\epsilon(\epsilon + a)^2 - \epsilon^2(\epsilon + a)} \,. \tag{4.51}$$

These definitions have the appropriate continuum limit. As in Sec. 4.2, we restrict ourselves to the case where $\psi^{(1)} = 0$ and we define the order parameter to be $\langle O_2 \rangle \equiv \sqrt{2}\psi^{(2)}$, following the conventions of Ref. [15]. Although $\psi^{(1)}$ and $\psi^{(2)}$ do not have the same holographic interpretation in the deconstructed theory away from the continuum limit, our definitions provide an accurate measure of whether a nonvanishing profile of the ψ_j has been dynamically generated.

4.4 Results

In this section, we numerically solve the discretized theory of Sec. 4.3 for $N \in \{5, 10, 100, 1000\}$. In the case of $N = 1000$, for the purpose of connecting with the continuum theory, we fix the UV cutoff $z_1 = \epsilon = 10^{-1}$, while for other N we set $\epsilon = a$, the

bulk lattice spacing. We fix the lattice spacing at the horizon $a_H = 10^{-5}$. In all cases, we impose the following boundary conditions:

$$\phi_1' = -\rho = -1, \quad \psi^{(1)} = 0, \quad \phi_N = 0, \quad \text{and } \psi_{N-1}' = \frac{2}{3z_N}\psi_N, \quad (4.52)$$

where we have used the scaling symmetry of the theory to fix T_c by setting $\rho = 1$. Searching for nonvanishing ψ_j solutions as we vary the temperature, we find there is a critical temperature for each N at which the operator $\langle O_2 \rangle$ condenses, as shown in Fig. 4.2. We note that there are numerous non-zero solutions for ψ_j but, as in the continuum model [15], we retain only the monotonic solutions. For $N = 5$, $N = 10$, $N = 100$, and $N = 1000$ we find the critical temperatures $T_c = 0.076\,\rho^{1/2}$, $T_c = 0.088\,\rho^{1/2}$, $T_c = 0.111\,\rho^{1/2}$, and $T_c = 0.118\,\rho^{1/2}$ respectively. Here we reintroduced the factor of $\rho^{1/2}$ as indicated by the scaling relations. It is interesting to see that for all N we retain the square root behavior of the phase transition. We find that the curves in Fig. 4.2 near T_c are well fit by the form $\langle O_2 \rangle = C_N T_c^2 (1 - T/T_c)^{1/2}$. The values we obtain for the coefficients are $C_{1000} = 127$, $C_{100} = 20$, $C_{10} = 58$, and $C_5 = 93$, as compared to the continuum value $C = 144$ [15].

We would also like to study the behavior of the complex conductivity away from the continuum limit. Using the expression for the current Eq. (4.48), we find the following expression for the conductivity:

$$\sigma = \frac{j^x}{E_x} = \frac{j^x}{\dot{A}_x} = -\frac{if_1(A_{x2} - A_{UVx})/a}{\omega A_{UVx}}. \quad (4.53)$$

As discussed in Sec. 4.3, we impose the ingoing-wave boundary condition, Eq. (4.44), n
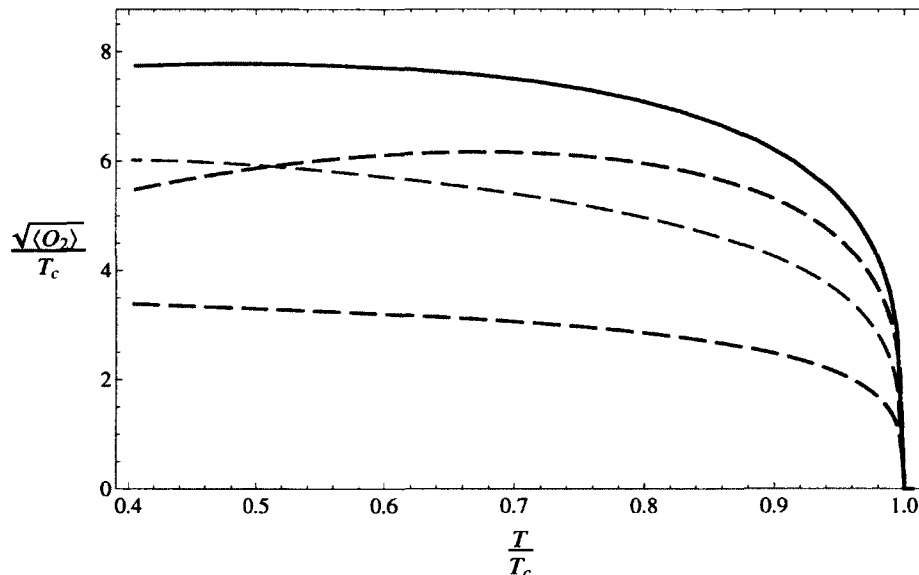
FIG. 4.2: This figure displays the condensation phase transition at critical temperature $T = T_c$. The top curve is the $N = 1000$ curve and below that the dashed curves from top to bottom around T_c are $N = 5$, $N = 10$, and $N = 100$, respectively. The 1000-site curve includes a fixed UV cutoff ϵ, which allows for a smooth continuum limit.

sites away from the horizon. In particular, we set

$$A_{xN-n} = 1 \quad \text{and} \quad A_{xN-n-1} = 1 - \frac{i\omega a}{f_{N-n-1}}, \tag{4.54}$$

where we have fixed the arbitrary normalization $A_{xN-n} = 1$. Our choices for the shift n for $N = 1000, 100, 10$ and 5 are $n = 20, 10, 2$ and 2, respectively. With these boundary conditions for A_{xj} we compute the real and imaginary parts of σ, as shown in Figs. 4.3 and 4.4. It is important to note that the graphs of $\text{Im}[\sigma(\omega)]$ in the superconducting phase exhibit a simple pole at $\omega = 0$. This implies the presence of a delta function contribution to the real part, $\text{Re}[\sigma(\omega)] \propto \delta(\omega)$, as discussed in Sec. 4.2. For $N = 10$ there are a series of peaks in $\text{Re}[\sigma(\omega)]$ with a corresponding pole-like structure in the imaginary part as follows from the Kramers-Kronig relation Eq. (4.17). Finally, the oscillatory behavior of $\text{Re}[\sigma(\omega)]$ at large ω displayed in the $N = 100$ and $N = 1000$ plots is consistent with our expectation

from Eq. (4.19) given that our boundary condition is only approximately ingoing wave.

FIG. 4.3: Complex conductivities. The $(N, T/T_c)$ values for the top and bottom rows are given by $(1000, 0.55)$ and $(100, 0.53)$, respectively. The dotted (red) curve is the normal (n) phase while the dashed (blue) curve is the superconducting (sc) phase. The vertical arrow represents a delta function. The solid (black) curve is the ratio: $\text{Re}(\sigma_{sc})/\text{Re}(\sigma_n)$.

4.5   Outlook

Dimensional deconstruction is a powerful technique for finding lower-dimensional theories that share some of the interesting phenomenological features of their higher-dimensional progenitors. In this paper, we have considered the dimensional deconstruction of four-dimensional holographic theories of superconductivity. We have shown how the AdS/CFT prescriptions for computing physical quantities of interest (for example, charge densities and currents) emerge in the lower-dimensional, discretized theory. We have also
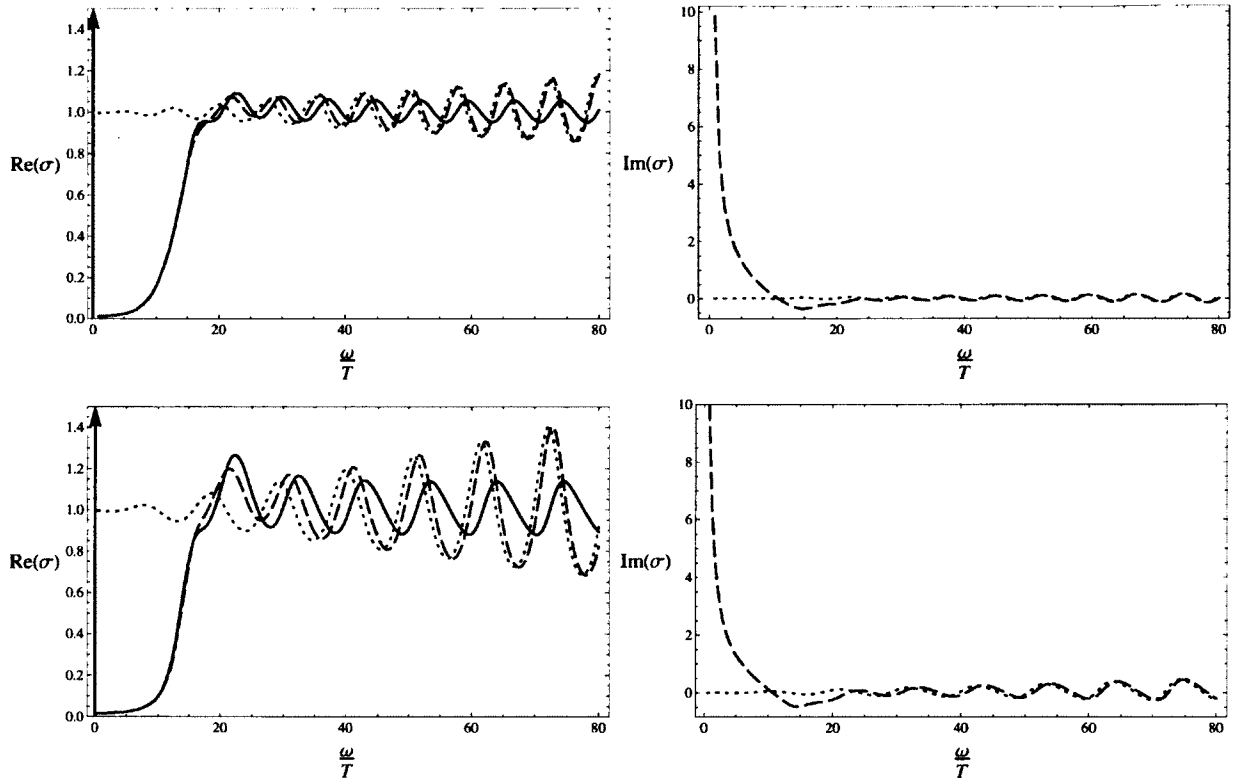
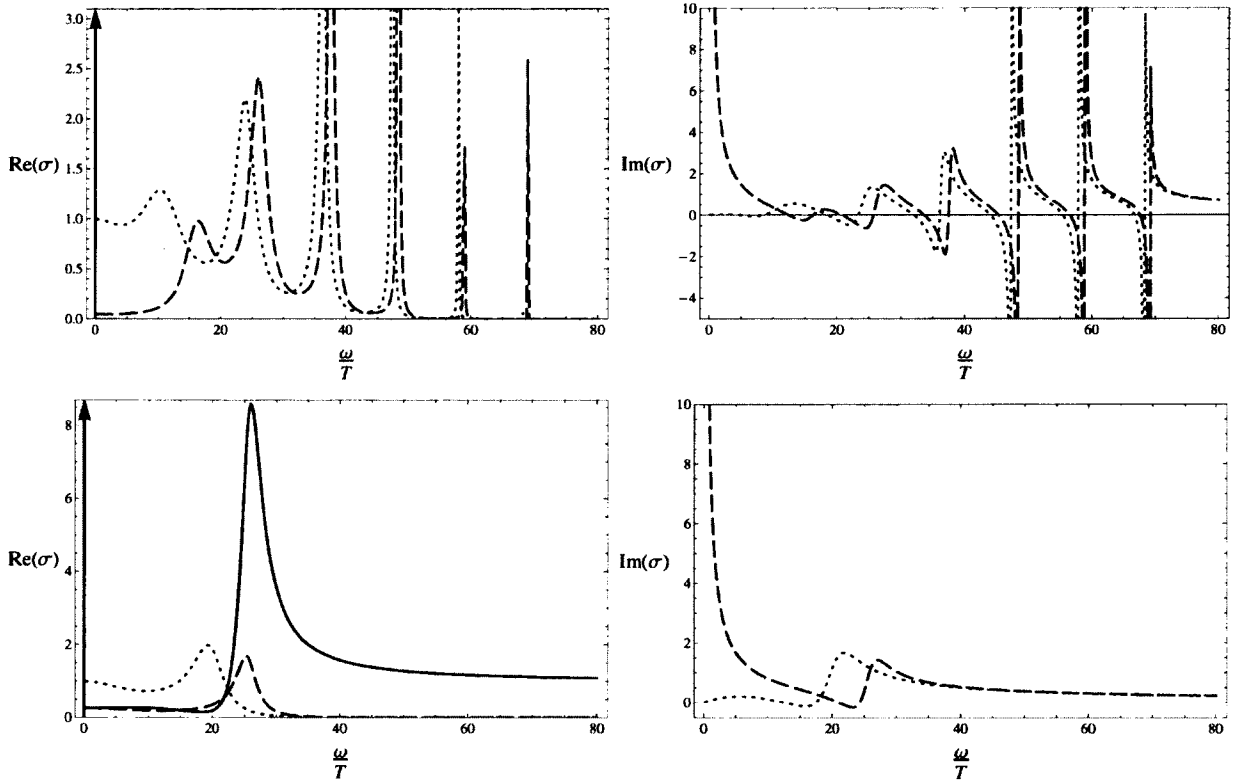FIG. 4.4: Complex conductivities. The $(N, T/T_c)$ values for the top and bottom rows are given by (10, 0.54) and (5, 0.50), respectively. The dotted (red) curve is the normal (n) phase while the dashed (blue) curve is the superconducting (sc) phase. The vertical arrow represents a delta function. The solid (black) curve (omitted for $N = 10$, for clarity) is the ratio: $\mathrm{Re}(\sigma_{sc})/\mathrm{Re}(\sigma_n)$.

demonstrated that deconstructed theories with a relatively small number of lattice sites (here taken ≥ 5) do indeed retain enough of the physics of the continuum limit to provide possible models of superconductivity on their own.

The results presented in this chapter are preliminary, in the sense that we have only considered the deconstruction of one of the simplest, s-wave holographic superconductors that were proposed in the first papers on the application of the AdS/CFT correspondence to this problem. Much of what we have found leads to questions and suggestions for future study:

- Dimensional deconstruction also motivates new models of p- and d-wave superconductors. It would be interesting to study the phenomenology of those models.

- In the our approach, the photon field is not included as a dynamical degree of freedom in the deconstructed theory. However, the theory can be easily modified by gauging the electromagnetic U(1) symmetry and adding an associated gauge kinetic term.

- The deconstructed model suggests the possibility of hidden local symmetries in the interactions between Cooper pairs and excitons. Perhaps absorption studies would be able to test the existence of these states and interactions.

- If one deviates from a strict matching to the continuum holographic theory, then one has greater freedom in constructing a model that is based on a very small number of replicated gauge groups (for example, two or three). Would a two- or three-site model of superconductivity be phenomenologically viable? How would we build in the quasinormal mode behavior?

- The deconstructed model introduces temperature-dependent couplings inferred by a holographic model. It would be important to deduce these couplings instead from a microscopic description.

- In our presentation, the fluctuations of the link fields were ignored, consistent with the tacit assumption that these fields are heavy. However, these fields, which have no counterpart in the continuum holographic theory, might also have a physical interpretation.

CHAPTER 5

Conclusion

Holographic methods have the potential to be important calculational tools applicable to real materials. In the preceding chapters, we saw the AdS/CFT correspondence used to model a variety of physical systems. We used the general framework presented in the Introduction to model QCD (Chapters 2 and 3) and superconductors (Chapter 4). In the applications to QCD, the hard-wall model has only a few free parameters and allows for predictions accurate on the 10% level. Although the model has since been improved upon, it is representative of how well a simple holographic model can perform. In the application to superconductors, we studied a minimal holographic superconductor [15]. Although it too has been improved upon for more realistic phenomenology, this holographic superconductor represents a proof of principle: it was one of the very first examples of a holographic superconductor and demonstrated the holographic methods involved in calculating strongly-coupled superconducting physics. Using the idea of dimensional deconstruction we constructed some simple superconducting models in their natural (lower) spacetime dimension, which retain some of the qualitative features of the extra-dimensional holographic model. This was an example of a general idea, that can

be applied to extra-dimensional models. In this work, we covered only a narrow slice of research on the topic of applied AdS/CFT. The reader is encouraged to follow the literature where there are a number of excellent papers, articles, and reviews. A selection of my personal favorites are Refs. [26, 28, 29, 30, 31, 32, 33, 34, 127, 128, 129, 130, 131].

Hopefully it is clear that the holographic framework reviewed and demonstrated in this work is very flexible and well suited for model building. Once symmetries and relevant operators are identified, one can proceed to construct a holographic model and make predictions. It is important to point out that (at present) there is somewhat of a disconnect between constructing the holographic theory and identifying it with concrete, real-world systems. We can make holographic predictions but we don't know the specifics of the microscopic theory: for instance, in condensed matter applications, there's no direct contact with a specific lattice structure. There has, however, been much progress toward applying holography to real materials. Some of the most interesting results come from general considerations – trying to derive universal holographic truths. For example, as mentioned in the Introduction, there are various holographic sum rules and holographic bounds. If these results are obeyed in strongly-coupled materials, there's hope for a dual gravitational description. Encouraging progress has also been in the form of universality. Different microscopic models and holographic models flow to the same IR fixed point which may describe sought-after physics, such as the "strange metallic" behavior of the high-T_c cuprate superconductors [129, 132, 133]. Indeed, significant progress has been made on the classification of IR asymptotics for holographic theories [134]. This kind of unified viewpoint provides added incentive for the possible applicability of holographic models. Developing applications of holographic dualities to real-world physical systems is a very active area of research with exciting opportunities, and we can look forward to many interesting advances following this line of reasoning.

APPENDIX A

A Purely Dynamical ψ

Here we present a simple generalization to the analysis presented in Chapter 4. Recall it was assumed in Chapter 4 that the ψ_j fields at the ends of the moose, ψ_1 and ψ_N, were background fields. Here we show that the same boundary conditions would be obtained in the continuum limit if we allow all the ψ_j to be dynamical fields. The Lagrangian that is relevant in this case is a minor modification of Eq. (4.33); the third sum in this expression, which runs from $j = 2$ to $N - 1$, is changed to one which runs from $j = 1$ to N (with $a_N = a_H$) for the first two terms in square brackets and from $j = 2$ to N for the mass squared term. We also shift z_N away from its previous value by ϵ_H, which serves as a cutoff to regulate the divergence in $1/f_N$. Eq. (4.35) remains unaltered, but now there are two additional equations of motion, for ψ_1 and ψ_N:

$$\frac{1}{a}\psi_1' + \frac{1}{f_1^2}\phi_1^2\psi_1 = 0\,, \tag{A.1}$$

and

$$-\frac{1}{a_H}\psi_{N-1}' + \frac{z_{N-1}^2}{z_N^2 f_N f_{N-1}}\phi_N^2\psi_N + \frac{2z_{N-1}^2}{f_{N-1}z_N^4}\psi_N = 0\,, \tag{A.2}$$

where $\psi'_{N-1} = (\psi_N - \psi_{N-1})/a_H$. These equations can be viewed as dictating the boundary conditions for Eq. (4.33), which, in our previous approach, were chosen freely to mimic the boundary conditions of the continuum theory. Eq. (A.1) reduces in the continuum limit to the boundary condition $\psi'_1 = 0$. Since $\phi_N \equiv 0$, the second term in Eq. (A.2) vanishes ($1/f_N$ is finite for finite cutoff ϵ_H). Hence,

$$\psi'_{N-1} = \left[\frac{2a_H z_{N-1}^2}{f_{N-1} z_N^4}\right] \psi_N. \tag{A.3}$$

The quantity in brackets can be expanded in powers of a_H while maintaining $\epsilon_H \ll a_H$; one finds

$$\psi'_{N-1} = \left[\frac{2}{3z_H} - \frac{2}{3z_H^2}a_H + \mathcal{O}(a_H^2)\right] \psi_N. \tag{A.4}$$

In the limit $a_H \to 0$ we recover the boundary condition in Eq. (4.38). In summary, the effect of treating the ψ_j as dynamical fields everywhere is to modify the form of the boundary conditions away from those of the continuum limit:

$$\psi'_1 = -\frac{a}{f_1^2}\phi_1^2\psi_1, \quad \text{and} \quad \psi'_{N-1} = \left[\frac{2}{3z_H} - \frac{2}{3z_H^2}a_H\right] \psi_N. \tag{A.5}$$

BIBLIOGRAPHY

[1] J. M. Maldacena, *"The large N limit of superconformal field theories and supergravity,"* Adv. Theor. Math. Phys. **2**, 231 (1998) [Int. J. Theor. Phys. **38**, 1113 (1999)] [arXiv:hep-th/9711200].

[2] E. Witten, *"Anti-de Sitter space and holography,"* Adv. Theor. Math. Phys. **2**, 253 (1998) [arXiv:hep-th/9802150].

[3] S. S. Gubser, I. R. Klebanov and A. M. Polyakov, *"Gauge theory correlators from non-critical string theory,"* Phys. Lett. B **428**, 105 (1998) [arXiv:hep-th/9802109].

[4] C. Csaki, H. Ooguri, Y. Oz and J. Terning, *"Glueball mass spectrum from supergravity,"* JHEP **9901**, 017 (1999) [hep-th/9806021].

[5] J. Polchinski and M. J. Strassler, *"The string dual of a confining four-dimensional gauge theory,"* arXiv:hep-th/0003136.

[6] S. J. Brodsky and G. F. de Teramond, *"Light-front hadron dynamics and AdS/CFT correspondence,"* Phys. Lett. B **582**, 211 (2004) [arXiv:hep-th/0310227].

[7] G. F. de Teramond and S. J. Brodsky, *"The hadronic spectrum of a holographic dual of QCD,"* Phys. Rev. Lett. **94**, 201601 (2005) [arXiv:hep-th/0501022].

[8] J. Babington, J. Erdmenger, N. J. Evans, Z. Guralnik and I. Kirsch, *"Chiral symmetry breaking and pions in non-supersymmetric gauge / gravity duals,"* Phys. Rev. D **69**, 066007 (2004) [arXiv:hep-th/0306018].

[9] M. Kruczenski, D. Mateos, R. C. Myers and D. J. Winters, *"Towards a holographic dual of large-N(c) QCD,"* JHEP **0405**, 041 (2004) [arXiv:hep-th/0311270].

[10] T. Sakai and S. Sugimoto, *"Low energy hadron physics in holographic QCD,"* Prog. Theor. Phys. **113**, 843 (2005) [arXiv:hep-th/0412141];

T. Sakai and S. Sugimoto, *"More on a holographic dual of QCD,"* Prog. Theor. Phys. **114**, 1083 (2005) [arXiv:hep-th/0507073].

[11] J. Erlich, E. Katz, D. T. Son and M. A. Stephanov, *"QCD and a Holographic Model of Hadrons,"* Phys. Rev. Lett. **95**, 261602 (2005) [arXiv:hep-ph/0501128].

[12] L. Da Rold and A. Pomarol, *"Chiral symmetry breaking from five dimensional spaces,"* Nucl. Phys. B **721**, 79 (2005) [arXiv:hep-ph/0501218].

[13] J. Hirn and V. Sanz, *"Interpolating between low and high energy QCD via a 5D Yang-Mills model."* JHEP **0512**, 030 (2005) [arXiv:hep-ph/0507049].

[14] S. S. Gubser, *"Breaking an Abelian gauge symmetry near a black hole horizon,"* Phys. Rev. D **78**, 065034 (2008) [arXiv:0801.2977 [hep-th]].

[15] S. A. Hartnoll, C. P. Herzog and G. T. Horowitz, *"Building a Holographic Supercon-ductor,"* Phys. Rev. Lett. **101**, 031601 (2008) [arXiv:0803.3295 [hep-th]];

S. A. Hartnoll, C. P. Herzog and G. T. Horowitz, *"Holographic Superconductors,"* JHEP **0812**, 015 (2008) [arXiv:0810.1563 [hep-th]].

[16] S. S. Gubser and S. S. Pufu, *"The Gravity dual of a p-wave superconductor,"* JHEP **0811**, 033 (2008) [arXiv:0805.2960 [hep-th]];

M. Ammon, J. Erdmenger, V. Grass, P. Kerner and A. O'Bannon, *"On Holographic p-wave Superfluids with Back-reaction,"* Phys. Lett. B **686**, 192 (2010) [arXiv:0912.3515 [hep-th]];

R. -G. Cai, Z. -Y. Nie and H. -Q. Zhang, *"Holographic p-wave superconductors from Gauss-Bonnet gravity."* Phys. Rev. D **82**, 066007 (2010) [arXiv:1007.3321 [hep-th]];

J. -W. Chen, Y. -J. Kao, D. Maity, W. -Y. Wen and C. -P. Yeh, *"Towards A Holographic Model of D-Wave Superconductors,"* Phys. Rev. D **81**, 106008 (2010) [arXiv:1003.2991 [hep-th]];

F. Benini, C. P. Herzog and A. Yarom, *"Holographic Fermi arcs and a d-wave gap,"* Phys. Lett. B **701**, 626 (2011) [arXiv:1006.0731 [hep-th]].

[17] S. A. Hartnoll and C. P. Herzog, *"Impure AdS/CFT correspondence,"* Phys. Rev. D **77**, 106009 (2008) [arXiv:0801.1693 [hep-th]].

[18] S. A. Hartnoll, J. Polchinski, E. Silverstein and D. Tong, *"Towards strange metallic holography,"* JHEP **1004**, 120 (2010) [arXiv:0912.1061 [hep-th]].

[19] G. T. Horowitz, *"Introduction to Holographic Superconductors,"* arXiv:1002.1722 [hep-th].

[20] C. C. Homes *et al.*, *"A universal scaling relation in high-temperature superconductors."* Nature **430**, 539 (2004).

[21] J. Erdmenger, P. Kerner and S. Muller, *"Towards a Holographic Realization of Homes' Law,"* arXiv:1206.5305 [hep-th].

[22] G. T. Horowitz and M. M. Roberts, *"Zero Temperature Limit of Holographic Superconductors,"* JHEP **0911**, 015 (2009) [arXiv:0908.3677 [hep-th]].

[23] Y. V. Kovchegov, *"AdS/CFT applications to relativistic heavy ion collisions: a brief review,"* arXiv:1112.5403 [hep-ph].

   J. Casalderrey-Solana, H. Liu, D. Mateos, K. Rajagopal and U. A. Wiedemann, *"Gauge/String Duality, Hot QCD and Heavy Ion Collisions,"* arXiv:1101.0618 [hep-th].

   S. S. Gubser and A. Karch, *"From gauge-string duality to strong interactions: A Pedestrian's Guide,"* Ann. Rev. Nucl. Part. Sci. **59**, 145 (2009) [arXiv:0901.0935 [hep-th]].

[24] H. Liu, J. McGreevy and D. Vegh, *"Non-Fermi liquids from holography,"* Phys. Rev. D **83**, 065029 (2011) [arXiv:0903.2477 [hep-th]].

   S. -S. Lee, *"A Non-Fermi Liquid from a Charged Black Hole: A Critical Fermi Ball,"* Phys. Rev. D **79**, 086006 (2009) [arXiv:0809.3402 [hep-th]].

[25] A. Bayntun, C. P. Burgess, B. P. Dolan and S. -S. Lee, *"AdS/QHE: Towards a Holographic Description of Quantum Hall Experiments,"* New J. Phys. **13**, 035012 (2011) [arXiv:1008.1917 [hep-th]].

[26] S. A. Hartnoll, *"Lectures on holographic methods for condensed matter physics,"* Class. Quant. Grav. **26**, 224002 (2009) [arXiv:0903.3246 [hep-th]].

[27] C. P. Herzog, *"Lectures on Holographic Superfluidity and Superconductivity,"* J. Phys. A A **42**, 343001 (2009) [arXiv:0904.1975 [hep-th]];

[28] J. McGreevy, *"Holographic duality with a view toward many-body physics,"* Adv. High Energy Phys. **2010**, 723105 (2010) [arXiv:0909.0518 [hep-th]].

[29] S. Sachdev, *"Condensed Matter and AdS/CFT,"* Lect. Notes Phys. **828**, 273 (2011) [arXiv:1002.2947 [hep-th]].

[30] S. Sachdev, *"Strange metals and the AdS/CFT correspondence,"* J. Stat. Mech. **1011**, P11022 (2010) [arXiv:1010.0682 [cond-mat.str-el]].

[31] S. Sachdev, *"The landscape of the Hubbard model,"* arXiv:1012.0299 [hep-th].

[32] S. A. Hartnoll, *"Horizons, holography and condensed matter,"* arXiv:1106.4324 [hep-th].

[33] S. Sachdev, *"What can gauge-gravity duality teach us about condensed matter physics?,"* Annual Review of Condensed Matter Physics 3, 9 (2012) arXiv:1108.1197 [cond-mat.str-el].

[34] N. Iqbal, H. Liu and M. Mezei, *"Lectures on holographic non-Fermi liquids and quantum phase transitions,"* arXiv:1110.3814 [hep-th].

[35] G. Policastro, D. T. Son and A. O. Starinets, *"The Shear viscosity of strongly coupled N=4 supersymmetric Yang-Mills plasma,"* Phys. Rev. Lett. **87**, 081601 (2001) [hep-th/0104066].

[36] S. Cremonini, *"The Shear Viscosity to Entropy Ratio: A Status Report,"* Mod. Phys. Lett. B **25**, 1867 (2011) [arXiv:1108.0677 [hep-th]].

[37] S. Sachdev, *"Quantum Phase Transitions,"* Cambridge, UK: Cambridge Univ. Pr. (1999) 353 p

[38] P. Kovtun and A. Ritz, *"Universal conductivity and central charges,"* Phys. Rev. D **78**, 066009 (2008) [arXiv:0806.0110 [hep-th]].

[39] W. Witczak-Krempa and S. Sachdev, *"The quasi-normal modes of quantum criticality,"* Phys. Rev. B **86**, 235115 (2012) [arXiv:1210.4166 [cond-mat.str-el]].

[40] I. R. Klebanov, *"From three-branes to large N gauge theories,"* hep-th/9901018.

M. R. Douglas and S. Randjbar-Daemi, *"Two lectures on the AdS / CFT correspondence."* In *Trieste 1998, Nonperturbative aspects of strings, branes and supersymmetry* 157-177 [hep-th/9902022].

J. L. Petersen, *"Introduction to the Maldacena conjecture on AdS / CFT."* Int. J. Mod. Phys. A **14** (1999) 3597 [hep-th/9902131].

P. Di Vecchia, *"An Introduction to AdS / CFT correspondence,"* Fortsch. Phys. **48**, 87 (2000) [hep-th/9903007].

I. R. Klebanov, *"TASI lectures: Introduction to the AdS / CFT correspondence."* hep-th/0009139.

E. Alvarez, J. Conde and L. Hernandez, *"Rudiments of holography,"* Int. J. Mod. Phys. D **12**, 543 (2003) [hep-th/0205075].

J. M. Maldacena, *"TASI 2003 lectures on AdS / CFT,"* hep-th/0309246.

[41] O. Aharony, S. S. Gubser, J. M. Maldacena, H. Ooguri and Y. Oz, "*Large N field theories, string theory and gravity,*" Phys. Rept. **323**, 183 (2000) [hep-th/9905111].

[42] C. V. Johnson, "*D-branes,*" Cambridge, USA: Univ. Pr. (2003) 548 p

[43] K. Becker, M. Becker and J. H. Schwarz, "*String theory and M-theory: A modern introduction,*" Cambridge, UK: Cambridge Univ. Pr. (2007) 739 p

[44] E. Kiritsis, "*String theory in a nutshell,*" Princeton University Press, 2007

[45] B. Zwiebach, "*A first course in string theory,*" Cambridge, UK: Univ. Pr. (2009) 673 p

[46] J. F. Donoghue, E. Golowich, B. R. Holstein and , "*Dynamics of the standard model,*" Camb. Monogr. Part. Phys. Nucl. Phys. Cosmol. **2**, 1 (1992).

[47] G. 't Hooft, "*A Planar Diagram Theory for Strong Interactions.*" Nucl. Phys. B **72**, 461 (1974).

[48] A. V. Manohar, "*Large N QCD,*" hep-ph/9802419.

[49] P. Di Francesco, P. Mathieu and D. Senechal, "*Conformal field theory,*" New York, USA: Springer (1997) 890 p

[50] S. W. Hawking and G. F. R. Ellis, "*The Large scale structure of space-time.*" Cambridge University Press, Cambridge, 1973

[51] L. Susskind and E. Witten, "*The Holographic bound in anti-de Sitter space,*" hep-th/9805114.

[52] J. Polchinski, "*Introduction to Gauge/Gravity Duality.*" arXiv:1010.6134 [hep-th].

[53] V. Balasubramanian, P. Kraus and A. E. Lawrence, "*Bulk versus boundary dynamics in anti-de Sitter space-time,*" Phys. Rev. D **59**, 046003 (1999) [hep-th/9805171].

V. Balasubramanian, P. Kraus, A. E. Lawrence and S. P. Trivedi, "*Holographic probes of anti-de Sitter space-times,*" Phys. Rev. D **59**, 104021 (1999) [hep-th/9808017].

[54] P. Breitenlohner and D. Z. Freedman, "*Positive Energy in anti-De Sitter Backgrounds and Gauged Extended Supergravity,*" Phys. Lett. B **115**, 197 (1982).

P. Breitenlohner and D. Z. Freedman, "*Stability in Gauged Extended Supergravity.*" Annals Phys. **144**, 249 (1982).

[55] I. R. Klebanov and E. Witten, "*AdS / CFT correspondence and symmetry breaking,*" Nucl. Phys. B **556**, 89 (1999) [hep-th/9905104].

[56] D. Z. Freedman, S. D. Mathur, A. Matusis and L. Rastelli, "*Correlation functions in the CFT(d) / AdS(d+1) correspondence,*" Nucl. Phys. B **546**, 96 (1999) [hep-th/9804058].

[57] E. Witten, "*Anti-de Sitter space, thermal phase transition, and confinement in gauge theories.*" Adv. Theor. Math. Phys. **2**, 505 (1998) [hep-th/9803131].

[58] D. T. Son and A. O. Starinets, "*Minkowski space correlators in AdS / CFT correspondence: Recipe and applications,*" JHEP **0209**, 042 (2002) [hep-th/0205051].

[59] J. D. Bekenstein, "*Black hole hair: 25 - years after,*" In *Moscow 1996, 2nd International A.D. Sakharov Conference on physics* 216-219 [gr-qc/9605059].

[60] S. S. Gubser, "*Phase transitions near black hole horizons,*" Class. Quant. Grav. **22**, 5121 (2005) [hep-th/0505189].

[61] G. Baym, "*Pion condensation in nuclear and neutron star matter.*" Phys. Rev. Lett. **30**, 1340 (1973).

[62] A. B. Migdal, A. I. Chernoutsan and I. N. Mishustin, "*Pion Condensation And Dynamics Of Neutron Stars.*" Phys. Lett. B **83**, 158 (1979).

[63] P. Haensel and M. Proszynski, "*Pion condensation in cold dense matter and neutron stars,*" Astrophys. J. **258**, 306 (1982).

[64] A. W. Steiner, M. Prakash, J. M. Lattimer and P. J. Ellis, "*Isospin Asymmetry in Nuclei and Neutron Stars,*" Phys. Rept. **411**, 325 (2005) [arXiv:nucl-th/0410066].

[65] A. B. Migdal, "*Stability of vacuum and limiting fields.*" Zh. Eksp. Teor. Fiz. **61**, 2209 (1971).

[66] A. B. Migdal, O. A. Markin and I. N. Mishustin, "*Pion Interaction In Nuclear Matter And Pi Condensation,*" Zh. Eksp. Teor. Fiz. **70**, 1592 (1976).

[67] R. F. Sawyer and D. J. Scalapino, "*Pion condensation in superdense nuclear matter,*" Phys. Rev. D **7**, 953 (1973).

[68] D. T. Son and M. A. Stephanov, "*QCD at finite isospin density,*" Phys. Rev. Lett. **86**, 592 (2001) [arXiv:hep-ph/0005225].

D. T. Son and M. A. Stephanov, "*QCD at finite isospin density: From pion to quark antiquark condensation,*" Phys. Atom. Nucl. **64**, 834 (2001) [Yad. Fiz. **64**, 899 (2001)] [arXiv:hep-ph/0011365].

[69] K. Splittorff, D. Toublan and J. J. M. Verbaarschot, "*Thermodynamics of chiral symmetry at low densities,*" Nucl. Phys. B **639**, 524 (2002) [arXiv:hep-ph/0204076].

[70] D. Toublan and J. B. Kogut, "*Isospin chemical potential and the QCD phase diagram at nonzero temperature and baryon chemical potential,*" Phys. Lett. B **564**, 212 (2003) [arXiv:hep-ph/0301183].

[71] L. He and P. Zhuang, "*Phase structure of Nambu-Jona-Lasinio model at finite isospin density,*" Phys. Lett. B **615**, 93 (2005) [arXiv:hep-ph/0501024].

[72] H. Abuki, R. Anglani, R. Gatto, M. Pellicoro and M. Ruggieri, "*The fate of pion condensation in quark matter: from the chiral to the real world,*" Phys. Rev. D **79**, 034032 (2009) [arXiv:0809.2658 [hep-ph]].

[73] J. B. Kogut and D. K. Sinclair, "*Lattice QCD at finite isospin density at zero and finite temperature,*" Phys. Rev. D **66**, 034505 (2002) [arXiv:hep-lat/0202028].

[74] P. de Forcrand, M. A. Stephanov and U. Wenger, "*On the phase diagram of QCD at finite isospin density,*" PoS **LAT2007**, 237 (2007) [arXiv:0711.0023 [hep-lat]].

[75] W. Detmold, M. J. Savage, A. Torok, S. R. Beane, T. C. Luu, K. Orginos and A. Parreno, "*Multi-Pion States in Lattice QCD and the Charged-Pion Condensate,*" Phys. Rev. D **78**, 014507 (2008) [arXiv:0803.2728 [hep-lat]].

[76] W. Detmold, K. Orginos, M. J. Savage and A. Walker-Loud, "*Kaon Condensation with Lattice QCD,*" Phys. Rev. D **78**, 054514 (2008) [arXiv:0807.1856 [hep-lat]].

[77] M. Bando, T. Kugo and K. Yamawaki, "*On The Vector Mesons As Dynamical Gauge Bosons Of Hidden Local Symmetries,*" Nucl. Phys. B **259**, 493 (1985).

[78] D. T. Son and M. A. Stephanov, "*QCD and dimensional deconstruction,*" Phys. Rev. D **69**, 065020 (2004) [arXiv:hep-ph/0304182].

[79] K. Y. Kim, S. J. Sin and I. Zahed, "*Dense hadronic matter in holographic QCD,*" arXiv:hep-th/0608046.

[80] O. Aharony, K. Peeters, J. Sonnenschein and M. Zamaklar, *"Rho meson condensation at finite isospin chemical potential in a holographic model for QCD."* JHEP **0802**, 071 (2008) [arXiv:0709.3948 [hep-th]].

[81] P. Basu, J. He, A. Mukherjee and H. H. Shieh, *"Superconductivity from D3/D7: Holographic Pion Superfluid,"* JHEP **0911**, 070 (2009) [arXiv:0810.3970 [hep-th]].

[82] A. Karch, M. Kulaxizi and A. Parnachev, *"Notes on Properties of Holographic Matter,"* JHEP **0911**, 017 (2009) [arXiv:0908.3493 [hep-th]].

[83] K. I. Kim, Y. Kim and S. H. Lee, *"Isospin matter in AdS/QCD,"* arXiv:0709.1772 [hep-ph].

[84] S. J. Brodsky and R. Shrock, *"Maximum Wavelength of Confined Quarks and Gluons and Properties of Quantum Chromodynamics,"* Phys. Lett. B **666**, 95 (2008) [arXiv:0806.1535 [hep-th]].

[85] A. Deur, V. Burkert, J. P. Chen and W. Korsch, *"Determination of the effective strong coupling constant $\alpha_{s,g_1}(Q^2)$ from CLAS spin structure function data,"* Phys. Lett. B **665**, 349 (2008) [arXiv:0803.4119 [hep-ph]].

[86] P. M. Hohler and M. A. Stephanov, *"Holography and the speed of sound at high temperatures,"* Phys. Rev. D **80**, 066002 (2009) [arXiv:0905.0900 [hep-th]].

[87] A. Cherman, T. D. Cohen and A. Nellore, *"A bound on the speed of sound from holography,"* Phys. Rev. D **80**, 066003 (2009) [arXiv:0905.0903 [hep-th]].

[88] B. H. Lee and D. W. Pang, *"Notes on Properties of Holographic Strange Metals,"* arXiv:1006.4915 [hep-th].

[89] D. B. Kaplan and A. E. Nelson, *"KAON CONDENSATION IN DENSE NUCLEONIC MATTER."* preprint HUTP-86/A023; Phys. Lett. B **175**, 57 (1986).

[90] G. Colangelo, J. Gasser and H. Leutwyler, *"pi pi scattering,"* Nucl. Phys. B **603**, 125 (2001) [arXiv:hep-ph/0103088].

[91] J. Gasser and H. Leutwyler, *"Chiral Perturbation Theory To One Loop,"* Annals Phys. **158**, 142 (1984).

[92] J. Erlich and C. Westenberger, *"Tests of Universality in AdS/QCD,"* Phys. Rev. D **79**, 066014 (2009) [arXiv:0812.5105 [hep-ph]].

[93] Z. Abidin and C. E. Carlson, "*Strange hadrons and kaon-to-pion transition form factors from holography,*" Phys. Rev. D **80**, 115010 (2009) [arXiv:0908.2452 [hep-ph]].

[94] C. Csaki, M. Reece and J. Terning, "*The AdS/QCD Correspondence: Still Undelivered,*" JHEP **0905**, 067 (2009) [arXiv:0811.3001 [hep-ph]].

[95] M. Shifman, "*Highly excited hadrons in QCD and beyond.*" hep-ph/0507246.

[96] A. Karch, E. Katz, D. T. Son and M. A. Stephanov, "*Linear confinement and AdS/QCD,*" Phys. Rev. D **74**, 015005 (2006) [hep-ph/0602229].

[97] D. Albrecht and J. Erlich, "*Pion condensation in holographic QCD,*" Phys. Rev. D **82**, 095002 (2010) [arXiv:1007.3431 [hep-ph]].

[98] R. Wilcox, "*The Pion in AdS/QCD,*" Thesis (B.S.), College of William and Mary (2011).

[99] O. Domenech, G. Panico and A. Wulzer, "*Massive Pions, Anomalies and Baryons in Holographic QCD,*" Nucl. Phys. A **853**, 97 (2011) [arXiv:1009.0711 [hep-ph]].

[100] E. Witten, "*Multitrace operators, boundary conditions, and AdS / CFT correspondence,*" hep-th/0112258.

[101] M. Berkooz, A. Sever and A. Shomer, "*'Double trace' deformations, boundary conditions and space-time singularities,*" JHEP **0205**, 034 (2002) [hep-th/0112264].

[102] D. Albrecht, J. Erlich and R. J. Wilcox, "*Nonlinear Boundary Dynamics and Chiral Symmetry in Holographic QCD,*" Phys. Rev. D **85**, 114012 (2012) [arXiv:1112.5643 [hep-ph]].

[103] C. D. Carone and H. Georgi, "*Technicolor with a massless scalar doublet,*" Phys. Rev. D **49**, 1427 (1994) [hep-ph/9308205].

[104] C. D. Carone, J. Erlich and J. A. Tan, "*Holographic Bosonic Technicolor,*" Phys. Rev. D **75**, 075005 (2007) [hep-ph/0612242].

[105] A. Cherman, T. D. Cohen and E. S. Werbos, "*The Chiral condensate in holographic models of QCD,*" Phys. Rev. C **79**, 045203 (2009) [arXiv:0804.1096 [hep-ph]].

[106] L. Da Rold and A. Pomarol, "*The Scalar and pseudoscalar sector in a five-dimensional approach to chiral symmetry breaking,*" JHEP **0601**, 157 (2006) [hep-ph/0510268].

[107] T. M. Kelley, S. P. Bartz and J. I. Kapusta, *"Pseudoscalar Mass Spectrum in a Soft-Wall Model of AdS/QCD,"* Phys. Rev. D **83**, 016002 (2011) [arXiv:1009.3009 [hep-ph]].

[108] R. Casero, E. Kiritsis and A. Paredes, *"Chiral symmetry breaking as open string tachyon condensation,"* Nucl. Phys. B **787**, 98 (2007) [hep-th/0702155 [HEP-TH]].

I. Iatrakis, E. Kiritsis and A. Paredes, *"An AdS/QCD model from Sen's tachyon action,"* Phys. Rev. D **81**, 115004 (2010) [arXiv:1003.2377 [hep-ph]].

I. Iatrakis, E. Kiritsis and A. Paredes, *"An AdS/QCD model from tachyon condensation: II,"* JHEP **1011**, 123 (2010) [arXiv:1010.1364 [hep-ph]].

[109] G. Panico and A. Wulzer, *"Effective action and holography in 5D gauge theories,"* JHEP **0705**, 060 (2007) [hep-th/0703287].

[110] C. Csaki, C. Grojean, H. Murayama, L. Pilo and J. Terning, *"Gauge theories on an interval: Unitarity without a Higgs,"* Phys. Rev. D **69**, 055006 (2004) [hep-ph/0305237].

[111] J. G. Bednorz and K. A. Muller, *"Possible high Tc superconductivity in the Ba-La-Cu-O system,"* Z. Phys. B **64**, 189 (1986).

[112] W. L. McMillan, *"Transition Temperature of Strong-Coupled Superconductors,"* Phys. Rev. **167**, 331 (1968).

[113] J. W. Loram, K. A. Mirza, J. R. Cooper and W. Y. Liang, *"Electronic specific heat of YBa2Cu3O6+x from 1.8 to 300 K,"* Phys. Rev. Lett. **71**, 1740 (1993);

T. Timusk and B. Statt, *"The pseudogap in high-temperature superconductors: and experimental survy,"* Rep. Prog. Phys. **62**, 1 (1999).

[114] Z. A. Xu, et al., *"Vortex-like excitations and the onset of superconducting phase fluctuation in underdoped $La_{2-x}Sr_xCuO_4$,"* Nature **406**, 486 (2000).

[115] Y. Kamihara, T. Watanabe, M. Hirano and H. Hosono, *"Iron-Based Layered Superconductor La[O1-xFx]FeAs (x = 0.050.12) with Tc = 26 K"* J. Am. Chem. Soc. **130**, 11 (2008).

[116] H. B. Nielsen and P. Olesen, *"Vortex Line Models for Dual Strings,"* Nucl. Phys. B **61**, 45 (1973).

[117] N. Arkani-Hamed, S. Dimopoulos and G. R. Dvali, *"The Hierarchy problem and new dimensions at a millimeter,"* Phys. Lett. B **429**, 263 (1998) [hep-ph/9803315];

I. Antoniadis, N. Arkani-Hamed, S. Dimopoulos and G. R. Dvali, *"New dimensions at a millimeter to a Fermi and superstrings at a TeV,"* Phys. Lett. B **436**, 257 (1998) [hep-ph/9804398].

[118] L. Randall and R. Sundrum, *"A Large mass hierarchy from a small extra dimension,"* Phys. Rev. Lett. **83**, 3370 (1999) [hep-ph/9905221];

L. Randall and R. Sundrum, *"An Alternative to compactification,"* Phys. Rev. Lett. **83**, 4690 (1999) [hep-th/9906064].

[119] H. Davoudiasl, J. L. Hewett and T. G. Rizzo, *"Phenomenology of the Randall-Sundrum Gauge Hierarchy Model,"* Phys. Rev. Lett. **84**, 2080 (2000) [hep-ph/9909255];

L. J. Hall and C. F. Kolda, *"Electroweak symmetry breaking and large extra dimensions,"* Phys. Lett. B **459**, 213 (1999) [hep-ph/9904236].

[120] K. R. Dienes, E. Dudas and T. Gherghetta, *"Extra space-time dimensions and unification,"* Phys. Lett. B **436**, 55 (1998) [hep-ph/9803466];

K. R. Dienes, E. Dudas and T. Gherghetta, *"Grand unification at intermediate mass scales through extra dimensions,"* Nucl. Phys. B **537**, 47 (1999) [hep-ph/9806292].

[121] N. Arkani-Hamed, A. G. Cohen and H. Georgi, *"(De)constructing dimensions,"* Phys. Rev. Lett. **86**, 4757 (2001) [hep-th/0104005];

C. T. Hill, S. Pokorski and J. Wang, *"Gauge invariant effective Lagrangian for Kaluza-Klein modes,"* Phys. Rev. D **64**, 105005 (2001) [hep-th/0104035].

[122] N. Arkani-Hamed, A. G. Cohen and H. Georgi, *"Electroweak symmetry breaking from dimensional deconstruction,"* Phys. Lett. B **513**, 232 (2001) [hep-ph/0105239];

N. Arkani-Hamed, A. G. Cohen, T. Gregoire and J. G. Wacker, *"Phenomenology of electroweak symmetry breaking from theory space,"* JHEP **0208**, 020 (2002) [hep-ph/0202089];

N. Arkani-Hamed, A. G. Cohen, E. Katz, A. E. Nelson, T. Gregoire and J. G. Wacker, *"The Minimal moose for a little Higgs,"* JHEP **0208**, 021 (2002) [hep-ph/0206020];

C. Csaki, J. Erlich, C. Grojean and G. D. Kribs, *"4-D constructions of supersymmetric extra dimensions and gaugino mediation,"* Phys. Rev. D **65**, 015003 (2002) [hep-ph/0106044];

S. Dimopoulos, D. E. Kaplan and N. Weiner, *"Electroweak unification into a five-dimensional $SU(3)$ at a TeV,"* Phys. Lett. B **534**, 124 (2002) [hep-ph/0202136].

[123] M. Bando, T. Kugo, S. Uehara, K. Yamawaki and T. Yanagida, "*Is Rho Meson A Dynamical Gauge Boson Of Hidden Local Symmetry?*," Phys. Rev. Lett. **54**, 1215 (1985);

R. Casalbuoni, S. De Curtis, D. Dominici and R. Gatto, "*Effective Weak Interaction Theory with Possible New Vector Resonance from a Strong Higgs Sector.*" Phys. Lett. B **155**, 95 (1985).

[124] J. Frenkel, "*On the Transformation of light into Heat in Solids. I,*" Phys. Rev. **37**, 17 (1931).

[125] D. T. Son and M. A. Stephanov, "*QCD and dimensional deconstruction,*" Phys. Rev. D **69**, 065020 (2004) [hep-ph/0304182].

[126] J. D. Jackson, *Classical Electrodynamics*, Third Edition, Wiley (1998).

[127] C. P. Herzog, P. Kovtun, S. Sachdev and D. T. Son, "*Quantum critical transport, duality, and M-theory.*" Phys. Rev. D **75**, 085020 (2007) [hep-th/0701036].

[128] S. A. Hartnoll, "*Quantum Critical Dynamics from Black Holes,*" arXiv:0909.3553 [cond-mat.str-el].

[129] T. Faulkner, N. Iqbal, H. Liu, J. McGreevy and D. Vegh, "*From Black Holes to Strange Metals,*" arXiv:1003.1728 [hep-th];

H. Liu, "*From black holes to strange metals,*" Physics Today **65**, 6 (2012).

[130] S. A. Hartnoll and A. Tavanfar, "*Electron stars for holographic metallic criticality,*" Phys. Rev. D **83**, 046003 (2011) [arXiv:1008.2828 [hep-th]].

[131] N. Iqbal, H. Liu and M. Mezei, "*Semi-local quantum liquids,*" JHEP **1204**, 086 (2012) [arXiv:1105.4621 [hep-th]].

[132] S. Sachdev, "*Holographic metals and the fractionalized Fermi liquid,*" Phys. Rev. Lett. **105**, 151602 (2010) [arXiv:1006.3794 [hep-th]].

[133] J. McGreevy, "*Viewpoint: In pursuit of a nameless metal.*" Physics **3**, 83 (2010).

[134] C. Charmousis, B. Gouteraux, B. S. Kim, E. Kiritsis and R. Meyer, "*Effective Holographic Theories for low-temperature condensed matter systems,*" JHEP **1011**, 151 (2010) [arXiv:1005.4690 [hep-th]].

B. Gouteraux and E. Kiritsis, "*Generalized Holographic Quantum Criticality at Finite Density,*" JHEP **1112**, 036 (2011) [arXiv:1107.2116 [hep-th]].

B. Gouteraux and E. Kiritsis, *"Quantum critical lines in holographic phases with (un)broken symmetry,"* arXiv:1212.2625 [hep-th].

VITA

Dylan Albrecht

Dylan Albrecht was born May 22, 1984 and raised in Winchendon, Massachusetts. Since childhood his primary interests changed from various sports, to chess, to mathematics, to computer programming, and then to math and physics. He began school at the Waldorf School in Keene, NH. Then after a year of home-schooling he transferred for middle school to The Well School in Peterborough, NH, where they allowed for independent study in mathematics. After one year of high school at Buxton School, he decided to get his GED. Instead of going to high school he studied computer science, while dabbling in mathematics and physics, from home. In the Spring semester of 2004, he entered the University of Massachusetts Amherst as a math major. He graduated *cum laude* in 2007, with a double major in math and physics. In 2007 he entered the Physics PhD program at the College of William and Mary. During the course of his graduate studies he became interested in formal aspects of particle physics, quantum field theory, and gravity. After completion of the Master degree requirements he began research in theoretical high energy particle physics with Professor Josh Erlich. They started research in extra-dimensional model building based on the AdS/CFT correspondence, and have recently turned to possible condensed matter applications. He looks forward to continuing this line of research in the future.